Effect of Water Injection on Boiler Performance

by

Mitchell Kane

A Doctoral Thesis

Submitted in partial fulfilment of the requirements

for the award of

Doctor of Engineering of Loughborough University

September 2018

Abstract

A 20kW commercial boiler has been modified to enable the injection of water into its combustion air, with the aim of reducing the emissions of carbon monoxide (CO) and oxides of nitrogen (NO_x) and increasing heat transfer efficiency.

It was identified that water injection had been used for efficiency and emissions control in both gas turbine and internal combustion engines. NO_x reductions were consistently achieved however CO reductions were application dependant. The lack of literature relating to water injection in boilers provided an opportunity for novel research.

An experimental setup was designed to investigate the effect of water injected into the combustion air on the heat-transfer efficiency of the boiler system, as well as its emissions of CO and NO_x. The differences between liquid water and steam, injecting at points internal and external to the burner, and with or without the use of nozzles was also explored.

NO_x and CO reductions of up to 40% and 93% were achieved with water injected inside the burner through a nozzle with no significant change in heat-transfer efficiency. The CO reduction effectiveness was found to be dependent on several factors. These included: the method and location of the injection, whether the fluid was vaporised, and the air-to-fuel equivalence ratio. The majority of experimental cases resulted in NO_x reductions.

Acknowledgements

I would like to thank Spirax-Sarco Limited for sponsoring the research.

My appreciation also extends to the following people:

Prof. Jeremy Miller – for proposing and supporting the research.

Dr. Andrew Clarke – for guidance and accommodating my remote working.

Dr. Nashtara Islam – for getting me started on the journey.

Laura – for putting up with me.

Table of Contents

List of Figures

Nomenclature

a_{ki}	Subscript to kth element in molecular species i
b_k	Moles of element k in basis amount of chemical system
h	Specific enthalpy, kJ/kg
i	Index
j	Index
k	Index
m	Index
$\dot{m}$	Mass flow rate, kg/s
M	Number of elements
$\mathbf{n}$	Species-abundance vector with entries n_i
n_i	Number of moles of species i
N'	Number of species excluding inert species
$\dot{Q}$	Heat transfer rate, kW
R	Molar gas constant, 8.3143 kJ/kmol.K
T	Temperature, °C or K
η	Efficiency
λ	Lagrange multiplier or air-fuel equivalence ratio
μ_i	Chemical potential of species i
ψ	λ_k/RT

1. Introduction

Contents

1.1. The Use of Hydrocarbon Fuels

The combustion of hydrocarbon fuels, specifically fossil fuels, has driven global growth since the first industrial revolution. This is due to their high energy density, chemical stability, and geographic abundance, which means that they are convenient and economical. They influence every aspect of society, from power generation and industry to transport and domestic heating.

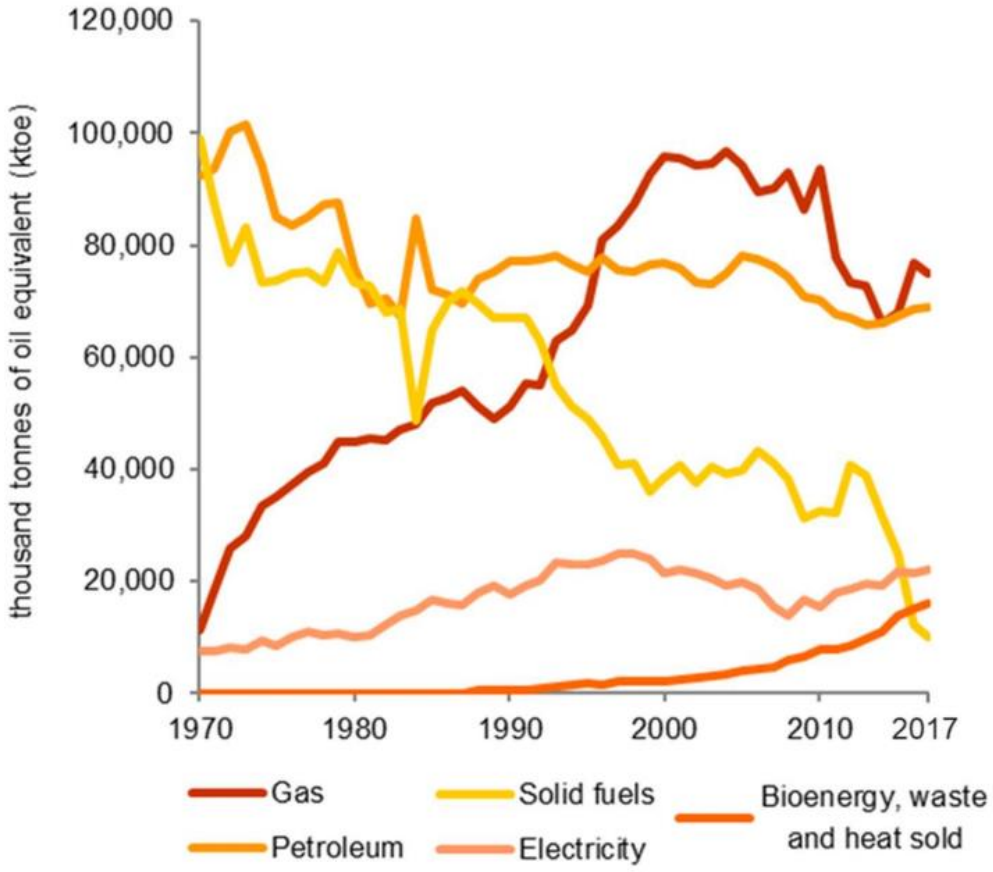

Figure 1-1 – UK energy consumption in primary energy equivalents by fuel type (BEIS, 2018)

Despite their advantages, Figure 1-1 shows that the usage of oil and solid fuels saw a significant decline between 1970 and 2017. The resultant energy deficit was partially addressed by bioenergy and renewable power, though primarily by natural gas, which rose by a factor of four.

While Figure 1-1 shows no indication of a significant decline in gas or petroleum usage in recent years, there is much debate around an eventual departure from fossil fuels. However, the National Grid (2018) conducted a study regarding future pathways for energy development. They concluded that although the uptake of low-carbon and renewable energy sources will significantly increase, the transition will take time. Indeed, by 2030 all four of their proposed scenarios indicated that gas would still provide more power than electrical means, and that by 2050 only one of the four scenarios would see electricity as the primary energy source. This suggests that fossil fuels will still be in use for decades to come.

1.2. The Problem

The World Energy Council (2017) proposed a three-part definition for energy sustainability, named the "energy trilemma". This comprises of "energy security", "energy equity", and "environmental sustainability". Hydrocarbon fuels are a finite resource, however they are readily available in the UK at an accessible cost, therefore the energy security and energy equity aspects are lesser issues. Their significant disadvantage, and the cause of their decreased usage, is their poor environmental sustainability.

Hydrocarbons release a range of pollutants during the combustion process, each with their own environmental concerns. The emission of oxides of nitrogen (NO_x) can combine with atmospheric water to form nitric acid, causing acid rain, which can damage plant life and structures (Pabian *et al.*, 2012; Livingston, 2016). Additionally, carbon monoxide (CO) can cause photochemical smog, which carries various public health concerns (Guttikunda and Kopakka 2014).

Though the issues caused by NO_x and CO are significant, it is the release of CO_2 from hydrocarbons which is of greatest interest, as it is well established that CO_2 contributes to climate change. The Department for Business Energy & Industrial Strategy (2018) stated that the rise in global temperature associated with CO_2 release can lead to rising sea levels, extreme weather conditions, and poverty. Furthermore, the IPCC (2014) predicted that to prevent global temperatures rising above 2°C from pre-industrial levels, CO_2 concentrations would need to be 40% to 70% lower in 2050 than they were in 2010. Also, since the IPCC (2014) also estimated that fossil fuels and industry contributed approximately 78% of greenhouse gas emissions between 1970 and 2010, it is clear to see why hydrocarbon fuels lack environmental sustainability.

1.3. Legislation

To force improved sustainability in the UK, the Government has set targets for future CO_2 emissions. It is aiming for a 30% reduction from 2,782 MtCO2e in the 2013 to 2017 period, to 1,950 MtCO2e in the 2023-2027 period (Department for Business Energy & Industrial Strategy, 2018). The Government also actively penalises the use of carbon fuel derived energy through the Climate Change Levy, an environmental tax (Government Digital Service, 2018).

Historically only greenhouse and ozone-depleting gases were legislated against, hence there were no set limits on NO_x or CO emissions. However, the Medium Combustion Plant Directive (EU) 2015/2193 (European Union 2015) became law on 20th December 2018 and sets fixed limits for the NO_x emissions from 1MW to 5MW installations. This is set to 80ppm for new developments, and 200ppm for existing systems. The directive only recommends that future limits are set for CO, therefore it is currently only mandatory to monitor it.

These policies set out the challenges for emissions reductions, and industry will need to adapt through the implementation of new technologies in order to meet those challenges.

1.4. Mitigation Techniques

1.4.1. Combating Emissions

Technologies have been developed to reduce emissions through preventing their formation or release. Kuprianov (2005) defined a system that uses the recirculation of flue gases to cool the combustion zone and reduce the concentration of oxygen, leading to reduced NO_x emissions. Similarly, Mathioudakis (2002) investigated a gas turbine system that used steam injection rather than flue gas to reduce NO_x. Pang *et al.* (2017) investigated the benefits of carbon capture and storage, which can remove the CO_2 produced in the combustion process and store it in reservoirs. This process was described by Xiong, Zhao and Zheng (2011) as “perhaps the only choice” for the effective control of CO_2.

1.4.2. Replacing Fossil Fuels

The more obvious method of reducing emissions would be to cease using fossil fuels, which could be achieved by changing from hydrocarbon energy sources to electrical ones. For example, rather than using natural gas to generate steam for industrial processes, electrical heating elements could be used. This option would certainty reduce the emission of pollutants, however it faces many challenges.

Firstly, the source of the electricity would itself have to be emission free, else the pollutants would simply be released at the power plant. This effectively means that either renewable or nuclear sources would be required, however, as stated by the National Grid (2018), the complete withdrawal from hydrocarbon fuels by 2050 is not a viable scenario. This is due to the time it will take for cleaner technologies to be developed and commissioned to meet the energy demand. As shown in Figure 1-1, most energy consumption is served by hydrocarbon fuels, and as previously stated, it is unlikely that electrical energy will even meet the energy output of natural gas by 2050, let alone replace it.

Secondly, the capital cost of switching from hydrocarbon fuels to electrical sources would be significant. A moderately sized steam generator producing 10 tonnes of steam an hour would consume around 6.7MW of thermal power, therefore replacing a natural gas fuelled system with an equivalent electrical solution would be a considerable investment.

The factors preventing the short-term, mass migration from hydrocarbon fuels to electrical energy lead to the conclusion that fossil fuels will be used for the foreseeable future, and that alternative measures are required to improve environmental sustainability.

1.4.3. Reducing Fuel Usage

Rather than replacing hydrocarbon fuels, improving the efficiency of the processes they are used in would also reduce emissions, as less fuel would be required for the same heating duty. In a typical combustion system efficiency is lost due to many factors, such as poor insulation or incomplete combustion, however the primary loss of efficiency is through the combustion gases themselves. This is due to those gases carrying a large proportion of the heat of combustion out of the system, and in the worst cases, straight to the atmosphere.

Technologies do exist for improving efficiency by reducing combustion gas losses. For example, a typical household condensing boiler can recover a portion of the sensible heat of the flue gases, and the latent heat of the steam produced during combustion. This results in significant efficiency gains. Similar technologies, such as industrial flue gas economisers, can also reclaim heat from the flue gas, and use it for other working fluids, thus saving energy. Another method of improving efficiency is to remove the nitrogen from the combustion air, i.e., to only use oxygen. Nitrogen serves no useful purpose in the combustion process, and yet absorbs heat and forms pollutants. All of these efficiency improving measures do incur additional cost and complexity however.

1.5. Research Application Aims and Objectives

The field of hydrocarbon fuels is well researched, therefore this research was focussed on a specific application that had received little attention: improving the environmental sustainability of natural gas-fired steam boilers.

This resulted in the following objectives:

1. A reduction of NO_x emissions
2. The reduction of CO emissions
3. An improvement in heat-transfer efficiency, and thus a reduction in fuel consumption

To achieve these objectives the use of injecting water into the combustion process was investigated, which has been proven effective in gas turbine systems (Peltier, 2006), where NO_x and CO reductions were achieved whilst improving efficiency. Although a gas turbine system is significantly different from a boiler system, the combustion chemistry is similar therefore this was determined to be a viable route for research.

1.6. Contributions to Knowledge

Specific contributions to knowledge from this research include:

1. Emissions reductions on a 20kW scale system

   This research is the first known instance of the application of water injection for the reduction of CO and NO_x in a ~20kW scale commercial system. Emissions reductions of up 64% CO and 28% NO_x were achieved with no apparent effect on heat-transfer efficiency.

   This has proven that it is technically viable to introduce the environmental benefits of water injection to commercial/domestic-scale boilers. As there are over 20 million of these in the UK alone (Randall and Beaumont, 2011), the opportunity is significant.

   The effects of water injection on combustion systems have previously been investigated in laboratory environments (Ge, Zang and Guo, 2009) and on industrial-scale systems such as gas turbines for power generation (Arsenie *et al.*, 2015), but not for domestic/commercial scale systems.

   Though the research is focused on a 20kW-scale system, the principle of operation for boilers is similar, and the research output will result in the development of a product for an industrial system.

2. Retrofitting a commercially available burner for NO_x/CO reduction

   This research is the first known study of a retrofitted commercially available burner for water or steam injection. Prior research has featured the design of burners for water injection, however in this research a standard burner was modified to incorporate the same functionality.

   The aforementioned emissions reductions achieved in this work demonstrate that retrofitting is a viable alternative to the replacement of a burner unit, which is advantageous as it enables water injection to be implemented into systems at a reduced cost.

3. Reducing emissions to access lower fuel-air equivalence ratios, thus improving efficiency

   This research has led to a patent submission for a multi-variable optimisation system that reduces NO_x, CO, and SO_x emissions, in addition to improving potential efficiency.

   This is achieved by controlling the air/fuel and water/fuel ratios, which enables operating the burner under richer conditions than would normally be accessible. Typically, emissions increase as excess air is reduced, however operating closer to stoichiometric offers efficiency improvements. By harnessing the emissions reducing potential of water injection, the system can operate close to stoichiometric whilst maintaining an acceptable emissions output.

   This research is the first documented proposal of such a system, hence its contribution to knowledge.

4. Identification of the importance of injection location to the performance of water injection systems for boilers

   The research investigated the effect of water injection point and the use of atomising nozzles on the CO and NO_x emissions from the system. The locations included inside the burner before the swirl diffuser, and into the air supply before the burner air intake. Experiments were conducted both with and without nozzles, and on steam and water, at each location.

   It was identified that the injection point and the nozzle type used for the water injection was critical to the resultant emissions of the boiler system, as injecting internally and with the use of a nozzle offered clear improvements. This had not previously been investigated for this application.

1.7. Thesis Structure

This work details the process involved in conducting the research exercise, including the experimental approach, presentation and analysis of results, and recommendations for further work. The work is structured as follows:

1. Introduction

   An overview of the research topic and an outline of the thesis structure.

2. Literature Review

   A review of current knowledge and experimental techniques that were used to identify areas for novel research, develop a methodology, and generate a theoretical model.

3. Theoretical Analysis

   An overview of the mathematical modelling used to predict the output of the boiler system. This also aided in the design of the experimental arrangement.

4. Experimental Arrangement

   The presentation of the experimental setup with reasoning as to why the equipment was chosen.

5. Preliminary Experiments

   An exploration of the capability of the experimental setup, as well as the identification of required improvements and the analysis of the initial results.

2. Literature Review

2.1. Effects of Steam Injection on Combustion

The first section of this literature review explores the effect of steam and water injection on the combustion characteristics of various air/fuel mixtures and evaluates relevant experimental methodologies for use in the research. The information was used to guide the design of an experimental setup for water injection into a boiler system, and to determine the most suitable experimental approach.

2.1.1. Fundamentals of Combustion

As the research goals focussed on a natural-gas fuelled system, understanding the combustion processes of hydrocarbon fuels is a necessity. Kuo (2005) stated the following overall reaction for the stoichiometric combustion of hydrocarbon fuels:

$$C_xH_y + n_{air}(O_2 + 3.762N_2) \rightarrow xCO_2 + (y/2)H_2O + 3.762n_{air}N_2$$

This overall reaction must be expanded to investigate how CO and NO_x are formed, and the effect that water addition has. Skevis *et al.* (2004) published the seven stage methane mechanism displayed in Figure 2-1, however it was not designed for use with water addition and the seven reactions would not capture its effects.

I	CH_4	+	OH	=	$2.5H_2$	+	CO
II	2CO	+	O_2	=	$2CO_2$		
III	$2H_2$	+	O_2	=	$2H_2O$		
IV	H_2	+	O_2	=	2OH		
V	H_2			=	2H		
VI	N_2	+	$0.5O_2$	=	N_2O		
VII	N_2	+	O_2	=	2NO		

Figure 2-1 – Seven stage reaction mechanism for methane combustion (Skevis et al., 2004)

However, the Smith *et al.* (2000) Gas Research Institute (GRI) 3.0 mechanism comprised of 325 reactions with 53 species and was designed for the detailed chemical modelling of natural gas. From this, Park *et al.* (2004) identified 6 reactions that contributed most significantly to the generation of CO, which are shown in Figure 2-2.

$$O + C_2H_2 \rightarrow CO + CH_2 \quad (R23)$$
$$H + HCO \rightarrow H_2 + CO \quad (R55)$$
$$H + HCCO \rightarrow CH_2(s) + CO \quad (R79)$$
$$HCO + H_2O \rightarrow H + CO + H_2O \quad (R166)$$
$$HCO + M \rightarrow H + CO + M \quad (R167)$$
$$O + CH_3 \rightarrow H + H_2 + CO \quad (R284)$$

Figure 2-2 – CO formation reactions, (Park et al., 2004), where the reaction numbers reference GRI-3.0 (Smith et al., 2000)

$$N + NO \leftrightarrow N_2 + O \quad (R178)$$
$$N + O_2 \leftrightarrow NO + O \quad (R179)$$
$$N + OH \leftrightarrow NO + H \quad (R180)$$

Figure 2-3 – Zeldovich mechanism for NO formation (Park et al., 2004), where the reaction numbers reference GRI-3.0 (Smith et al., 2000)

Similarly, the reactions in Figure 2-3 were noted as contributing to the generation of NO_x via the Zeldovich mechanism. According to Glassman, Yetter and Glumac (2014), the Zeldovich mechanism applies to “thermal” NO_x generated due to heat in the post-flame region, however there is also “prompt” NO_x and fuel-bound NO_x.

Prompt NO_x was stated to form in the flame region via the following reactions:

$$CH + N_2 \leftrightarrow HCN + N$$

$$C_2 + N_2 \leftrightarrow 2CN$$

The HCN, N, and CN then react with O, O_2, and OH to form oxides of nitrogen. Fuel-bound NO_x refers to nitrogen contained within the fuel which reacts during the combustion process, and does not apply to natural gas combustion.

To achieve the research aims of reducing emissions, the CO and NO_x forming reactions will need to be influenced, potentially through the direct chemical action of introducing water into the combustion process, or by altering the temperature of the flame to change the chemical equilibria. Section 2.1.2 identifies studies into water-added combustion and its effects on chemical kinetics.

2.1.2. Chemical Kinetics

Landman, Derksen and Kok, (2006) conducted an experimental study on a natural gas-fired combustor, comparing the effects of both steam and nitrogen addition on the flame. In order to eliminate the thermal effect of the additives the inlet conditions were varied, which resulted in an approximately constant adiabatic flame temperature. The effect of oxygen deficiency with steam injection was also eliminated by matching the mole fraction of steam with nitrogen during the nitrogen addition experiments. “Significant” reductions in the emission of oxides of nitrogen (NO_x) were found, with steam being twice as effective as nitrogen. It was concluded that this was due to the steam “influencing the pathways of the chemical reactions taking place in the combustion zone”, though the mechanism for this was not proposed.

A more recent combustor study by Göke *et al.* (2014) presented both experimental data and a verified theoretical model for steam-enhanced combustion. Their results, which are displayed in Figure 2-4, again demonstrate the effect of steam on combustion chemistry. It can be seen that the addition of 20% steam (as a percentage of the mass flow of air), reduced the experimentally measured NO_x from 18ppm to 12ppm at a flame temperature of 1900K. The theoretical data suggests that this was due to a reduction in NO_x generated from the thermal and N_2O pathways of ~84% and ~75% respectively, although the contribution of the prompt pathway increased by 107%. An exponential increase in NO_x with temperature was also observed, dominated by thermal NO_x with contributions from prompt NO_x. The N_2O pathway appeared unaffected by temperature.

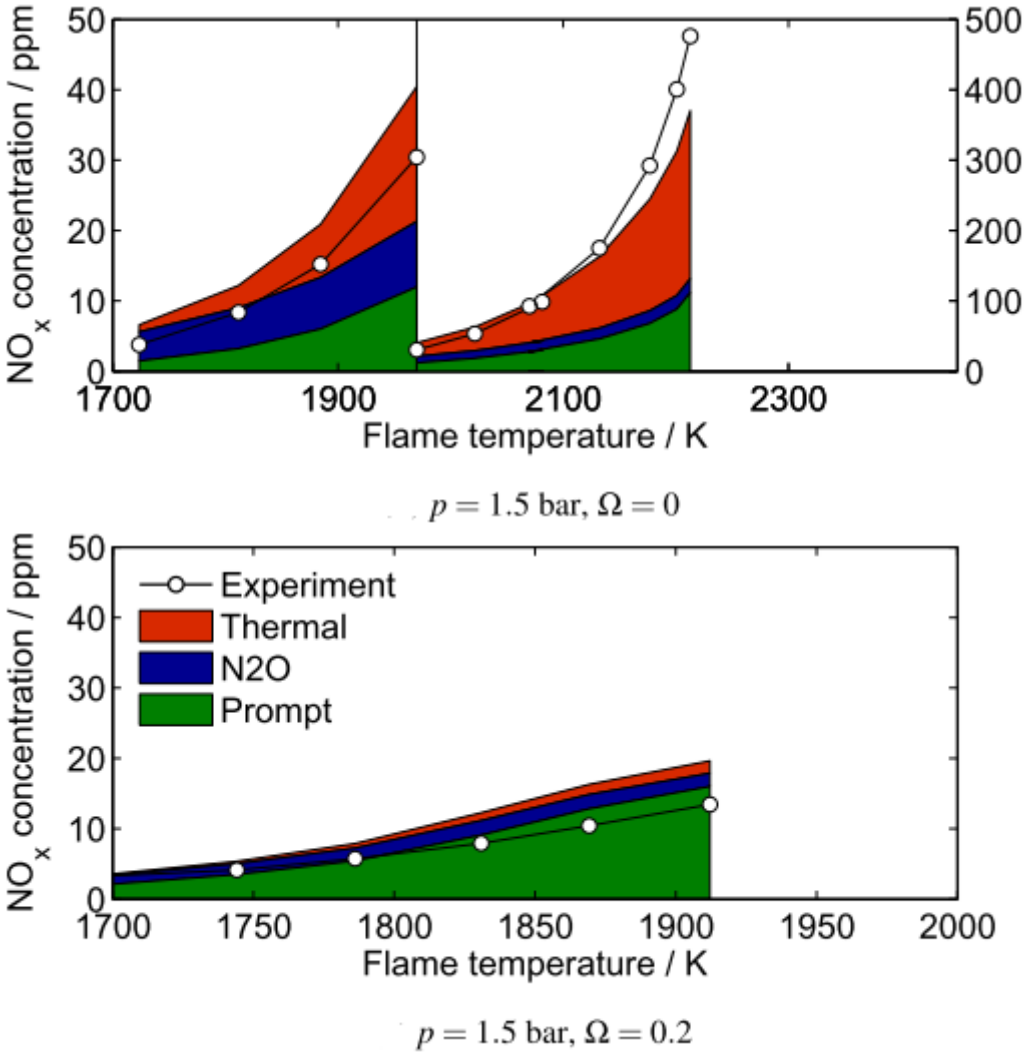

Figure 2-4 – Contribution of the NO_x formation pathways, where p is combustor pressure and Ω is the steam/air ratio, (Göke et al., 2014)

Earlier work by Touchton (1984) also investigated steam/air/natural gas combustion over the same range of steam to fuel ratios as those studied by Göke et al. (2014), but the adiabatic flame temperature was artificially held constant by heating the reactants. It was concluded that the effect of steam on NO_x production was purely due to a reduction in flame temperature, and not to chemical effects such as changes in hydroxyl (OH) concentration. This conflicts with the findings from both Landman, Derksen and Kok (2006) and Göke et al. (2014). All three studies focussed on combustor

applications, though the steam to fuel mass ratio in Landman, Derksen and Kok (2006) was 2.6, whereas the ratios explored by Touchton (1984) ranged from 0.6 to 2.0. This could have been the cause of the discrepancy, though Landman, Derksen and Kok (2006) may have affected NO_x production by changing the inlet conditions to maintain the adiabatic flame temperature. The combustion models by Touchton (1984) and Göke *et al.* (2014) both achieved agreement with their test data yet reached conflicting conclusions. This is likely due to either variations in the designs of the combustors, or the fact that the Touchton model assumed a negligible prompt NO_x contribution and was therefore unable to resolve it. The Touchton model was also fit to previous experimental data, therefore both factors may have resulted in the prompt NO_x contribution being misrepresented as thermal NO_x.

Peltier (2006) presented experimental data for a steam-injected gas turbine demonstrating NO_x and CO levels at 2 ppm or lower. Although the excess oxygen was relatively high at 15%, the effect of steam injection was substantial. The NO_x reduction was attributed to a lower flame temperature and shorter residence time. Claeys *et al.* (1993) observed similar trends in their gas turbine application, though to a lesser extent. De Jager, Kok and Skevis (2007) ran a numerical analysis of gas turbine combustors and found that although nitric oxide (NO) decreased, there was a “moderate” rise in CO. An experimental study by Li *et al.*, (2017) supported this, showing no benefit of steam addition for CO addition for any of their tested cases. This can be seen in Figure 2-5, where CO increases with steam addition in all cases other than those around 1925K.

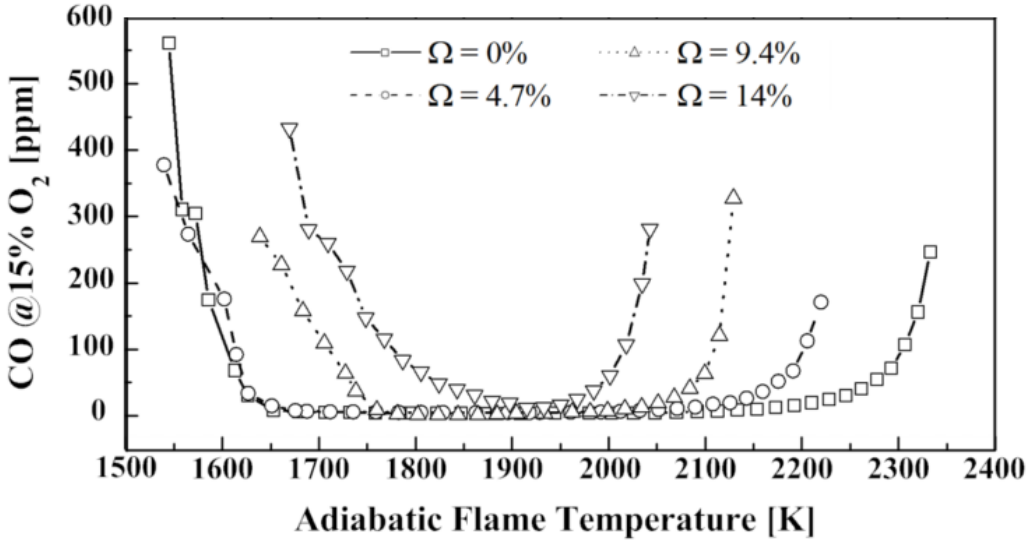

Figure 2-5 – CO vs. AFT at various steam/air ratios, (Li *et al.*, 2017)

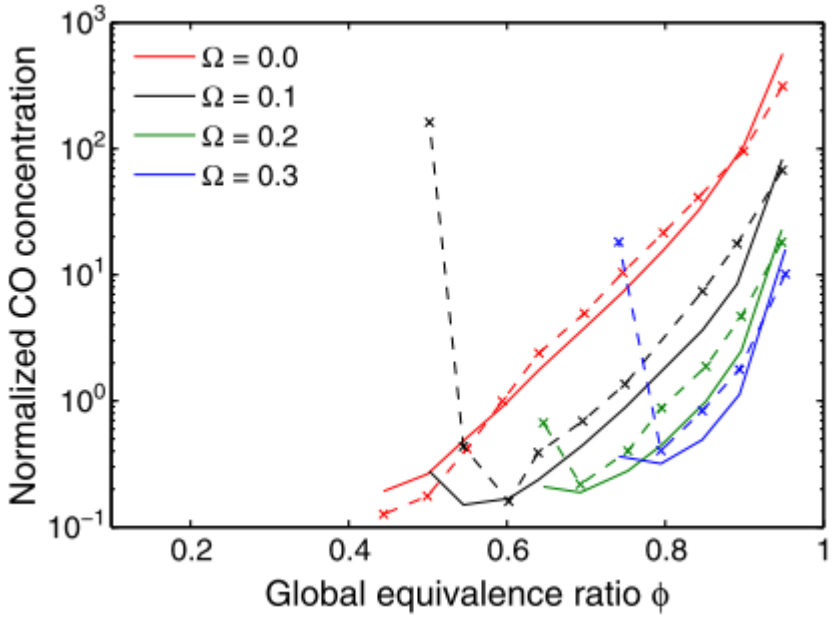

Figure 2-6 – CO vs. equivalence ratio at various steam/air ratios for a natural gas combustor, with experimental data (dotted) and modelled data (solid), Göke *et al.*, (2013)

Göke *et al.* (2013) and Larionov *et al.* (2016) observed similar NO_x and CO reduction trends to Peltier (2006). In the study by Göke *et al.* (2013), “low” NO_x emissions were achieved with steam injection even “near” stoichiometric conditions, which were attributed to both flame temperature reduction and chemical effects. As shown by Figure 2-6, CO reductions were also achieved across fuel-air equivalence ratio (Φ) values of approximately 0.6 to 0.9, dependant on steam/air ratio (Ω). For Ω greater than 0.0, CO began to increase towards leaner conditions. The point at which the increase began occurred at higher Φ values with higher Ω values, meaning that optimisation of Φ and Ω is required to achieve the lowest CO emissions. De Paepe *et al.* (2016) also observed CO reductions with steam injection, noting that it allowed higher Φ operating states to be achieved compared with dry combustion.

Larionov *et al.* (2016) investigated an experimental propane-air application rather than natural gas and air. They attributed their decrease in CO with steam addition to both a reduction in flame temperature and the increased availability of oxygen and hydrogen radicals, however none of the emissions reductions were quantified.

An experimental investigation into the effects of superheated steam on a premixed methane-air flame by Kobayashi *et al.* (2009) demonstrated a 27% reduction of CO with 10% steam addition (as a percentage of air + steam mass flow). The study proposed that the increase in H_2O enhances the water-gas-shift reaction, $CO + H_2O = CO_2 + H_2$, resulting in more complete combustion.

A numerical study by Zhao *et al.*, (2002) studied the interaction of steam with a methane/air diffusion flame, drawing several conclusions which reinforced the claims of a chemical influence on NO_x reductions observed by the experimental studies by Landman, Derksen and Kok (2006) and Göke *et al.* (2014). The model suggested that for a fixed maximum flame temperature the addition of steam increased the concentration of OH radicals, due to steam decomposition (GRI 93 and GRI 86) and the suppression of OH consumption reactions (GRI 193)

$$CH + H_2O = OH + CH_2 \text{ (-GRI 93)}$$

$$O + H_2O = OH + OH \text{ (-GRI 86)}$$

$$NH + OH = N + H2O \text{ (GRI 193)}$$

$$N + OH = NO + H \text{ (GRI 180)}$$

$$CH + N_2 = HCN + N \text{ (GRI 240)}$$

The OH radicals caused an increased in NO_x generation through R180, however steam addition also caused a greater reduction in CH concentration through R93 which lead to a decrease in prompt NO formation via R240. This resulted in an overall reduction in NO_x. The model was not experimental validated, however it was noted that data regarding the formation of OH radicals in combustion with steam was scarce.

Cong and Dagaut (2009) also undertook a kinetic analysis of a premixed flame, again noting a decrease in maximum flame temperature and NO_x with steam injection, however they attributed the NO_x reduction to dilution and thermal effects rather than chemical effects. The difference may be due to a variation in the contribution of prompt NO in each application. Katoh *et al.* (2006) performed an experimental study on the effect of steam addition

on OH distribution in a flame using laser-induced fluorescence, which showed that although water decomposition increased OH production, the decrease in maximum flame temperature lowered the overall concentration of radicals and the associated NO_x production, which correlated with the theoretical model proposed by Zhao *et al.*, (2002).

The reduction on NO_x with steam addition appears well established; (Toqan *et al.* (1992) reported reductions of 10ppm with 0.12kg_{steam}/kg_{gas} in their experimental study, and Park *et al.* (2004) and Skevis *et al.* (2004) noted similar effects in their numerical studies and determined it was due to a suppression of the thermal mechanism. Roy, Schlader and Odgers (1974) also documented experimental NO_x reductions, but noted that the combustion efficiency decreased at steam/fuel ratios greater than 0.5 due to increased hydrocarbon content in the flue gas.

2.1.3. Flame Characteristics

Sohn *et al.* (1999) investigated the effect of steam addition on hydrogen (H_2) and air flames, finding that it had both a thermal and chemical effect and reduced the burning velocity, though the study was numerical in nature and was reportedly difficult to validate experimentally due to variations in empirical data.

Terhaar, Oberleithner and Paschereit (2014) also investigated H_2/air flames, finding that the flow field and flame shape for a premixed, swirl-induced flame were significantly affected by the rate of steam addition. Their results are shown in Figure 2-7, where, for a fixed overall mass flow of steam and air, increasing quantities of steam shift the profile from a “V flame” to a “trumpet flame” and then to a “detached flame”. It can also be seen that the bulk velocity increases 10% from 66.1m/s for the 0% steam/air V flame to 72.9m/s for the 20% steam/air “detached flame”, and that the laminar burning velocity decreases 34% from 0.59 to 0.39 m/s. The increase in bulk velocity coupled with the decrease in burning velocity is likely the cause of the flame extending downstream with increasing steam/air ratio, resulting in detachment at 20% steam/air. Increasing this ratio further would therefore likely have resulted in lift-off.

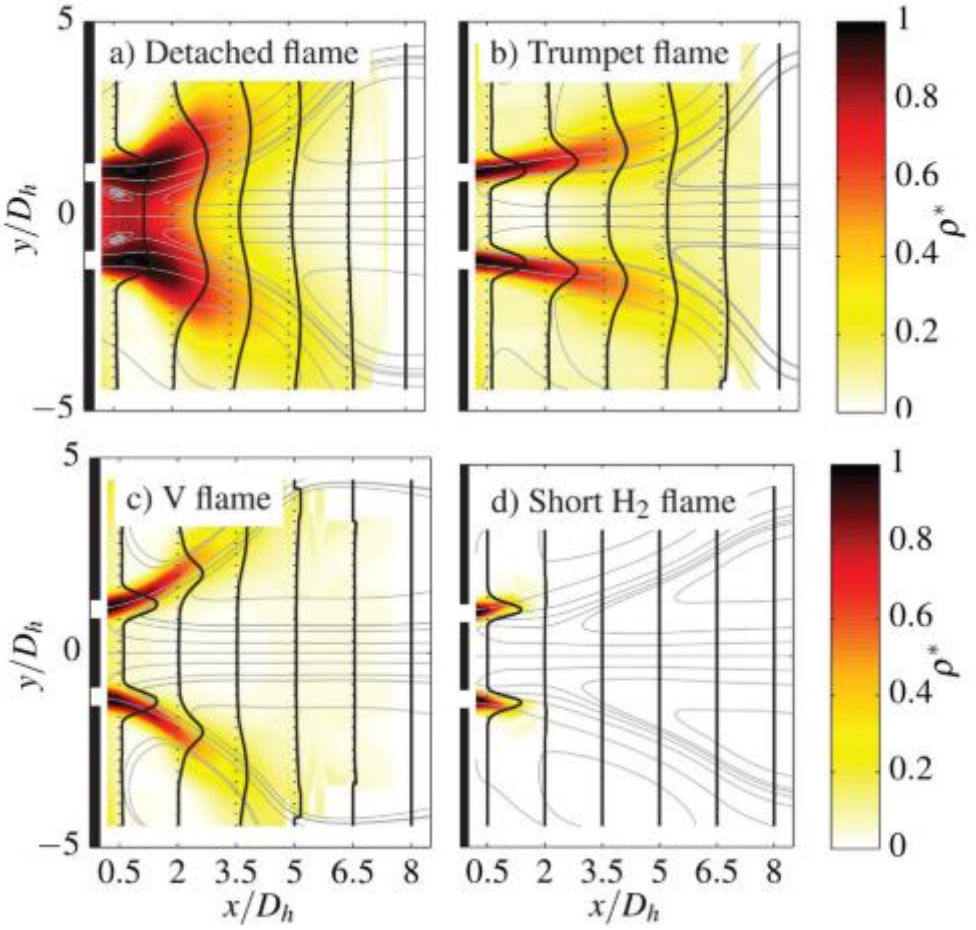

Type	$T_{in}/1K$	$T_{ad}/1K$	ϕ	Fuel	Ω	$u_0/1m/s$	$S_L/1m/s$
Detached	620	1850	0.8	CH_4	0.2	72.9	0.39
Trumpet	620	1850	0.68	CH_4	0.1	69.6	0.48
V flame	620	1850	0.56	CH_4	0	66.1	0.59
Short H_2	540	1850	0.5	H_2	0	65.8	2.58

Figure 2-7 – (Terhaar, Oberleithner and Paschereit, 2014) Streamlines of the time-averaged flow fields and radial profiles of the estimated normalized density (solid lines ρ) superimposed on the estimated normalized density distribution, where Ω is the steam/air mass ratio, u_0 is the bulk velocity at the combustor inlet, and S_L is the laminar burning velocity*

Liu and MacFarlane (1983) found that in addition to the reduction in burning velocity, steam addition reduced the overall rate of combustion. Steam addition was also linked to lower flame speeds by Cong and Dagaut (2009).

Steam addition has also been investigated for syngas flames, where Singh *et al.* (2012) reported that the burning velocity decreased for 50/50 H_2/carbon monoxide (CO) syngas with steam injection, while for 5/95 syngas the burning velocity increased with up to 20% steam and then decreased with further addition. It was explained that the differing effect on burning velocity was due to competing chemical and thermal influences. Up to 20% steam addition the increase in OH radical concentration resulted in increased reaction and flame speeds, however successive increases in steam addition resulted in a dilution of the fuel and a lower flame temperature, reducing the burning velocity. The thermal dilution dominated for the 50/50 flame from the outset, thus there was no initial increase in flame speed.

Larionov *et al.* (2016) investigated a range of flame characteristics affected by water vapour for a propane-air flame. They found that the flame changed from laminar to turbulent, accompanied by a changed in its sound and luminosity. It was also found that the flame colour shifted from yellow to blue, which was stated to be due to reduced free carbon in the flame, and could indicate that combustion efficiency was improving as a result of the turbulent flow increasing mixing.

Though the H_2 and propane studies did not utilise methane as their fuel they do show that steam does not act as an inert substance in the combustion process.

Xin, Shusheng and Bing (2007) studied the effect of steam addition on methane diffusion flames, finding that it destabilised the flame by reducing the momentum of the air, leading to decreased flow circulation. Ge, Zang and Guo (2009) and Terhaar, Oberleithner and Paschereit (2014) also reported that steam injection radically affected the structure of diffusion flames, and also their stability. Conversely, for gas turbine applications, Peltier (2006) described how steam addition to the fuel increased the rate of diffusion and improved the rate of combustion, and De Paepe *et al.* (2016) reported that steam had a stabilising effect on combustion at lower equivalence ratios. The applications and scales of the studies were significantly different which is likely to be the cause of the dissimilarity. This indicates that the geometry of a burner and the conditions it is used under has at least as much of an influence on the flame characteristics as the species involved in the combustion.

2.2. Effects of Liquid Water Injection

Claeys *et al.* (1993) showed that for gas fuel, water caused NO_x emissions reductions of 63% at a 0.5 water/fuel mass ratio, greater than the 40% reduction observed for steam. This is likely due to the increased thermal dilution caused by heat in the combustion process being utilised for vaporising the water, resulting in lower flame temperatures and therefore less thermal NO_x.

For oil fuel, CO emissions reduced by 15% and 20% for water and steam injection respectively, at a 0.5 water/fuel ratio. Unfortunately, the water with natural gas experimental data was rendered invalid due to an equipment failure. No theory was presented as to why the steam and water results differed, however it was likely related to the additional heat absorbed during the evaporation of the liquid water evaporation. The extra cooling of the flame could have caused a reduction in the reaction rate of CO and O, resulting in incomplete combustion.

Water injection was also shown to reduce unburnt hydrocarbons by up to 21%, although data was also presented that indicated an increase in unburned hydrocarbons with decreasing firing temperature, indicating that the cooling effect of the water was not beneficial. Cheikhravat *et al.* (2015) presented a significantly different application, however one observation was notable as it described how water droplets increased combustion turbulence, which was suggested to result in more complete combustion. This improved combustion turbulence could explain how water reduced unburnt hydrocarbons in the Claeys *et al.* (1993) despite lowing the flame temperature.

2.3. Experimental Methods

Singh *et al.* (2012) described a particle image velocimetry (PIV) experiment that involved heating water to evaporation in a water chamber and then passing it through to a combustion chamber. Of particular note was the series of thermocouples that were used to ensure that the water remained in the gaseous phase until it reached the combustion chamber. Xin, Shusheng and Bing (2007) undertook a similar approach for their PIV application, however they explicitly stated that they were generating superheated steam. The steam was also mixed with dry air before it entered the combustor rather than injecting it directly. Katoh *et al.* (2006) mixed aerosolised water with dry air in a heating chamber which evaporated the water.

Peltier (2006) illustrated how a gas turbine combustor was modified to produce NO_x emissions as low as 5 ppm using steam injection. Although the boiler application is significantly different, the approach indicates that modifying an existing system is viable. Claeys *et al.*, (1993) also tested a gas turbine, and used a dedicated steam generator for steam injection with an air atomiser for water injection.

Landman, Derksen and Kok (2006) built a custom combustion system featuring a scaled-down industrial burner nozzle and a spark igniter. Flue gases were cooled using water and the resulting condensate was drained. Air was provided by a compressor and then cleaned, dried, and preheated, and natural gas was supplied from gas bottles. A computer monitored and controlled mass flows and temperatures. A steam generator was used, with steam flow measured with a weight balance.

Experiments by Cheikhravat *et al.* (2015) were conducted in a spherical vessel regulated at a specific temperature. The vessel featured quartz windows for optical access and tungsten electrodes for ignition. Two types of nozzle were used for water injection, a mono-fluid and a bi-fluid variant. The water droplet sizes were measured with a third-party laser light diffraction device.

For the jet stirred reactor application presented by Cong and Dagaut, (2009), all the gases were preheated before entering the reactor. Thermal mass-flow controllers were used to regulate the gas flow rates. Platinum-rhodium thermocouples housed within a silica thermowell measured the reactor temperature. An infrared gas analysing technique was used to measure relevant species, fed by a heated sample line.

The test rig used by Terhaar, Oberleithner and Paschereit (2014), the results of which were discussed in section 2.1.3, featured a premixed burner with optical access and variable swirl generator. Superheated steam was mixed with the air before reaching the burner, at ratios ranging from 0 to 0.5 of the air mass flow. The outlet temperature was estimated rather than measured. Göke *et al.* (2014) tested a gas-fired combustor which again featured air/steam mixing ahead of the swirl generator of the burner and optical access. An oil-fired steam generator generated saturated steam for injection. Mass flows were measured with Coriolis meters, and inlet, outlet, and fuel temperatures were measured with type K thermocouples. Steam-to-air mass flow ratios ranged from 0 to 0.25.

Toqan *et al.* (1992) designed and built a 1.5 MW experimental burner to investigate fluid dynamics effects on flame properties. It featured preheated combustion air, primary, secondary, and tertiary air intakes, as well as automatic control of mass flows. Concentrations of CO, carbon dioxide (CO_2), oxygen (O_2), and NO_x were measured at various points throughout the system, and steam was injected at a ratio of 0.12 of the *fuel* mass flow. It was found that without flue gas recirculation (FGR) or steam injection, 70ppm of NOx and 56ppm CO was achievable, and with both FGR and steam injection, 15ppm NO_x and <10ppm CO were achievable. The effect of steam injection was not separated from the effect of FGR, though the data suggests that it provided a 10ppm reduction in NO_x over FGR alone.

Roy, Schlader and Odgers (1974) ran experiments on a baffle combustor that could be operated with premixed or diffusion flames. Orifice plates and a venturi were used to measure steam and air flows respectively. Steam injection rates ranged from 0 to 2.2 of the fuel mass flow. The steam injection rates used by Toqan *et al.* (1992) and Roy, Schlader and Odgers, (1974), which are based on steam to *fuel* mass ratios of 0 to 2.2, are significantly lower than the 0 to 0.5 steam to *air* ratios used by Terhaar, Oberleithner and Paschereit (2014) and Göke *et al.* (2014). This variation may be due to advances in combustor technology, as there is a 22-year difference between the two sets of sources.

The boilers of interest to this research are fuelled by natural gas, however Kayadelen (2017) found that natural gas composition varied “widely” between sources, and also over time for the same source. These variations in composition affected multiple aspects of the combustion process, including flame temperature and emissions.

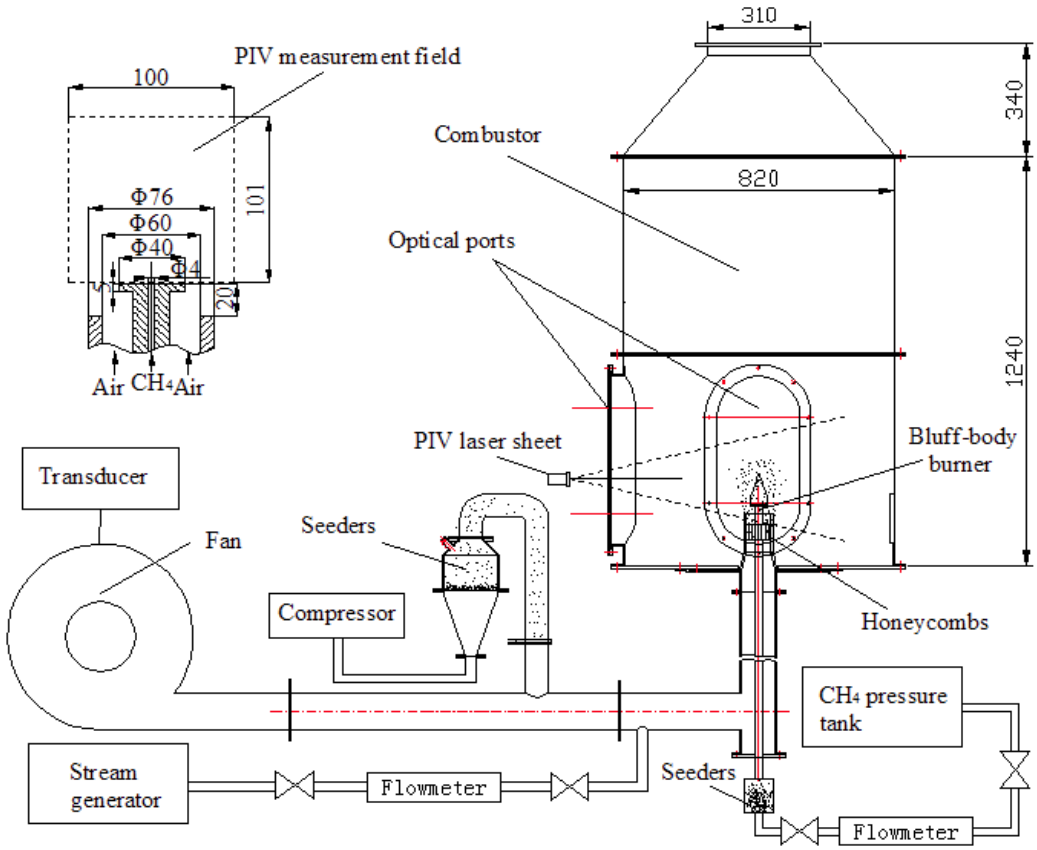

Figure 2-8 - Experimental rig from (Ge et al. 2009)

The experimental setup shown by Ge, Zang and Guo (2009) in Figure 2-8 featured a bluff-body burner housed within an optically accessible combustor. It can be seen that the steam is metered then mixed with the air before entering the combustor, with the fuel being metered and entering the combustion chamber through the centre of the bluff body to create a diffusion flame. The air was also seeded and PIV equipment was used to capture the flow field. Terhaar, Oberleithner and Paschereit (2014) also used PIV to investigate their swirl-stabilised combustor, which housed a premixed flame. The results of this setup can be seen in Figure 2-7.

Sun *et al.* (2016) also experimented with an optically accessible setup which is shown in Figure 2-9, where the key differences from Figure 2-8 are the lack of combustor and flow seeding, and the heating of all the reactants in a preheating furnace. It can also be seen that the water flow rate is measured using a piston pump before it is evaporated, rather than after.

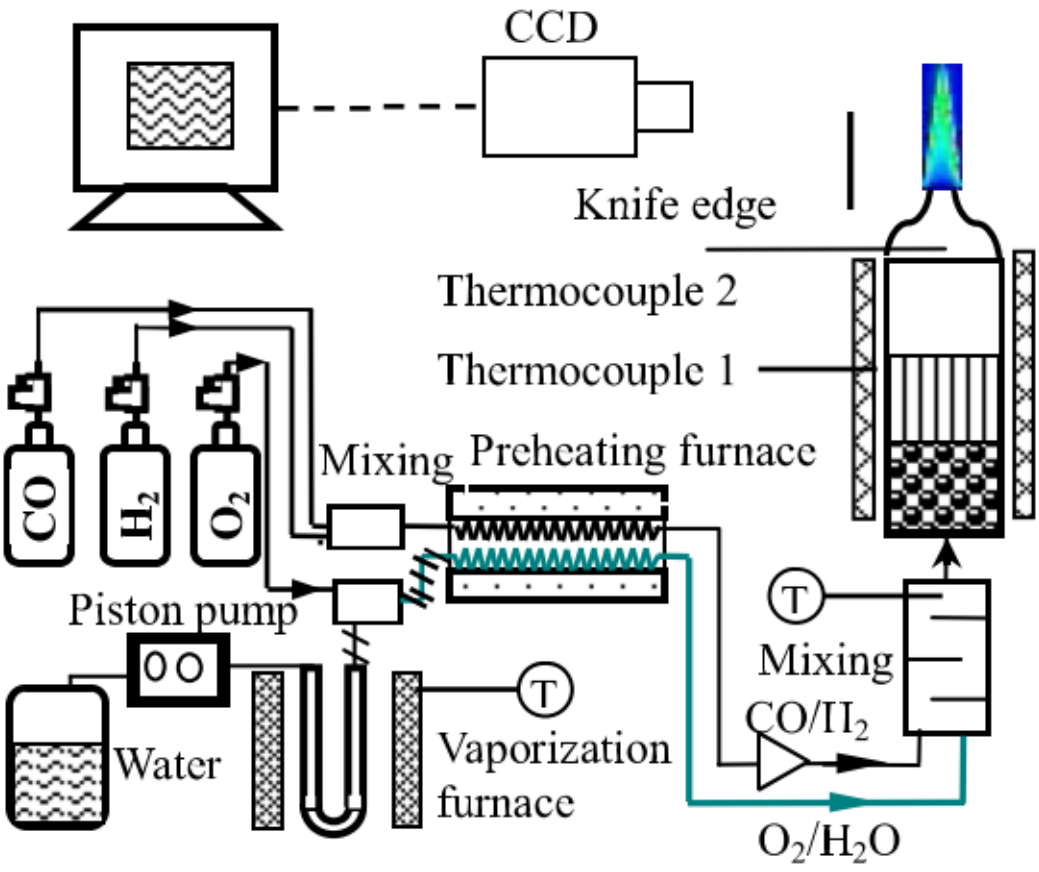

Figure 2-9 – Experimental setup from (Sun *et al.*, 2016)

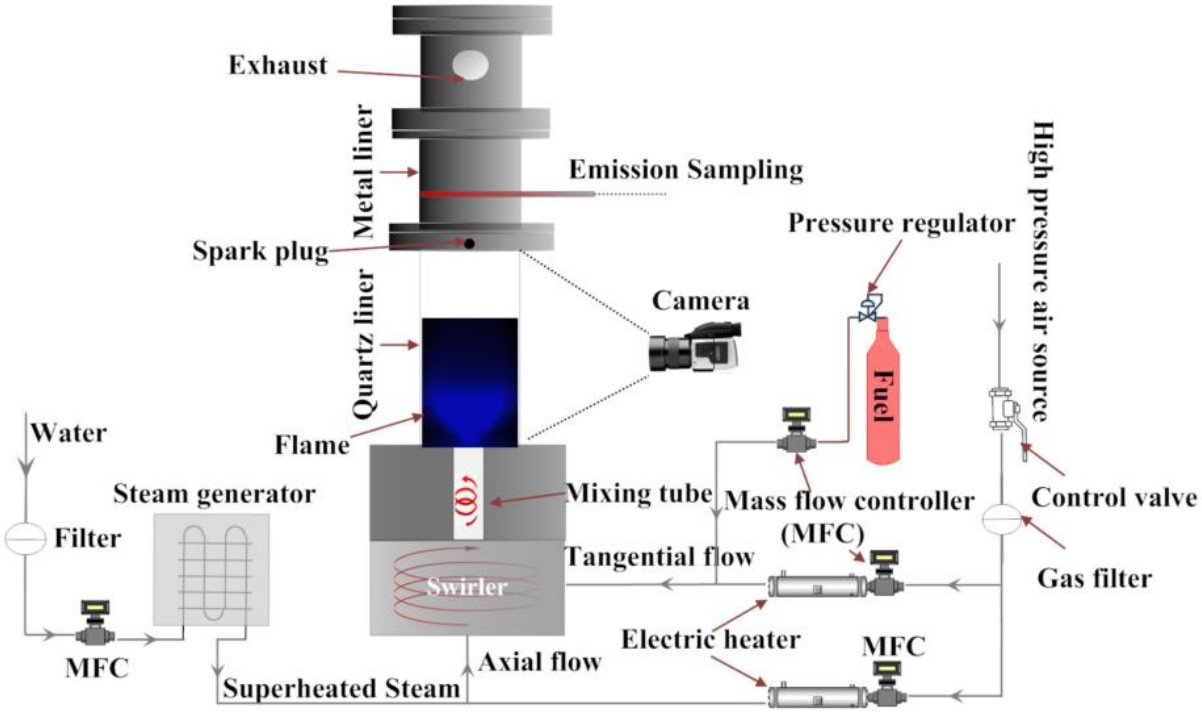

Figure 2-10 – Experimental setup from (Li *et al.*, 2017)

Li *et al.*, (2017) used the experimental setup shown in Figure 2-10, which differs from Figure 2-8 and Figure 2-9 as the burner featured both an axial and tangential flow which were independently measured.

2.4. Appraisal

Numerous studies of air/methane/steam combustion had already been conducted, though these appeared to be mostly lab-scale or focused on non-boiler applications such as gas turbines or internal combustion engines. The most relevant study found was the burner application presented by Toqan *et al.* (1992), which featured a diffusion flame rather than the premixed flames used in the application of interest to the research, and did not investigate the modified burner's use in an actual system.

It was beyond the financial resources of the research project to purchase a megawatt-scale steam boiler or to modify an existing one. Therefore, a sub-50kW burner was purchased with a compatible boiler, generating a premixed, methane/air jet flame in order to emulate a larger scale steam boiler as closely as possible. This was then modified for steam and water injection, with the steam initially generated by an electric heater.

Previous studies have investigated the fundamental theory of air/methane/steam flames, however it was also apparent that the influence of the system design and the various parameters on the actual efficiency and emissions of the system is not easily predicted. Therefore, as no literature was found for steam boilers nor for domestic-scale boilers, an opportunity for novel research was identified. The research focussed on the effect that steam injection had on the heat-transfer efficiency of the system and the emissions it generated. An increase in efficiency and reductions in NO_x, CO_2, and CO emissions were the aims, and although boiler applications do not benefit from the mass-flow increase as in a gas turbine, it was hypothesized that optimising the system could result in positive heat-transfer efficiency gains.

Lastly, Kayadelen (2017) found that variations in gas composition affected combustion performance and emissions, which were the very properties the research is aiming to influence. To remove the risk of fuel composition interfering with the experimental work it was necessary to use methane instead of natural gas, which could be obtained at specific purity grades.

2.5. Conclusions

Significant evidence was found showing that steam or water addition had an effect on the combustion process. Some sources suggested this was only due to thermal effects, others stated that there was a chemical effect, but all showed a reduction in NO_x emissions. In certain applications CO emissions were also reduced, however in most it increased. These differences were likely application specific and it was difficult to predict how a gas-fired steam boiler would be affected, hence the opportunity for research.

As a result of the literature review, it was decided that the research would investigate a scaled-down system that was representative of an industrial steam boiler. It was impractical to use a full-size system due to the cost, particularly without knowing if beneficial effects could be realised.

2.6. Calculating Chemical Equilibrium

The second half of this literature review aimed to determine the most appropriate method of modelling chemical equilibria in the combustion of methane with air. The creation of a model was essential as it allowed the prediction of reaction products and was used as a guide to design experiments and determine critical factors. In other applications models could be used to reduce carbon monoxide generation based on reactants or environmental conditions, or to optimise the air to fuel ratio for an internal combustion engine. There were also many other examples that include inorganic and organic chemistry, rocket propellants, and energy conversion (Smith and Missen, 1982).

2.7. Approaches to Solving Equilibrium

Several approaches to modelling chemical equilibrium were identified which were categorised as either stoichiometric or non-stoichiometric (Li *et al.*, 2001). Stoichiometric models relied upon using equilibrium constants, while non-stoichiometric models followed methods such as minimising Gibbs free energy (Sreejith, Arun and Muraleedharan 2013). It was generally agreed that the two approaches were based on the same concept (Jarungthammachote and Dutta, 2007; Barba *et al.*, 2011).

2.7.1. Stoichiometric Approaches

Rashidi (1997) built a stoichiometric model to evaluate a specific combustion reaction involving 13 chemical species. This involved simultaneously solving 9 non-linear algebraic equations representing equilibrium reactions as well as 4 elemental balances. It was reported that the Newton-Raphson method was often used to solve the equations by substituting them with a series of linear equations which were solved more easily using matrix inversion, Gaussian elimination, or the Gauss-Seidel approach. Another method, successive substitution, was also explored which appeared to have involved estimating the initial molar concentrations and then cycling through a substitution process until the solution converged. It was found that the Newton-Raphson method was often slow to converge whereas the successive substitution method was up to 50 times faster but failed to converge with air-fuel equivalence ratios greater than 0.9. A combination of the two methods was found to perform well computationally, though the model was not validated.

Kayadelen and Ust (2013) also followed an equilibrium constant approach for a combustion application where an 11-equation system was firstly reduced to 8 equations using substitution, then solved by the Newton-Raphson and Gauss-Seidel methods. The model was compared with the software packages CHEMKIN and GASEQ which featured more complex reactions with up to 53 species. It was found to be “quite similar” to GASEQ and within “reasonable accuracy” of CHEMKIN, though the error was not quantified.

There are numerous examples of the development of stoichiometric equilibrium models for various types of gasifiers (Zainal *et al.*, 2001; Deydier *et al.*, 2011; Vaezi *et al.*, 2011). Deydier *et al.* (2011) created a model involving 11 chemical species found in refuse derived fuel, which involved solving a system of 24 equations. Several assumptions were made to reduce the number of species considered in the reaction and thus reduce the complexity of the model, such as non-organic content being inert and the absence of heavy molecules of tar. The assumptions appear to have been reasonable as the model output was almost identical to that from Ptasinski, Prins and Pierik (2007), who used the software Aspen Plus which employed the minimisation of Gibbs free energy approach. Neither model was experimentally validated, though the close similarity between the stoichiometric and non-stoichiometric approaches is noteworthy.

2.7.2. Non-Stoichiometric Approaches

Most non-stoichiometric equilibrium methods appeared to be derived from entropy consideration. For example, the minimisation of Gibbs free energy method involved applying temperature and pressure constraints to an entropy maximisation approach, while the minimisation of Helmholtz free energy involved constraining internal energy and specific volume (Jones and Rigopoulos, 2005; Gunawardena and Fernando, 2014). Assad, Penyazkov and Skoblya (2011) explain that “in accordance with the Duhem theorem the equilibrium state of a closed system, the initial mass of which is known, is determined by two independent variables independently of the number of phases, the number of components, and the number of chemical equilibria”. This meant that a variety of variable pairs could be used to constrain the entropy minimisation approach, such as pressure and enthalpy (Freitas and Guirardello, 2012), temperature and specific volume

(Assad, Penyazkov and Skoblya, 2011), and those used for the Helmholtz and Gibbs minimisations.

Rashidi (1997) reported that a NASA approach minimised both the Gibbs and Helmholtz functions simultaneously, which resulted in a model that was both robust and complex. Van Baten and Szczepanski (2011) also applied both methods but separately, dependant on the inputs given by the user.

As mentioned previously the Gibbs free energy method is constrained by temperature, therefore Sreejith, Arun and Muraleedharan (2013) applied their model to a range of reaction temperatures in order to determine the maximum possible energy released. This method was used to compare the performances of different gasifying agents within a gasification process and to optimise the process, and it was found to be suitable. Hosseini, Dincer and Rosen (2012) applied an energy balancing equation to their minimisation approach to determine the product temperatures.

Concerning reliability, Gunawardena and Fernando (2014) found that their Gibbs free energy model for a pyrolysis process corresponded to experimental data well for some species but not others, and it was suggested that this was due to the reaction mechanism used. Xiao and Song (2011) successfully used a Gibbs free energy approach to model a chemical looping combustion process, which they validated against their own data. Shabbar and Janajreh (2013) reported that their model for a coal gasifier did not match with experimental data, as it tended to over-predict methane and under-predict carbon monoxide. The variation was thought to have been due to a discrepancy between the pressure used by the experimental data and the model reference pressure. The most comprehensive validation study reviewed was by Freitas and Guirardello,

(2014), who used the Gibbs free energy model for a glycerol reforming process. They compared their approach to both experimental data and an existing model, and quantitatively reported the variations which varied from a 0.692 mean percentage error in the worst case to 0.039 in the best case. It was concluded that the model had “good predictive ability”.

The entropy maximisation approach was demonstrated by Assad, Penyazkov and Skoblya (2011), where they showed that by constraining their equation system by temperature and pressure it was possible to model the combustion of a range of fuels, with good agreement against the software package Chemkin and experimental data. By constraining temperature and pressure they were effectively following the Gibbs minimisation method. Freitas and Guirardello (2014) used entropy maximisation with pressure and enthalpy constraints to supplement their Gibbs energy minimisation approach, where it was used to calculate the equilibrium temperature. The combination was found to have a low computational time and compared reasonably well to experimental data.

2.7.3. Comparison of Equilibrium Models

Several sources provided insight into the applicability of the Gibbs free energy approach versus the equilibrium constant approach. Rashidi (1997) found that the equilibrium constant approach was simpler to implement and satisfactory for a variety combustion simulations, but required more data, experienced numerical difficulties with components, and was inflexible. Jarungthammachote and Dutta (2008) had similar findings, explaining that the equilibrium constant method was not suitable for complex models as information regarding the chemical reactions and equilibrium constants had to be supplied in advance, whereas the Gibbs free energy method needed

no chemical reactions to be defined. Both Jarungthammachote and Dutta, (2007) and Deydier *et al.* (2011) also reported that the minimisation of Gibbs free energy method was more difficult to implement due to its more complex mathematics.

The Gibbs free energy approach was referred to as the most commonly used method of finding equilibrium conditions by Faungnawakij, Viriya-Empikul and Tanthapanichakoon (2011), however De Souza *et al.*, (2014) argued that it was unsuitable for autothermal reforming processes as the reaction did not progress at constant temperature. Instead, they used entropy maximisation with pressure and enthalpy constraints, which they noted was rarely used. The approach was found to have good agreement with experimental data, with kinetic factors identified as the main source of error.

2.7.4. Related Non-Equilibrium Approaches

Li *et al.* (2001) found that equilibrium models were unsuitable for predicting carbon conversion within a coal gasifier due to the reaction being controlled by non-equilibrium factors. Similarly, for a wood gasifier application Altafini, Wander and Barreto (2003) suggested that kinetic models are more accurate than equilibrium models at temperatures below 1000K, as the reaction rate is slower and the assumption of equilibrium causes errors. It was also mentioned that kinetic models were highly complex as they were tailored for specific reaction systems, while the Gibbs minimisation approach was more general and simpler to program.

Asgari, Hannani and Ebrahimi (2012) stated that chemical equilibrium models based on the minimisation of Gibbs free energy alone could not correctly predict the concentration of oxides of nitrogen (NO_x) formed in a

combustion reaction, as the process was dependent on chemical kinetics. In an attempt to compensate for this, they coupled Gibbs minimisation with kinetics, specifically the extended Zeldovich mechanism, however they were still unable to accurately predict NO_x in comparisons with experimental data. They reasoned that the errors were due to the selection of the kinetic data for the extended Zeldovich mechanism.

2.8. Appraisal

Many examples have been found of the successful application of both stoichiometric and non-stoichiometric approaches, and the methods and algorithms were well documented, thus both approaches are technically feasible. For non-stoichiometric models the minimisation of Gibbs free energy approach appeared to be significantly more prevalent than the maximisation of entropy, therefore there is a greater risk associated with following the entropy route, although both have been shown to be viable. The stoichiometric method may be simpler to implement, however it is apparently less versatile and requires equilibrium constant data (Rashidi, 1997), which may cause difficulties when facing more complex reactions.

Adding chemical kinetics to equilibrium models was generally considered to be an enhancement, as alone they were found to performed poorly when reactions occurred more slowly or were dominated by non-equilibrium factors (Li *et al.*, 2001; Altafini, Wander and Barreto, 2003), however chemical kinetics modelling was also reported to be highly complex. Li *et al.* (2001) demonstrated that the kinetic-coupling approach is feasible, though Asgari, Hannani and Ebrahimi (2012) were unable to successfully apply it to their NO_x modelling.

The CFD route was also shown to be technically feasible by Sathiah and Roelofs (2014), but required details of specific geometries. There were also several examples utilising existing chemical modelling software, such as Aspen, CHEMCAD, and CHEMKIN, which carried less technical risk and were presumably easier to implement as they were commercial packages. There were also several disadvantages associated with commercial software however, such as: financial cost, increased difficulty of disseminating models due to their dependence on the software, and reduced control over the computational methods.

The non-stoichiometric approaches appeared to be more suitable than the equilibrium constant approaches, as there was a risk that the equilibrium constant method would become unwieldy when faced with complex reaction mechanisms or when new species of interest were added to the model.

The Gibbs minimisation method was applied to a simple case study to determine its relative performance and complexity. It was also proposed to build a model that allowed different thermodynamic properties to be held constant, from which the most effective combination could be determined.

Chemical kinetics modelling was determined to be necessary for predicting NO_x formation, and it was intended to be added to the model once the equilibrium model was completed.

Commercial chemical modelling software may have been faster to implement, but one of the goals of the research was to transfer knowledge back to the industrial sponsor, and this goal would have been hindered if the model ran exclusively within a 3rd party software package. It was also important to understand precisely what computational methods were being used so that they could be accounted for when appraising the model. This would have been difficult with a commercial package without access to proprietary code. A custom program was written in C++ to model chemical reactions for the project. The use of CFD was also considered, however it was thought that the complexity of a CFD approach would have warranted its own research project.

2.9. Conclusions

Three methods of calculating chemical equilibrium were identified as suitable for use in the research project, the stoichiometric equilibrium constant approach, and the non-stoichiometric minimisation of Gibbs free energy and maximisation of entropy approaches.

The inflexibility of the stoichiometric method was considered to be a greater disadvantage than the complexity of the non-stoichiometric methods, thus a non-stoichiometric approach was adopted for the research.

The Gibbs free energy approach was explored due to its widespread success in a variety of fields. A chemical kinetics model was also planned for modelling NO_x generation.

Initially a bespoke program was written to model the chemical reactions for the project, primarily due to concerns over binding the model to a commercial package, which would have cause difficulties with dissemination. The open-source chemical reaction package Cantera was also investigated. These models are discussed in Chapter 3.

3. Theoretical Analysis

The purpose of the theoretical analysis was to model the thermal and chemical components of the boiler system. The analyses were used to estimate the outputs of the system to support the design of the experimental setup, and to examine the fundamental processes involved within the combustion process to aid in the understanding and processing of the data. Additionally, it was used to predict the performance of other systems outside the scope of the experimental work.

Contents

3.1. Thermal Analysis

The objectives of the thermal analysis were to aid the design of the experimental arrangement, process collected data, and predict the performance of other related combustion systems.

The thermal model was a collection of modules created for the design of the system. They estimated such things as heat transfer rates to the water from the boiler and from the water through the radiator, water flow rates for the boiler and injection processes, pipe pressure losses for various fluids, and air humidity. The modules were later combined to form a thermal model for the system, which estimated its performance and outputs.

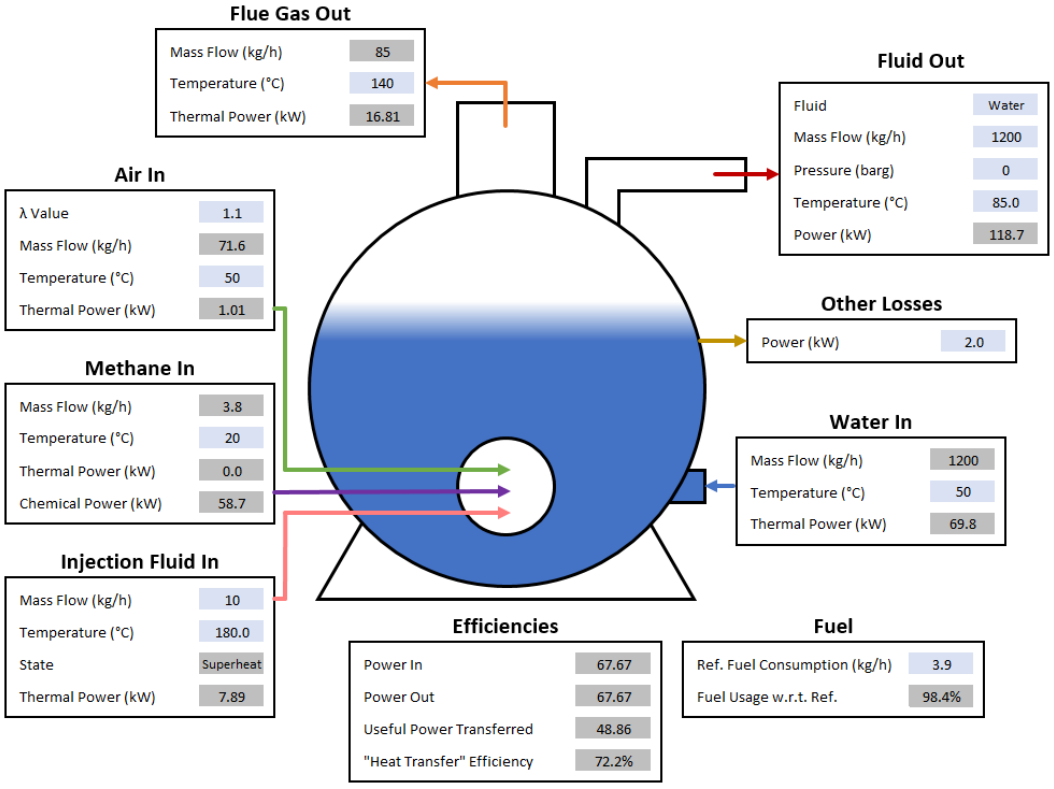

Figure 3-1 – Thermal model calculation diagram

The thermal model was also used to process test data, in which case the calculated output was compared with the actual output to validate the accuracy of the model. It was intended to use the validated model to predict the performance of other systems.

The model was built in Microsoft Excel with functions written in Visual Basic, as shown in Figure 3-1.

Other features of the model included the capability to add additional O_2 and H_2O to the input, change the exhaust and reactant temperatures, and estimate air flows, air-fuel ratios, exhaust flows, and exhaust composition. It also predicted the energy lost heating nitrogen (N_2) within the combustion air, the system operating costs based on fuel prices, and the savings that could be made by reducing excess O_2.

3.1.1. Setup

The thermal model was used to investigate the effects of λ value, flue gas temperature, and water/steam injection rate on the system's heat transfer efficiency and fuel usage. For the first study, the λ value was varied between 1.0 and 1.4. In the second study, the flue gas temperature was varied between 80°C and 200°C. The third study involved varying steam or water injection rates from 0g/min to 20g/min. Each study is based on a reference case where none of the flue gas heat was recovered. If heat was recovered in an economiser, then that would add to the useful heat output of the system and improve its efficiency.

The heat-transfer efficiency was defined as follows:

$$\eta_{heat-transfer} = \frac{\Delta P_{water}}{P_{input}}$$

Where:

$\eta_{heat-transfer}$	=	Heat transfer efficiency, the proportion of the power transferred to the heated fluid to the input power.
ΔP_{water}	=	Power transferred to the heated fluid between the inlet and outlet of the system.
P_{input}	=	Power in to the system.

$$\Delta P_{water} = P_{water,out} - P_{water,in}$$

Where:

$P_{water,out}$	=	Power of the heated water at the outlet of the system.
$P_{water,in}$	=	Power of the heated water at the inlet to the system.

$$P_{input} = P_{air,in} + P_{fuel,in} + P_{injection,in} + P_{combustion}$$

Where:

$P_{air,in}$	=	Thermal power of the air at the inlet to the system.
$P_{fuel,in}$	=	Thermal power of the fuel at the inlet to the system.
$P_{injection,in}$	=	Thermal power of the injection fluid at the inlet to the system.
$P_{combustion}$	=	Power released during complete combustion.

3.1.2. Results and Discussion

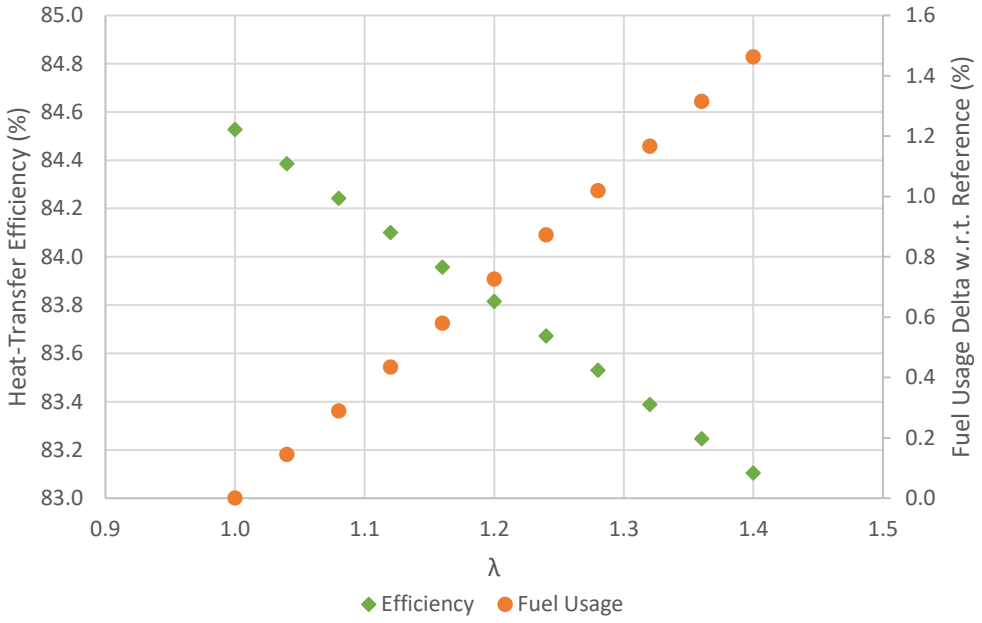

Figure 3-2 – Study 1: Efficiency, Fuel Usage vs λ

Figure 3-2 shows the result of the first study. In this case, as λ value increases from 1.0 to 1.4, the heat transfer efficiency decreases by 1.4%, from 84.5% to 83.1%. The model revealed that this was due to the energy lost through heating excess air from ambient to the flue gas temperature. The loss in efficiency coincides with an increase in fuel usage of 1.5% at a λ value of 1.4. This means that it is advantageous to operate closer to stoichiometric to optimise efficiency, though the chemical model showed that other factors must also be considered.

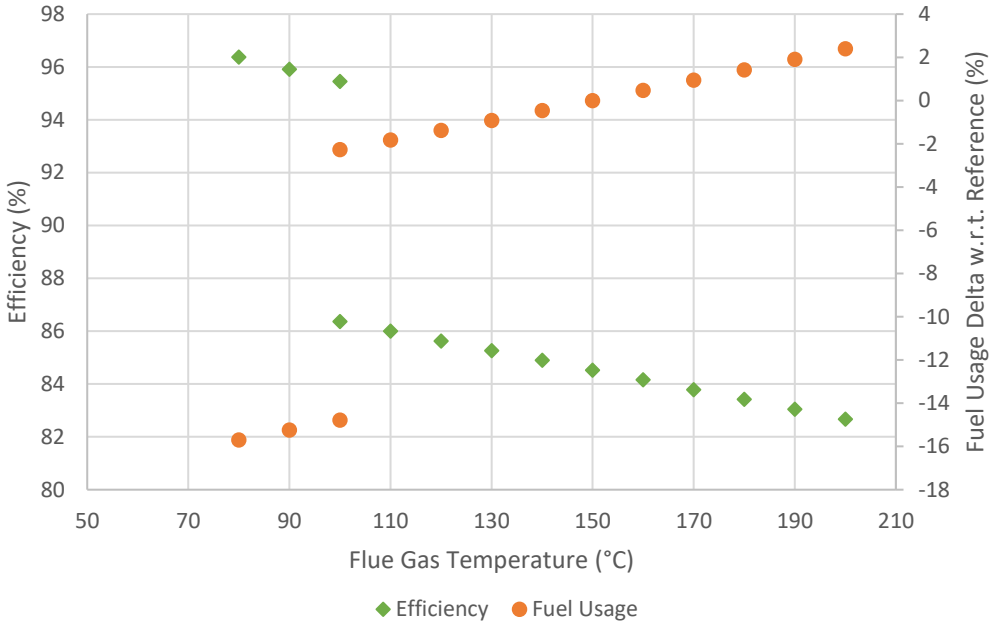

Figure 3-3 – Study 2: Efficiency, Fuel Usage vs Flue Gas Temp

Figure 3-3 highlights the significance of the flue gas temperature on the calculated heat transfer efficiency. It is shown that the efficiency decreases linearly by approximately 0.9% per 20°C temperature increase below 100°C, and 0.74% above. This linearity was due to the enthalpy changes in the system following a similar trend across the ranges of interest. The 9.1% decrease in efficiency at 100°C was due to the loss of the latent heat of the water from the combustion process, which in the theoretical system remained as steam above 100°C and was not recovered. This analysis demonstrated the significant energy savings available through utilising the exhaust gas, for example to preheat the boiler feed-water or combustion air, or even for other systems such as building heating.

The fuel usage follows an inverse trend to the efficiency, increasing linearly by approximately 0.9% per 20 °C temperature increase below 100 °C, and 0.94% above.

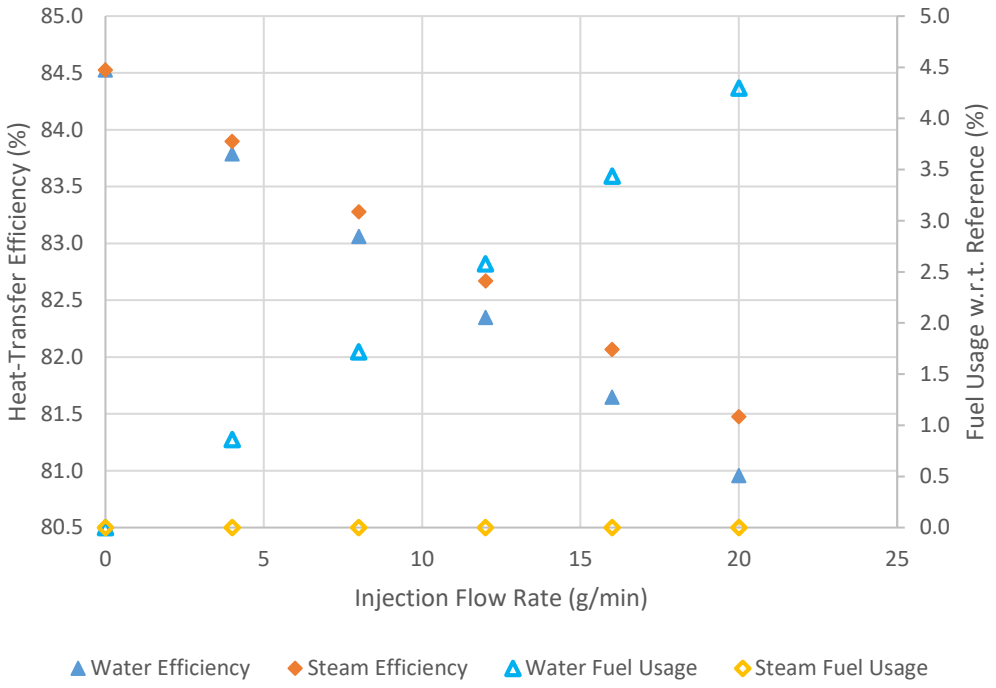

Figure 3-4 – Study 3: Efficiency, Fuel Usage vs Injection Rate

Figure 3-4 shows the effect of water or steam addition on the system's heat transfer efficiency and fuel usage. When water or steam was added, the heat transfer efficiency fell linearly across a range of 0g/min to 20g/min by 3.5% and 3.0% respectively. In both cases, the loss in heat transfer efficiency at 20g/min was greater than the gain in efficiency when reducing λ from 1.4 to 1.0, as shown in Figure 3-2. This indicates that high flow rates of water or steam addition could cause unwanted efficiency losses, and that some optimisation between λ value and injection is required. For study 3 the flue gas temperature was fixed, thus the effect of the fluid injection on the flue gas was not evaluated.

The fuel usage did not increase in the steam case as both the exhaust and the steam were set at 150°C and atmospheric pressure for the study. This means that although the fuel usage and heat transfer efficiency were approximately the direct inverse of one another in most of the studies, they would not be in most real systems. For example, if the injection steam was raised above the exhaust temperature then both the fuel usage and the heat transfer efficiency would decrease, as although the injected steam would supply extra heat to the boiler, requiring less fuel to be burnt, there would also be a higher amount of waste heat in the flue gas. This is particularly important when analysing the effect of combustion air pre-heating, as the model showed that if the flue gas temperature is held constant then the heat transfer efficiency does not increase with increasing air temperature, however fuel savings are still observed.

3.2. Chemical Analysis

The chemical analysis was key to understanding the combustion processes involved within the burner and predicting the emissions outputs of the system. Two models were applied, a custom-made literature-based model, which was used for the preliminary experiments, and an open-source model used for the main experiments.

3.2.1. Literature-based Model

The first model was used to model the combustion process, so that given a set of mass flows and ambient conditions, the heat release and flue gas species concentrations could be estimated. It was intended for it to be used to predict the performance of an industrial-scale steam boiler after being validated against the empirical results from the experimental boiler.

The model was written as a command-line based program, using the C++ programming language and Microsoft Visual Studio as the integrated development environment. The program's first function was to look up chemical properties including enthalpy, entropy, isobaric heat capacity, conductivity, thermal conductivity, using a temperature input. These were calculated from a set of polynomial coefficients listed by McBride, Gordon and Reno (1993).

The program's second function was to calculate adiabatic flame temperatures using the chemical properties from the first function and the method shown by Cengel and Boles (2015), which essentially consisted of determining the temperature that balances the following equation:

$$\sum N_p\left(\bar{h}_f^\circ + \bar{h} - \bar{h}^\circ\right)_p = \sum N_r\left(\bar{h}_f^\circ + \bar{h} - \bar{h}^\circ\right)_r$$

Where:

$\bar{h}$ = Specific enthalpy, kJ/kg

$\bar{h}^\circ$ = Specific enthalpy at 298K, 1atm, kJ/kg

$\bar{h}_f^\circ$ = Enthalpy of formation at 298K, 1atm, kJ/kmol fuel

N = Number of moles, kmol

$_p$ = Product

$_r$ = Reactant

A search algorithm was created that caused the product enthalpy to converge towards the reactant enthalpy by varying the temperature. The adiabatic flame temperature was the solution temperature.

The third and main function of the program was to determine the chemical equilibrium of a given set of species at a given temperature and pressure. The computational methods literature review found that the Gibbs minimisation method was the most suitable approach for the application. Several examples of the technique were found, including the Brinkley, NASA, and RAND variations, though the RAND approach detailed by Smith and Missen (1982) was used as the basis for the program. This involved solving the following set of non-linear equations for $\delta n_j^{(m)}$ and $\delta \psi_k^{(m)}$ until an acceptable element balance was reached:

$$-\frac{1}{RT}\sum_{j=1}^{N'}\left(\frac{\partial \mu_i}{\partial n_j}\right)_{\mathbf{n}^{(m)}} \delta n_j^{(m)} + \sum_{k=1}^{M} a_{ki}\delta\psi_k^{(m)} = \frac{\mu_i^{(m)}}{RT} - \sum_{k=1}^{M} a_{ki}\psi_k^{(m)}$$

$$\sum_{j=1}^{N'} a_{kj}\delta n_j^{(m)} = b_k - b_k^{(m)}$$

The values of $\delta n_j^{(m)}$ and $\delta \psi_k^{(m)}$ were then applied to the initial values to increment the iteration, with conditioning to ensure they did not cause negative molar quantities. When the element balance reached an acceptable residual error, the iterations ceased and the resultant molar quantities were identified. The intention was for the program to predict the composition of the flue gases from combustion with varying steam and water inputs, and for the results to then be validated with experimental data from the test rig.

3.2.2. Open-Source Model

The open-source software Cantera (Goodwin *et al.*, 2018) was used to validate the literature-based model and provide additional functionality. Mayur *et al.* (2019) described the software as a "simulation toolkit that provides interfaces for modelling complex chemical reaction systems", and as it includes thermodynamic, transport, and kinetic databases it can calculate chemical equilibrium, rates of reaction, and chemical properties (Acampora and Marra, 2015). Cantera was used by Langer *et al.* (2018) to create a model of an adiabatic reactor, which involved solving a set of ordinary differential equations for the species mass fractions and the temperature. It was found to agree "very well" with results from 3 other modelling packages. They also modelled a laminar, freely propagating, premixed flame, where the Chemkin laminar burning velocity results agreed with other open-source packages within 0.2 cm/s under most conditions, except for slightly rich mixtures, where Cantera reported velocities 0.45 cm/s lower.

One of the key limitations of Cantera was that although it could calculate the equilibrium of multi-phase or multi-component reactions, it could not solve reactions involving both. This meant that it was unable to accept liquid water as an input for a combustion reaction, thus it could not directly solve the water injection cases. As the equilibrium model was dimensionless, the principle difference between using liquid water and steam was the latent heat. It was therefore predicted that reducing the overall reactant enthalpy by the enthalpy of evaporation of water would result in a fair approximation of a liquid water reaction, as the equilibrium enthalpy of the products would be the same.

In the literature review some disagreement was found between whether the reduction in NO_x and CO was a chemical or a thermal effect. To investigate this, a set of Cantera simulations were performed with the adiabatic flame temperature (AFT) free to change as normal, and a second set were run where the AFT was fixed to match the 0 g/min case. This was intended to isolate the chemical effects from the thermal effects.

Four rates of steam injection were investigated for each of the "normal" and fixed AFT cases, ranging from 0g/min to 12g/min in line with the steam-to-fuel ratio used by Toqan *et al.* (1992).

The model parameters were set as shown in Table 3-1.

Table 3-1 – Theoretical study parameters

Study	Parameter 1	Parameter 2	Parameter 3	AFT
1	AFT	λ	Injection rate	Normal
2	CO	λ	Injection rate	Normal
3	CO	λ	Injection rate	Fixed
4	NO_x	λ	Injection rate	Normal
5	NO_x	λ	Injection rate	Fixed

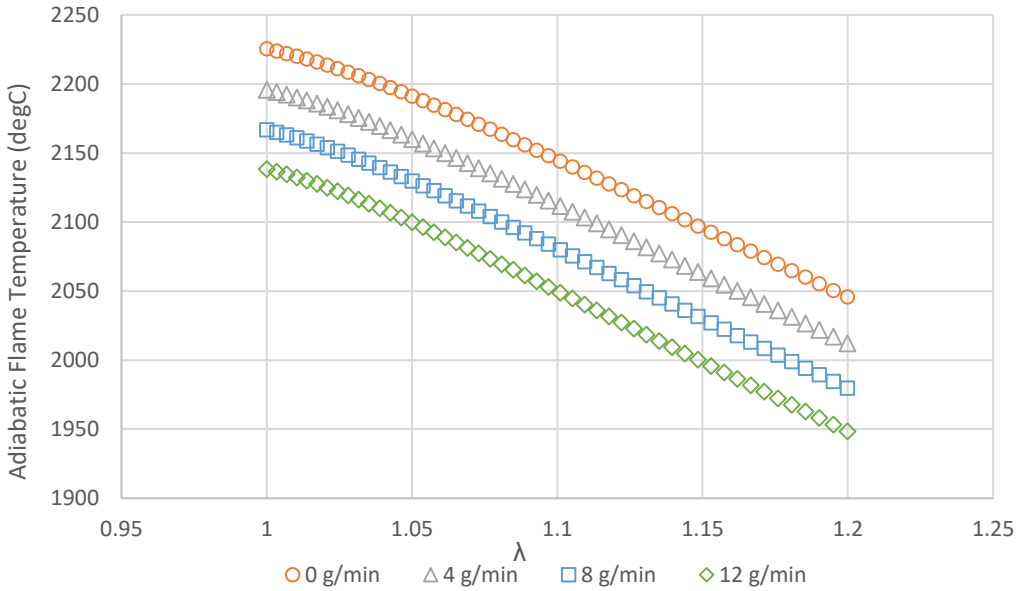

Figure 3-5 – Study 1 - Adiabatic flame temperature vs. λ value at various water injection rates

Figure 3-5 shows that steam injection reduced the adiabatic flame temperature by approximately 31°C, or 1.5%, with 4 g/min, and that the effect increased linearly with increasing steam flow rate. This was also consistent across the range of λ ratios simulated. A reduction was expected as steam injection results in the thermal dilution of the combustion gases, due the same enthalpy of combustion heating a greater mass.

Figure 3-6 shows that CO reduced with increasing steam flow, although the additional reduction appears to be diminishing. This is shown more clearly by Figure 3-7, where at λ = 1.2, 4 g/min of steam reduced CO by 24.5%, however 8 g/min of steam reduced CO by 42.9%, a disproportionately lower reduction. Additionally, the reduction in CO was dependent upon λ, where it decreases from 24.5% to 14.4% from λ = 1.2 to λ = 1.0 for the 4 g/min steam case. From Figure 3-6 it can also be seen in that CO increased as λ decreased, which is expected due to reducing oxygen availability, and is widely known trend. This means that the model was producing feasible results.

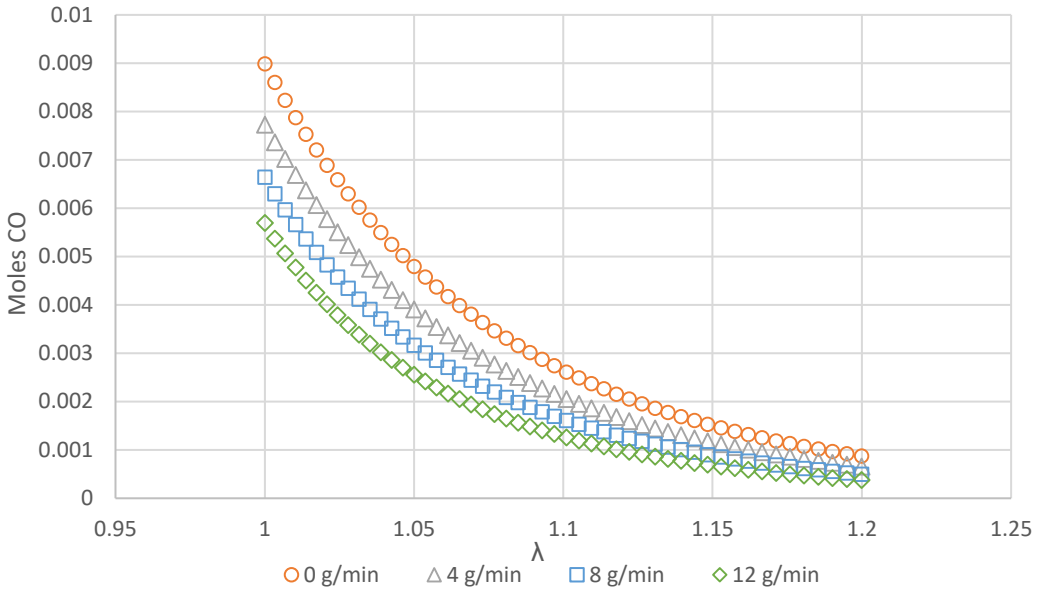

Figure 3-6 – Study 2 - Moles CO produced per mole of reactant CH4 vs. λ at various steam injection rates, AFT free to change

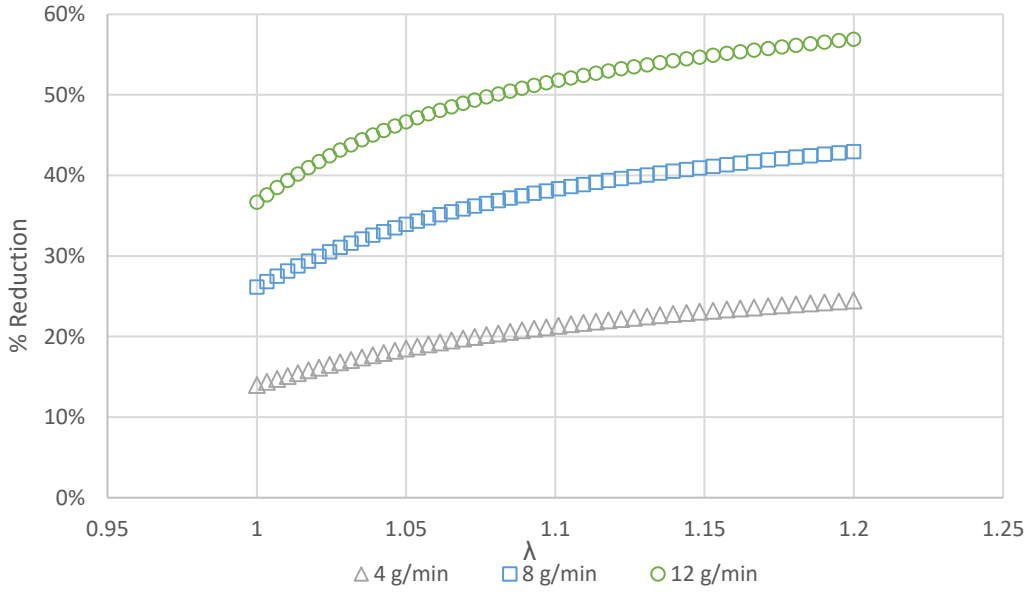

Figure 3-7 – Study 2 - As Figure 3-6 with CO as a % of the 0 g/min case for clarity

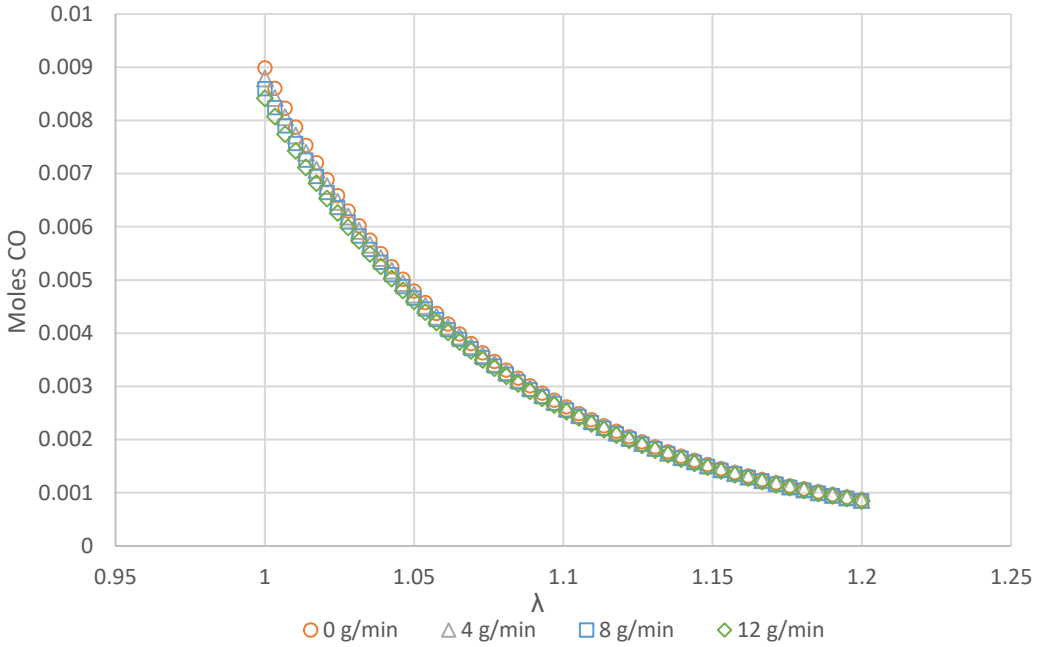

Figure 3-8 – Study 3 - Moles CO per mole produced of reactant CH_4 vs. λ at various steam injection rates, AFT adjusted to match 0ml case

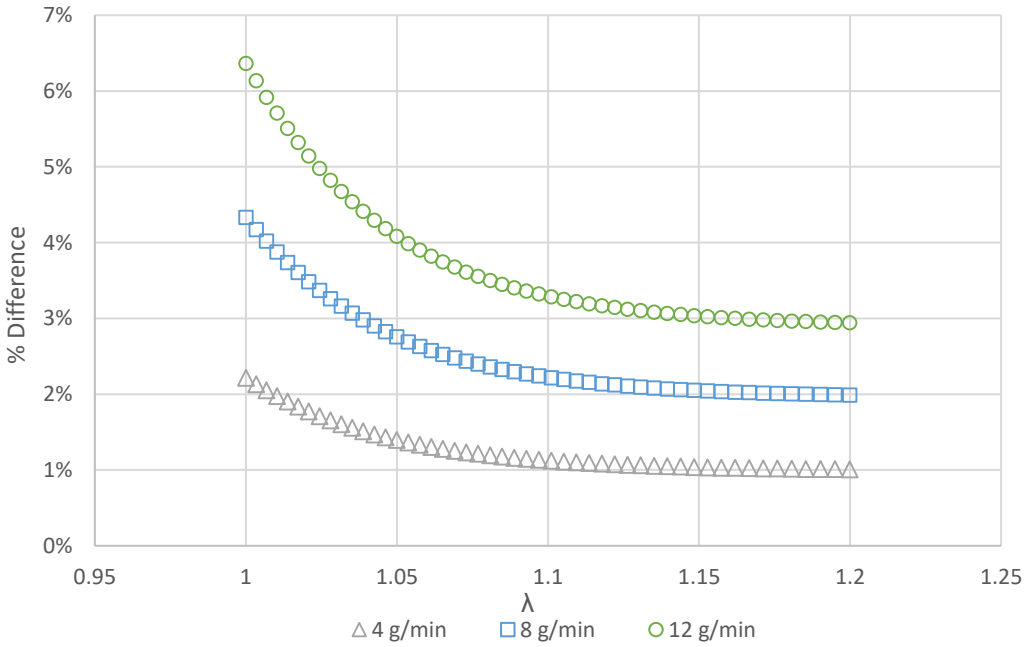

Figure 3-9 – Study 3 - As Figure 3-8 with CO as a % of the 0 g/min case for clarity

Comparing Figure 3-8 with Figure 3-6 shows that when the enthalpies of the reactants in the steam injection cases were matched to the “dry” case, the reduction in CO due to the steam was significantly reduced. Comparing Figure 3-9 with Figure 3-7 shows that the reduction in CO fell from 56.9% to 2.9% in the worst case when λ = 1.2, and from 14.4% to 2.1% in the best case, where λ = 1.2. This implies that the cooling effect of the steam on the reaction was more significant than its chemical effects, though the chemical effect is by no means insignificant.

In Figure 3-10 it can be seen that increasing steam injection rates caused a decrease in NO_x, and that the decrease in NO_x increased at higher λ values where more NO_x was present.

Figure 3-11 shows that, as a percentage compared with the 0ml case, the greatest NO_x reduction was achieved at a λ value of 1.0. It also shows that the reduction in NO_x with steam flow rate was not linear. For example, at λ = 1, the difference between the 0 g/min and 4 g/min cases was 12.2%, whilst the difference between the 8 g/min and 12 g/min cases was 9.5%.

Figure 3-12 shows that when the cooling effect of the steam on the AFT was negated, there was still a reduction in NO_x with steam injection, but to a lesser extent than for the cases shown in Figure 3-10.

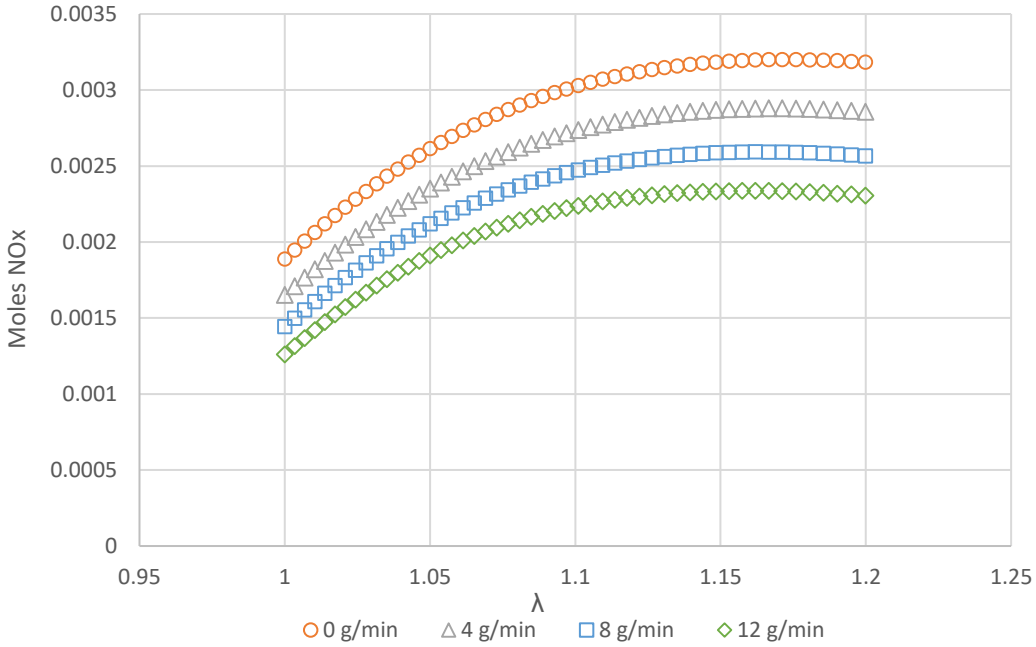

Figure 3-10 – Study 4 - Moles NO_x produced vs. λ at various steam injection rates, AFT normal

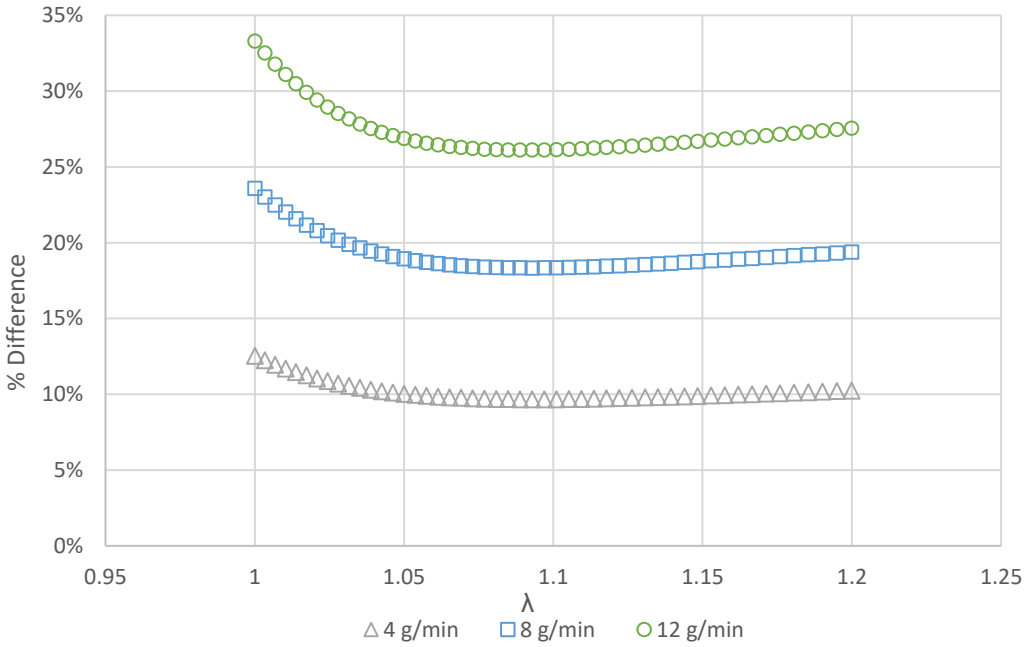

Figure 3-11 – Study 4 - As Figure 3-10 with NO_x as a % of the 0 g/min case for clarity, AFT normal

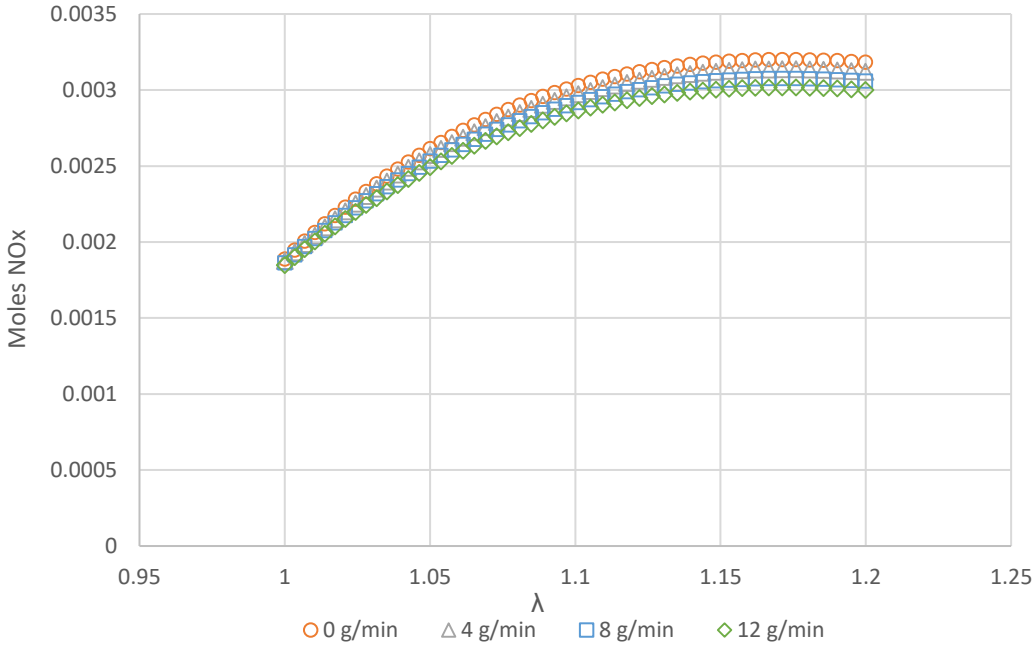

Figure 3-12 – Study 5 - Moles NO_x produced vs. λ at various steam injection rates, AFT fixed

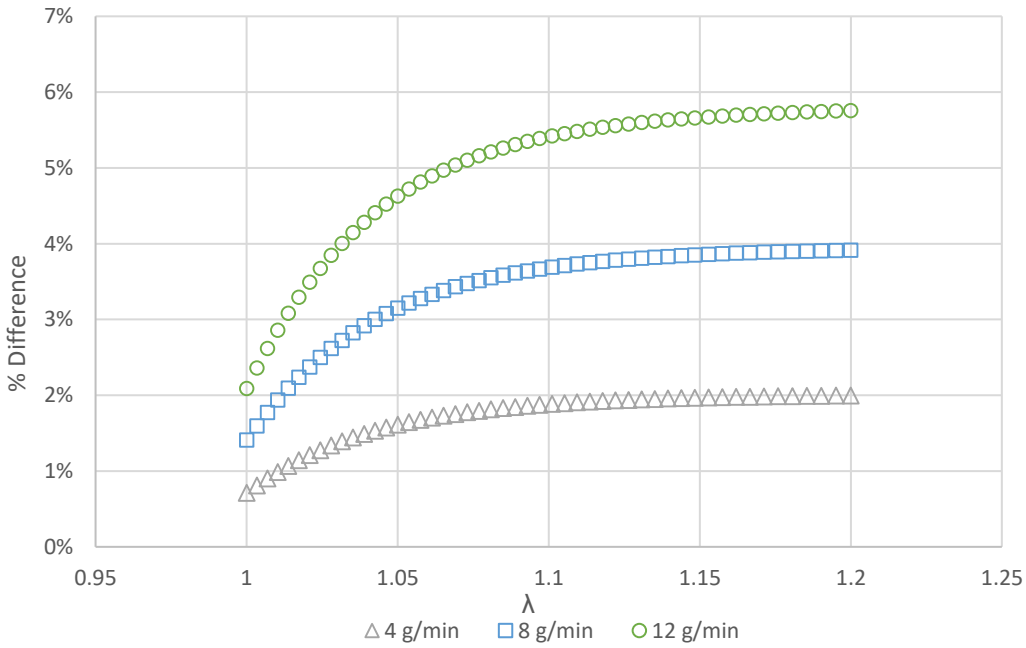

Figure 3-13 – Study 5 - As Figure 3-12 with NO_x as a % of the 0 g/min case for clarity, AFT fixed

Figure 3-13 shows that the maximum reduction in NO_x for the fixed AFT was 5.8% at a λ value of 1.2, whereas the maximum in the AFT free case, shown in Figure 3-11, was 32.5% at a λ value of 1.0. This means that the main cause for the reduction in NO_x in the AFT free case was the cooling effect of the steam rather than its chemical effect. It can also be seen that the chemical effect is greatest at higher λ values, for example in the 0.63ml/min case the reduction increases from 2.1% at λ = 1 to 5.8% at λ = 1.2. As with the "AFT free to change" cases, the reduction in NO_x was greatest between the 0ml/min and 0.21ml/min cases, and decreased between subsequent cases, though the difference was less significant. For example, at λ = 1.2, the change from 0ml/min to 0.21ml/min resulted in a 9.2% decrease in NOx, however the change from 0.42ml/min to 0.63ml/min resulted in only an 8.1% decrease.

The theoretical reductions in CO and NO_x were achieved under equilibrium conditions, however in reality the combustion process is limited by chemical kinetics. This means that the residence times of the various species within the actual flame affects the creation of products, thus the theoretical results only provided an indication of what to expect from the experiments. Similarly, the model did not account for the geometry of the burner, which is known to have a significant impact on the formation of pollutants (Toqan *et al.*, 1992). Investigating the design parameters of the burner would have required a full CFD model which was beyond the scope of the retrofit research.

3.3. Chapter Summary

This chapter has examined the thermal and chemical analyses undertaken in support of the experimental work. The thermal analysis was used to design the experimental arrangement, detailed in Chapter 4, and to model the performance of a range of boilers. The chemical analysis provided insight into the fundamental processes through which steam injection affected the combustion process. In the simulations steam injection reduced the quantity of both NO_x and CO in the products, primarily due to it reducing the AFT with a relatively minor chemical contribution.

Chapter 4 will detail the design of the experimental arrangement that explored whether the theoretical results could be replicated in actuality.

4. Experimental Arrangement

4.1. Introduction

The literature review identified that water and steam injection into the burner of a boiler was a viable technique for reducing combustion emissions. It was hypothesised that NO_x and CO emissions could be reduced simultaneously, potentially resulting in an indirect increase in combustion efficiency by enabling low-excess O_2 operation, which would normally be unsuitable due to excessive emissions.

The purpose of this chapter is to present the rationale behind the choice of experimental approach used in the research, and then examine the design of the various sections of the experimental setup in detail.

The majority of the setup was common between all aspects of the research, with alterations and modifications for individual experiments described in the relevant chapters.

Contents

4.2. Choice of Approach

The first stage of the experimental design involved choosing an approach which enabled the collection of data that could be used to calculate the overall efficiency of the system and the CO, HC, O_2, carbon dioxide (CO_2), and NO_x content of the exhaust gases. The literature review found that there were two main options: build an experimental rig centred on the modification of an existing product, or design a new system. Due to the industrial sponsor's interest in the boiler retrofit market, and the lack of literature in the area, it was decided that the modification route was most appropriate. This was due to it balancing the needs of the industrial sponsor and the requirement for the research to be novel. It was also predicted that developing a retrofit system would accelerate the development of the research into a commercial product.

Modifying a full-scale industrial steam boiler would have been ideal, however that route faced many challenges, such as the prohibitively high capital cost of a full-scale boiler, significant fuel costs, the requirement to adhere to steam boiler regulations, space practicalities, and water supply requirements. It was decided that a smaller, 20 kilowatt-scale steam boiler would be used to overcome these issues, however finding a commercial steam boiler of that size proved problematic, therefore a water heater ("boiler"), was used instead. This was considered a reliable representation of a larger steam-raising system as both systems shared common combustion principles.

4.3. Design of Experimental Arrangement

Having determined the scale of the test setup, a schematic showing its general principle was produced, displayed in Figure 4-1. This shows that the principle components of the rig: the boiler, burner, circulation pump, and heat sink.

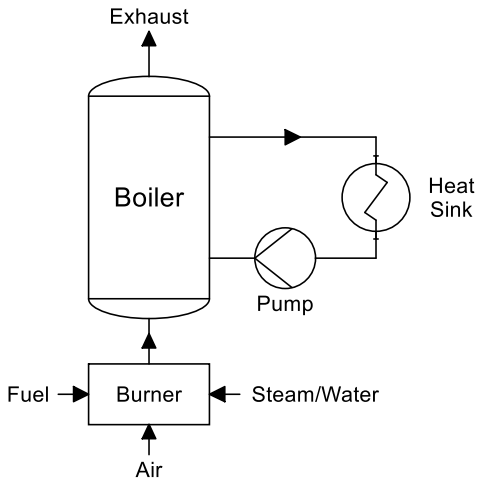

Figure 4-1 – Simple boiler system with steam/water injection

The main component in the system design was the boiler, as it determined which burner could be mounted and subsequently how much heat would need to be dissipated by the heat sink. In order to design an experimental system that was representative of a larger system, it was considered important that the standard three-pass fire tube layout was maintained for the experimental system, which significantly reduced the available options and eased the selection process. This layout can be seen in Figure 4-2, where the methane-air combustion gases cross the length of the boiler three times before exiting. The water to be heated enters the boiler at its base, surrounds the tube, and exits at the top. An injection point for external steam or water injection test can also be seen, which will be discussed in the relevant chapters.

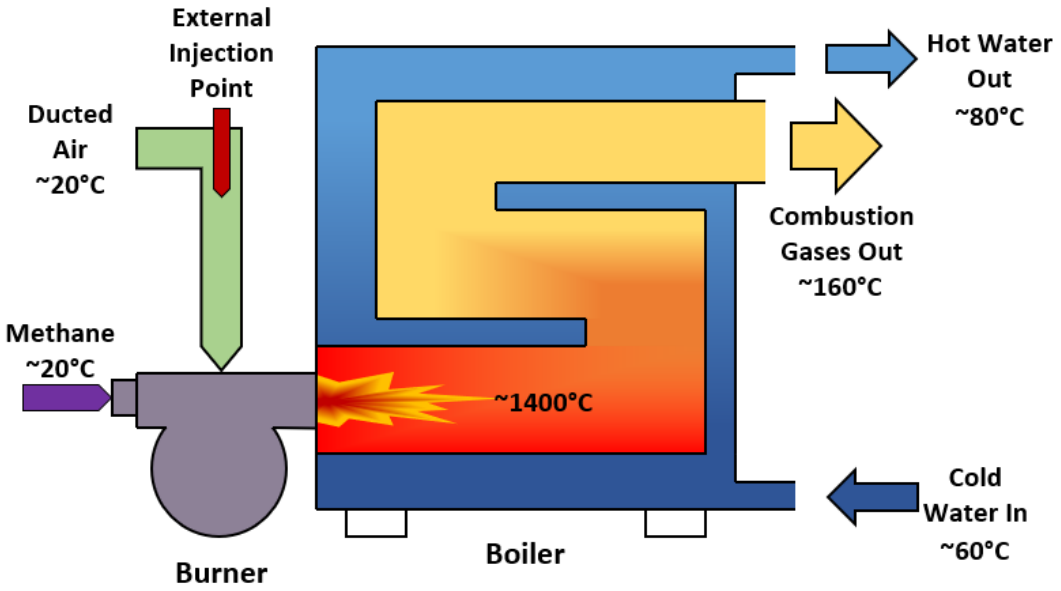

Figure 4-2 - Diagram of system arrangement

Sourcing a burner was straightforward as a number were recommended for the selected boiler, though both oil and gas options were available. It was known that gas burners were more common than oil, therefore a gas burner was selected as it was believed representative the largest portion of the burner market. The lowest output rating of 14.5kW was selected to minimise the heat dissipation and fuel requirements, which decreased the cost and footprint of the setup. A heat sink and pump were then chosen to match the heating load using the theoretical model as a guide.

Figure 4-3 illustrates the internals of the selected burner. Methane and air coaxially but separately enter the nozzle section with the methane at the core. Approximately 10mm before the swirl diffuser part of the fuel flow exits the core and is entrained into the air. The swirl diffuser promotes mixing of the air and methane and stabilises the flame, and remainder of the fuel flow exits radially approximately 5mm after the swirl diffuser. The internal injection point for steam or water is also displayed.

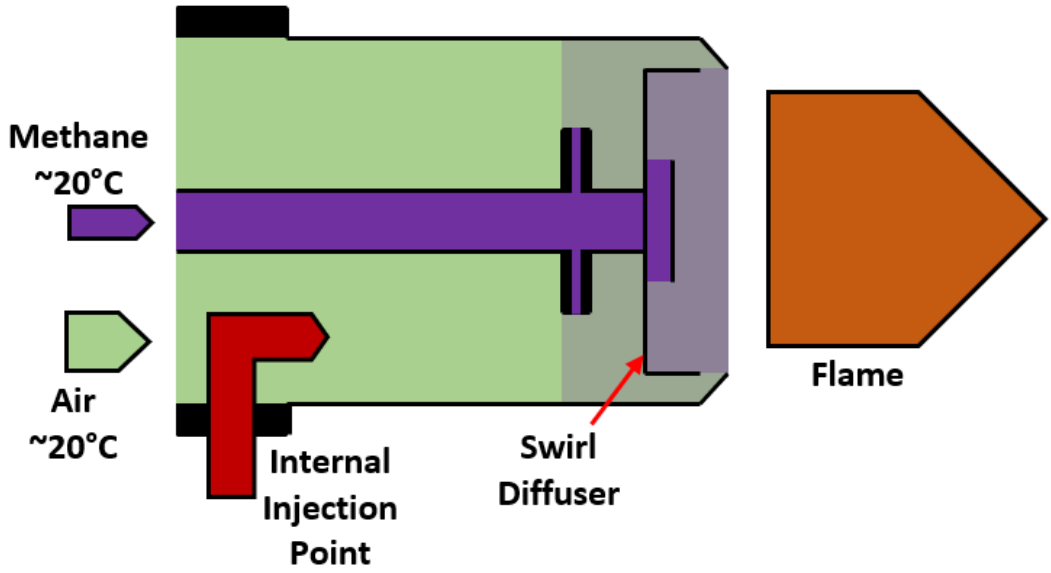

Figure 4-3 - Diagram of burner internals

The intended location of the experiment also influenced its design as it determined what space and utilities were available. It was originally planned to be housed at Loughborough University and to be small enough to be moved to the industrial sponsor if required. It was therefore designed as a self-contained unit with an independent steam supply, and was mounted on a mobile platform.

The remainder of the test setup, shown in Figure 4-4, was designed around the main components, and can be broken down into six sub-sections:

1. Fuel supply line
2. Air supply line
3. Water supply line
4. Boiler water circuit
5. Flue gas
6. Electrical and Electronics

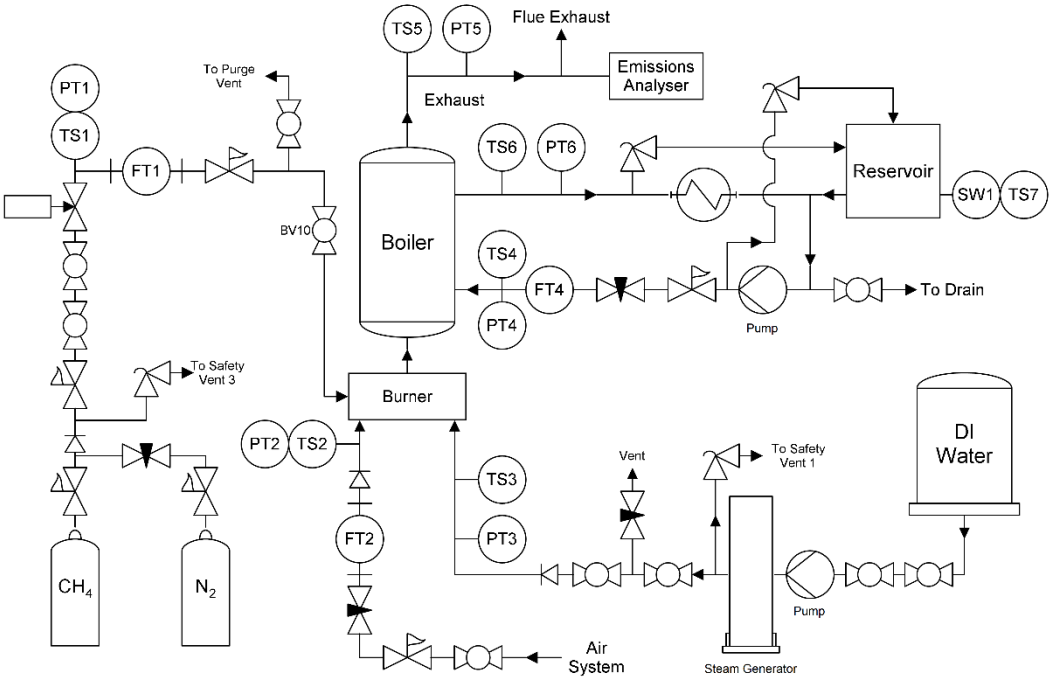

Figure 4-4 - Schematic of experimental setup for steam injection, where:

TS = Temperature sensor, PT = Pressure transmitter, FT = Flow transmitter, SW = Switch

4.3.1. Fuel Supply Line

Although the test rig was designed to emulate a natural gas boiler, Borman and Ragland (1998) showed that the composition of natural gas is not fixed, and it was predicted that the variations in composition would cause errors in the data and subsequently analysis. The use of gas chromatography to determine the precise composition of the gas supply was considered, however it was determined to be too costly.

Borman and Ragland (1998) also indicated that natural gas was 80-95% composed of methane, which was available in controlled purity levels, therefore it was decided that methane was a suitable substitute for the experiments. This required the use of cylinders rather than connecting to the gas main. The cylinders were costlier than natural gas per unit of fuel and required regulators to lower the gas pressure, but this was calculated

to be less than the cost of connecting to the natural gas supply and using gas chromatography.

The fuel line was designed to supply the 14.5kW burner. By calculating the enthalpies of the reactants and products it was found that the heat released during combustion was approximately 55500 kJ/kg, which resulted in a required fuel flow of 0.94kg/h. Investigations found that the largest cylinder able to be handled carried 8.1kg (50 litres) of methane, allowing for approximately 8 hours of experimentation. To reduce down-time 6 bottles were ordered at a time. The material safety data sheet (MSDS) for the methane stated that equipment should be purged of air before flowing methane to avoid creating potentially explosive atmospheres (BOC, 2015). A similarly-sized bottle of oxygen-free nitrogen was therefore chosen as a purge gas.

As the bottles were pressurised to 200 bar, and the burner required 25 mbar, a pressure regulation system was required. Due to stability concerns around using a single regulator, a three-stage system was designed. This included a BOC C202/2 special gas regulator to reduce from 200 to 4 bar, a BOC HP1900 regulator to reduce from 4 bar to 200mbar, and lastly a Fiorentini F30051 governor for the final reduction from 200mbar to 25mbar. The pipework size was then calculated using a pressure-drop approach.

The fuel line also required temperature, pressure, and mass flow measuring. A T-type thermocouple was chosen to measure the temperature due to its simplicity and relatively good accuracy of ±0.5°C. A PXM539-350IS transmitter was chosen to measure pressure as it was methane-compatible and featured an accuracy of 0.08% of full-scale. Lastly, a Nixon SC250 15100 variable area meter was selected to measure volume flow as

it offered a suitable accuracy of 1.6% of full-scale and a 4-20mA output, whilst being more cost-effective than a vortex or differential pressure meter.

4.3.2. Air Supply Line

The air was supplied from a 7 bar compressed air system. It was reduced to near-atmospheric pressure using a regulator and, for the preliminary tests, metered using a Nixon SC250 25160 volume flow meter, before entering the burner through a ducting adaptor. A rotameter was chosen due to its reasonable balance of cost and accuracy (1.6% of full-scale). The meter chosen also featured a 4-20mA output which could be read by the data acquisition system (DAQ).

As the flow meter was calibrated for 1.013 bara and 20°C any deviations of the air from the calibration values caused inaccuracies. To overcome this the pressure and temperature were measured using a Spirax EL2600 transmitter and a generic T-type thermocouple, which were then used to compensate for deviations by converting the output of the flowmeter to the equivalent volume of air at calibration conditions. The temperature and pressure were also used in determining the density and enthalpy of the fluid for the analysis.

As the research centred around adding various forms of water into the combustion process it was necessary to determine whether humidity in the combustion air would adversely affect the experiments. An investigation into the compressed air supply line was conducted, and it was found that there were filter-separators after the main air compressors to remove water, in addition to a filter-regulator on the supply to the experimentation area. An additional filter-regulator was installed inside the rig for greater control. It

was assumed that the three stages of filtration would remove any coalesced water in the air supply.

The error added to the water injection rates due to water vapour in the air was also calculated. For a typical test condition with a 15°C air supply, and assuming a worst case of 100% relative humidity, it was found that up to 4.8ml/min of water could be added to the combustion process. At the minimum injection flow rate of 4ml/min this resulted in an error of 120%. To overcome this issue, a dew-point sensor was installed so that a true reading of water vapour content could be included in the injection flow rate calculations. A coalescing filter was also installed to further reduce the humidity and ensure the integrity of the experiments.

4.3.3. Water/Steam Supply Line

The water supply for the injection system was fed from a tank of deionised water, through pipework that consisted of either galvanised or stainless steel. This was to ensure that the system was free of particulates and dissolved solids that may have been present had mains water or carbon steel pipe been used, which could have deposited inside the boiler or nozzles.

A Watson-Marlow Qdos60 peristaltic pump was used to both pump the water and measure its volume flow rate. It was also capable of being remotely controlled via a 4-20mA signal. A pulsation damper was installed near its outlet, as commissioning tests had found that it generated significant pressure oscillations.

4.3.4. Boiler circuit

The boiler water circuit featured a header tank that fed into a centrifugal pump, and the flow was regulated using a combination of pressure reducing and globe valves. The flow rate was measured using a Nixon NT11 turbine volume flow meter with an accuracy of 0.5% of reading. The pressure and temperature were measured at the entry and exit points to the boiler, the pressure with Spirax EL2600 pressure transmitters accurate to 0.5% of span, and the temperatures with class 1/10 4-wire platinum resistance thermometers (PRT) accurate to 0.1°C at 80°C. The water was passed through a fan-cooled radiator to reject heat to the atmosphere before it returned to the pump.

As the rig was outside considerations had to be made for environmental extremes, as radiators have been known to rupture due to ice formation. As a safeguard a mono-propylene glycol heat transfer fluid, Thermatrans Plus RP, was added to the boiler circuit. This altered the overall specific heat capacity of the heated fluid, however data obtained from the manufacturer was used to compensate for the difference, which proved to be minor.

4.3.5. Flue gas

The pressure and temperature of the flue gas were monitored with a Spirax EL2600 pressure transmitter and a T-type thermocouple respectively. A Testo 350 flue gas analyser was used to determine the composition of the flue gas, and was equipped with CO, HC, O_2, and NO sensors. The CO and NO sensors operated using the principle of ion selective potentiometry, whilst the HC and O_2 sensors were catalytic (heated bead) and Zirconia based, respectively (Testo Ltd., 2019).

The analyser was also able to derive CO_2 from the O_2 measurement and featured built-in sample cooling and condensate draining which ensured the quality of the sample.

4.3.6. Electronics and Software

A data capture system was designed to record the 10 4-20mA transmitter outputs and 13 thermocouple outputs, which featured a measurement computing USB-2416-4AO multi-function DAQ at its core. This allowed most of the sensors to be read by a single device, at 30 samples per second per channel. The DAQ output function also allowed external devices such as the peristaltic pump to be controlled.

The PRTs were connected directly to a Pico Technology PT-104 data logger, which featured improved accuracy compared to the thermocouples connected to the main DAQ. The PT-104 was measured through the PicoLog software.

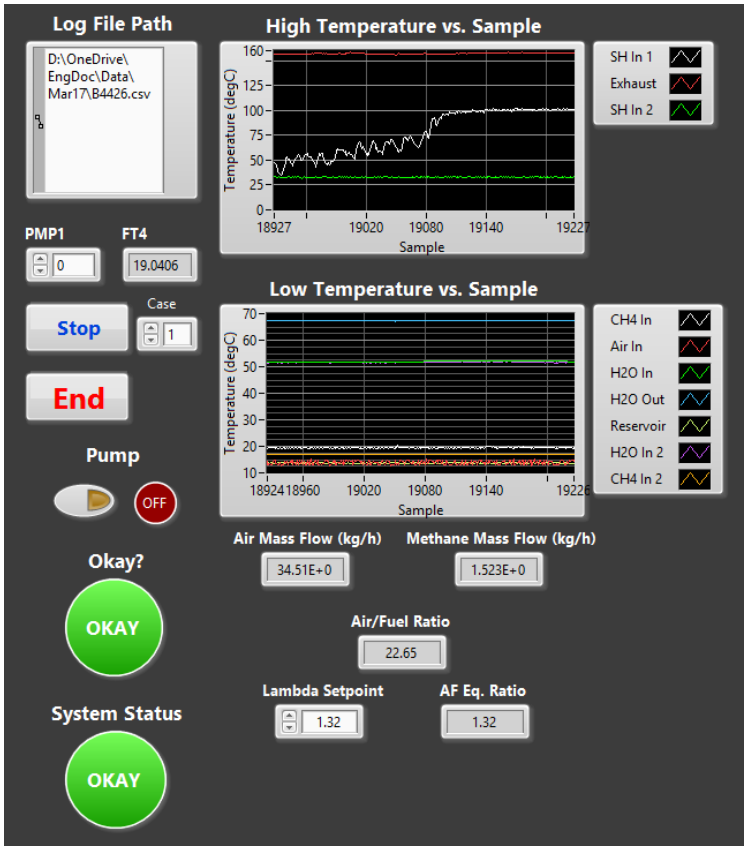

Figure 4-5 - LabVIEW program written for data capture

A LabVIEW program, shown partly in Figure 4-5, was written to interface with the main DAQ, monitor devices, collect data, and create log files. It was also programmed to capture data from PicoLog using dynamic data exchange.

A separate program, “easyEmission”, was used to collect and log data from the emissions analyser as it was designed specifically for the device. The manufacturer of the analyser offered limited LabVIEW support, and while some basic functionality was achieved with the supplied software components, it could not match the proprietary software which also provided diagnostic features.

4.3.7. Safety

A “what-if” risk assessment was conducted to identify operating risks. Several of these risks were associated with using the methane and nitrogen gas cylinders, as both presented explosion and asphyxiation risks and methane is highly flammable. Safeguards were incorporated to address this, including a safety relief valve vented to a safe location, continuous monitoring for methane in the atmosphere, and a flame arrestor to prevent flame travel through the fuel line. The methane sensor was wired to a relay panel which cut all power to the rig if the methane concentration in the experimental area reached 10% of the lower explosive limit. The burner also featured several built-in safety features such as flame detection and fuel shut-off solenoid valves.

The boiler was equipped with over-temperature protection to prevent the heated water from boiling. Also, each temperature and pressure sensor across the rig was monitored by the LabVIEW program. Under normal operation, the program sent out a 5V “okay” signal to a controller in the main rig panel. If one of the sensors reported an unexpected value, an error state would occur and the signal would be lost, triggering a relay in the controller to immediately shut-down the burner and steam generator. The circulation pump would then shut-down after a delay to ensure residual heat in the system did not boil the water. This process is illustrated in Figure 4-6.

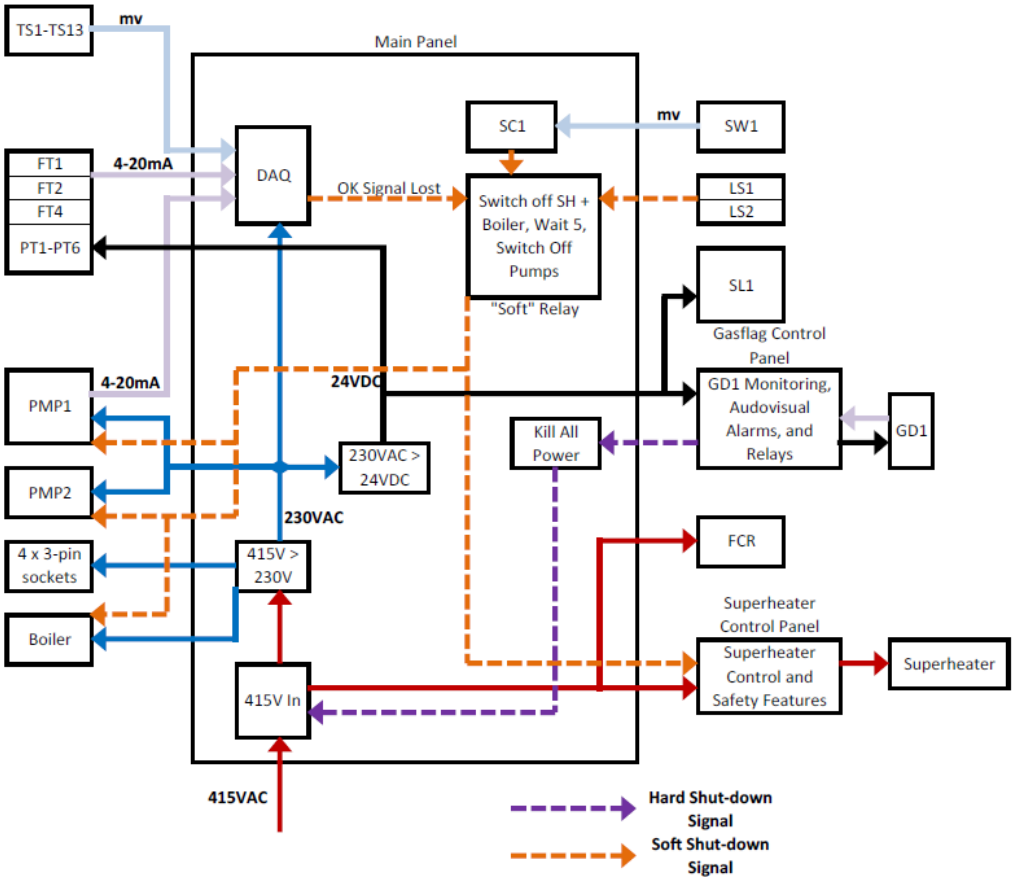

Figure 4-6 - Electrical function diagram

Other risk mitigations included writing a standard operating procedure, an inert gas purging process, reservoir level monitoring, steam and water safety valves, residual current devices, and check valves.

4.4. Experimental Build

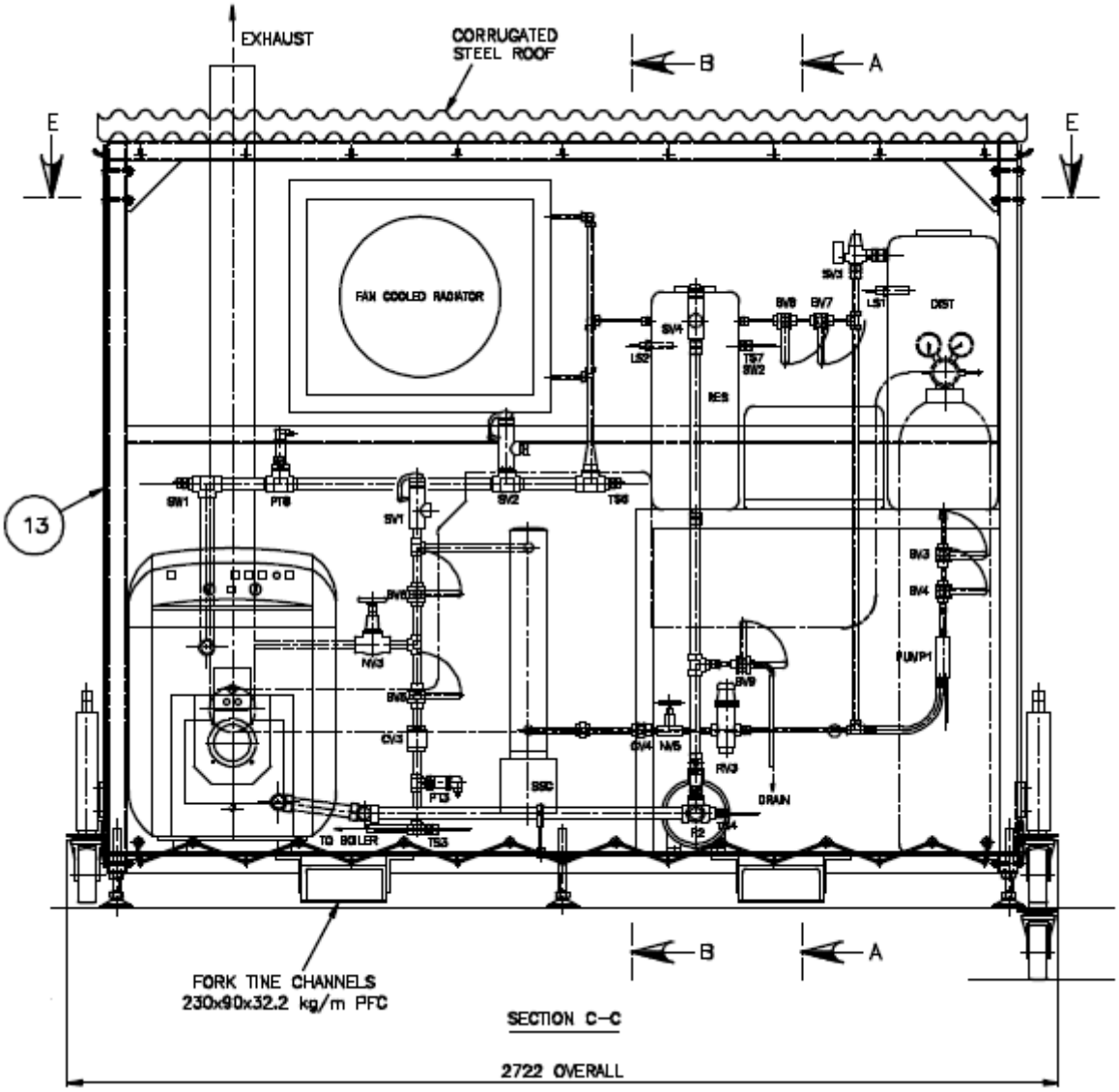

Figure 4-7 – Drawing of the front view of the test rig

After the experimental design was finalised the test rig build was organised. Ordering the selected components was relatively simple however a location for the rig had to be found, and a frame for the components needed to be fabricated. The original intention was for the rig to be small enough to be portable, however it quickly became apparent that the size of the rig would be substantial, and therefore more suited to a static location in the industrial sponsor's long-term experimentation area.

Figure 4-8 - The completed test rig

The experimentation area was located outside which simplified routing of the boiler flue, but required the rig to be weatherproofed. To expedite the build of the rig enclosure a draughtsman was commissioned who provided engineering drawings based on the established requirements, shown in Figure 4-7. This resulted in a roofed frame on a platform, which could be moved with jacking castors. Side curtains provided protection and could be pulled aside to allow entry and ventilation. Once the enclosure drawings were approved they were sent to an external company to be fabricated. Contractors were then arranged to build the control panel based on the diagram in Figure 4-6, and to fabricate and commission the gas and boiler pipework.

During the test rig assembly some modifications were made to the original design. The warm water rejected from the radiator was intended to be passed back into the reservoir as part of a closed loop system, but due to pressurisation concerns it was decided to use the reservoir as a vented header tank instead. This however meant that the radiator had to be relocated beneath the tank. The gas pipework also had to be changed to a larger size, as during commissioning the initial fuel demand caused a pressure drop which triggered the burner's safety shutdown. The finalised build can be seen in Figure 4-8.

4.4.1. Thermal Sizing

The burner heat output was stated in its documentation however the mass and volume flows of methane were required to calculate pipe sizes and estimate emissions. These were determined by calculating the enthalpy of combustion of the methane/air mix, which was then used to calculate the flow rates that would achieve the power output. The enthalpy values were calculated using the coefficients from NASA Technical Memorandum 4513 and the method outlined by Cengel and Boles (2015).

The water flow rates in the heating loop were calculated based on the boiler inlet and outlet temperature requirements. Flow rates and power requirements for water and steam injection were also evaluated. Steam properties were obtained from the program REFPROP, which incorporated NIST Standard Reference Database 23 (Lemmon *et al.*, 2018).

4.5. Chapter Summary

This chapter has explored the rationale behind the experimental setup chosen for the research, highlighted potential sources of error, and declared any assumptions used. It also detailed the design of each section of the test rig and its data collection capability.

It was shown that the test platform centres around a commercial-scale water heater with a jet burner, which was modified for water or steam injection. An emissions analyser was used for measuring the flue gas composition, and a combination of pressure, temperature, and volume flow meters were used to calculate the enthalpies of the fluid streams.

The methodologies and modifications for individual experiments will be detailed in the relevant chapters.

Chapter 5 describes the preliminary experiments conducted to validate the experimental arrangement.

5 Preliminary Experiments

This chapter details the experiments conducted at the start of the research. The main objectives of these experiments were to determine the capability of the experimental setup and to validate its output against literature and modelling predictions. This involved conducting a series of tests on the boiler whilst varying the excess oxygen content in the exhaust flow and determining their effects on the efficiency and emissions of the system.

A number of preliminary tests were also conducted for water and steam addition, which revealed that some improvements were required to the experimental setup before the main experimentation.

Contents

5.1. Methodology

5.1.1. Test Setup

To vary the excess oxygen in the flue gas it was necessary to adjust either the air or fuel mass flow, whilst keeping the other constant. It was decided to keep the fuel flow constant, as doing so maintained a constant chemical energy input into the system. The air flow was adjusted manually using an air regulator.

A start-up sequence was followed in order to ensure the accuracy and repeatability of the results. This involved initialising the data acquisition equipment and emissions analyser sampling 30 minutes before starting the rig, which allowed time for the devices to stabilise as recommended by the manufacturers. The main system was then turned on and given 30 minutes to achieve thermal equilibrium, as heating the system's thermal mass significantly reduced its heat transfer efficiency.

5.1.2. Analysis of Results

The properties of interest included the efficiencies of the system and the quantities of NO_x, CO, and O_2 in the flue gas.

For the preliminary experiments, three efficiencies were defined.

Firstly, the “Overall Efficiency” was defined as the ratio of power into the system to useful power out:

$$\eta_{overall} = \frac{\dot{Q}_{in}}{\dot{Q}_{useful}} \times 100$$

Power in was defined as the power available from the fuel in addition to the power required to raise the steam, ignoring inefficiencies:

$$\dot{Q}_{in} = \dot{Q}_{fuel} + \dot{Q}_{steam}$$

Power released by the fuel:

$$\dot{Q}_{fuel} = \dot{m}_{CH_4} \times HHV_{CH_4}$$

Power required to raise the steam:

$$\dot{Q}_{steam} = \dot{m}_{steam} \times \left(h_{steam,T_{in}} - h_{water,T_{reservoir}}\right)$$

The rate of useful output was defined as the heat transfer rate to the water:

$$\dot{Q}_{useful} = \dot{m}_{water} \times \left(h_{water,T_{exit}} - h_{water,T_{entry}}\right)$$

Secondly, the “Free Steam Efficiency” was defined as:

$$\eta_{free} = \frac{\dot{Q}_{fuel}}{\dot{Q}_{useful}} \times 100$$

The key difference in the “Free Steam” case was that the power required to raise the steam was not included, as this case assumes that the steam was provided rather than being generated, therefore took no additional power.

This case was used to determine whether efficiency increased if steam was available at no cost, such as in a situation where a low thermal quality steam source is available that would otherwise be vented to the atmosphere.

It can be seen that the “Free Steam” efficiency is simply the ratio of power available from the fuel to heat transferred to the water.

Thirdly, the “Condensing Efficiency” described a theoretical case where latent heat of the steam in the flue was recovered for a useful purpose, such as boiler water pre-heating:

$$\eta_{condensing} = \frac{\dot{Q}_{fuel}}{\dot{Q}_{useful,condensing}} \times 100$$

Where $\dot{Q}_{useful,condensing}$ is the useful heat transferred to the water in addition to the useful heat recoverable from the steam in the flue:

$$\dot{Q}_{useful,condensing} = \dot{Q}_{useful} + \dot{Q}_{condensing}$$

Where $\dot{Q}_{condensing}$ is the useful heat recoverable from the steam in the flue:

$$\dot{Q}_{condensing} = \dot{m}_{steam} \times \left(h_{steam,flue} - h_{water,T_{reservoir}}\right)$$

This case was used to identify whether changes to the “Overall” efficiency could be accounted for by the thermal energy absorbed by the steam or water.

Calculating the efficiencies required measuring the rates of energy inputs and outputs of the system. The volume flow, temperature, and pressure of CH_4 were used to calculate the mass flow of fuel, which, when multiplied by its calorific value, determined the rate of fuel energy input to the system. The calculated higher heating value of 55541 kJ/kg was used, which included the potential latent heat recovery when condensing the steam in the flue gas. The water volume flow, pressure, and temperature entering and exiting the boiler were used to derive the water mass flow, using a density calculated from the average of the inlet and outlet conditions. The enthalpies of water at T_{exit} and T_{entry} were calculated using the coefficients from McBride, Gordon and Reno (1993).

Data on CO, NO_x, and O_2 were also collected for examining the effect of parameter changes on emissions.

At each condition approximately three minutes of data was recorded for each property, which was then averaged to give a single value. This reduced the effect of random errors on the results.

5.1.3. Measurement Uncertainty

The measurement ranges, resolution, and uncertainties for the emissions data are shown in Table 5-1.

Table 5-1 – Emissions analyser sensor information (Testo Ltd., 2019)

Parameter	Range	Resolution	Uncertainty	Response (t90)
O_2	0 to 25% of vol.	0.01%	±0.2%	< 20s
CO	0 to 10000ppm	1ppm	±10ppm	<40s
NO	0 to 4000ppm	1ppm	±5ppm	<30s
HC	100 to 40000ppm	10ppm	±400ppm	<40s

The efficiency uncertainty was calculated by propagating the errors of the relevant instruments through the data analysis calculations. This resulted in a 2σ uncertainty of ±1.3% at a typical 80.8% overall efficiency. The most significant contributors to the error were the boiler water heat capacity calculation and the fuel mass flow meter output.

5.1.4. Test Programme

The minimum achievable quantity of oxygen in the exhaust was 2%, as reducing the air flow further increased the volume of CO beyond the limits of the emissions analyser, causing it to shut-down.

For the air/fuel experiment a total of 18 flue oxygen volume percentages were tested, distributed across a range of 2% to 16%. Each run was separated by a two minute period which allowed the test setup to reach equilibrium.

The water and steam injection experiments featured a fixed 6% flue O_2. Injection rates of 0 to 15ml/min and 0 to 130ml/min were tested for the water and steam injection experiments, respectively, where the steam injection flow rate was measured before it was vaporised.

5.2. Results and Discussion

5.2.1. Air/Fuel Experiments

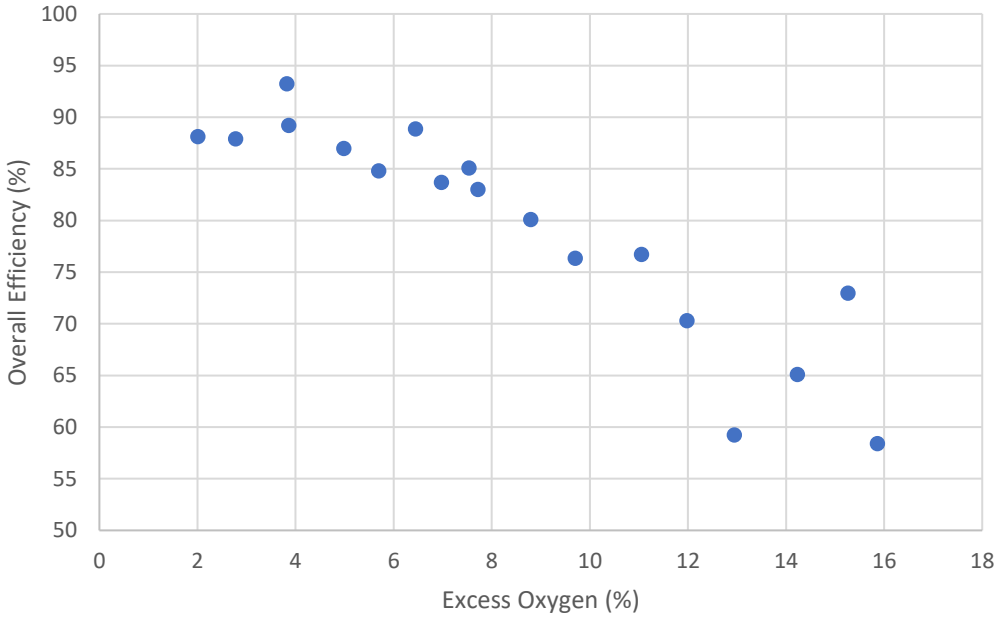

Figure 5-1 - Overall efficiency vs excess oxygen, no steam/water injection

Figure 5-1 shows an approximate 30% efficiency loss when the excess O_2 in the flue was adjusted from 2% to 15%. This was to be expected as increasing the excess O_2 required increasing the mass of air, which absorbed heat from the system and rejected it to the environment, rather than heating the water. The boiler was commissioned at 5% excess O_2, and reducing this by 1% resulted in an approximate 2.2% efficiency increase. The thermal model suggested that the same reduction in O_2 on a 4.5MW industrial steam boiler could yield over £14k fuel savings per annum, assuming 8000hr/yr operation. O_2 trim systems are reportedly widely available for industrial boilers (Washington State University, 2003), though no evidence had been found of a similar system for domestic boilers outside of academia (Conte, Scaradozzi and Cesaretti, 2006), likely due to the cost of the equipment involved (Carbon Trust, 2012).

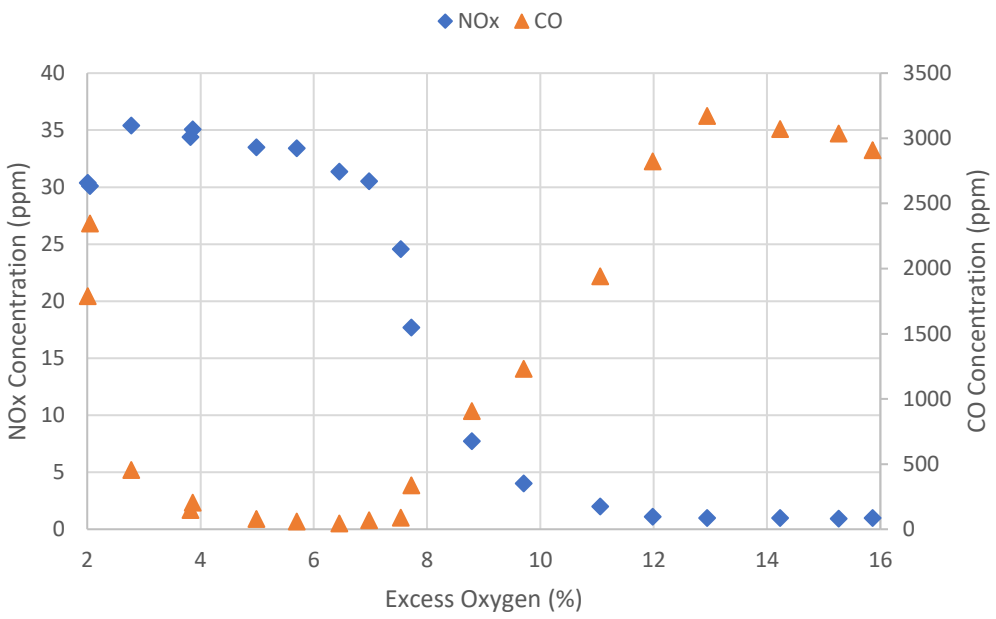

Figure 5-2 - Flue gas NO_x and CO vs excess oxygen

Figure 5-2 shows that there was a distinct increase in NOx concentration from 30.4ppm to 35.4 ppm when excess oxygen was increased from 2.0% to 2.8%, followed by a gradual 4.9ppm decrease between 2.8% and 7.0%, and a significant 26.5ppm decrease between 7.0% and 9.7%, then a gradual decrease with increasing excess oxygen. The initial increase may have been due to the increased oxygen availability, and the subsequent decrease is likely due to the flame cooling effect of excess air (Leonard and Stegmaier, 1994).

CO concentrations followed a reverse trend, starting at around 2000ppm at 2.0% excess oxygen, falling significantly to 455ppm at 2.8% oxygen, then decreasing more consistently to a minimum of 45.4ppm at 6.4% before rising again. The decrease in CO was expected due to the increased oxygen availability resulting in more complete combustion (Hanby, 1994), however the CO increase did not follow that logic, which was unexpected. Baukal *et al.* (2007) observed increases in CO emissions with decreasing furnace

temperature due to incomplete combustion, therefore the cooling effect of the excess air is theorised to have contributed to the CO rise. Another factor may have involved the increased air velocity disrupting the flame, perhaps causing flame lift-off or causing more swirl than the burner was designed for, which may have resulted in flame destabilisation and incomplete combustion.

5.2.2. Water Injection Tests

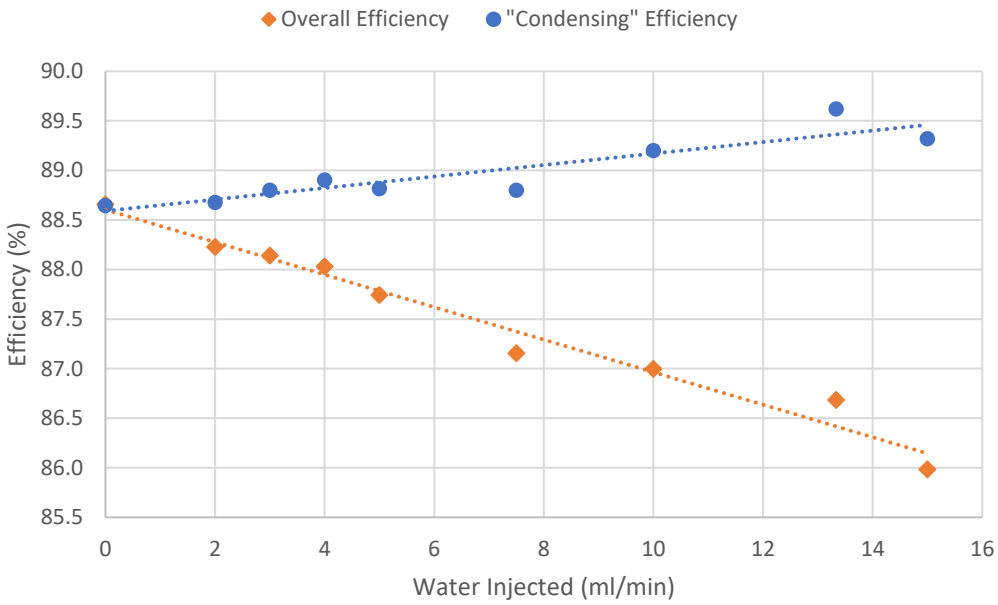

Figure 5-3 – Overall efficiency vs. water injected

The water experiments proved to be more reliable than their steam counterparts due to the less complex injection system. Figure 5-3 shows that overall efficiency decreased approximately 2.5% between the dry state and the 15ml/min water injection state in a linear fashion. As with the steam tests, there may have been a cooling effect on the flame which lead to incomplete combustion and the decrease in efficiency, as Figure 5-4 showed a rise in CO with water injection. The condensing efficiency

increased with increasing water injection, showing that the overall efficiency losses were accounted for by the energy absorbed in the latent and specific heats of the water/steam. The increase in condensing efficiency of approximately 0.9% is of interest as it indicates that water addition had a beneficial effect on efficiency if the detrimental thermal effects are discounted.

Figure 5-4 shows that the NO_x decreased with increasing water addition, though the step change seen in Figure 5-6 was not present. In the water case NO_x decreases 7.3ppm from 0ml/min to 10ml/min, while in the steam case it falls by 12.3ppm. This variation could be a result of the control issues with the steam generator. Regardless, the NO_x decrease with water addition shows that it may not be necessary to use steam, which could be beneficial as the water was simpler to control.

The CO levels increased by 32.4ppm from 0ml/min to 10ml/min for the water addition case, which was significantly less than the 316.2ppm increase for the steam case over the same range. This could indicate that water yielded more complete combustion than steam and is therefore a better injection option, or it may be the result of the steam control issues. This was investigated further in the relevant individual chapters.

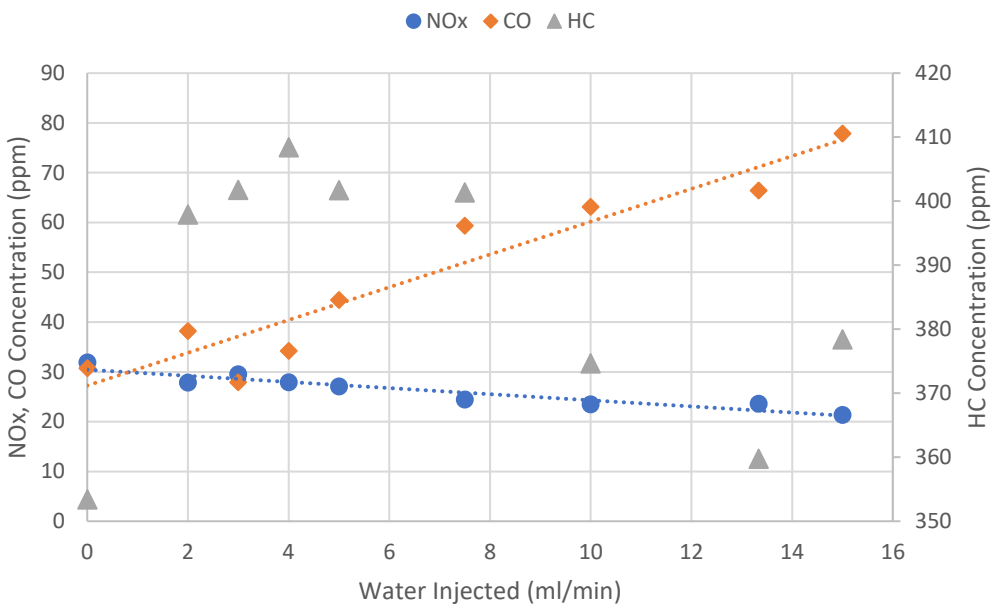

Figure 5-4 - Flue gas concentrations vs water injection

5.2.3. Steam Injection Tests

The initial steam addition experiments were subject to error due to issues with the steam generator control, described in Appendix A, however the data trends were still considered significant.

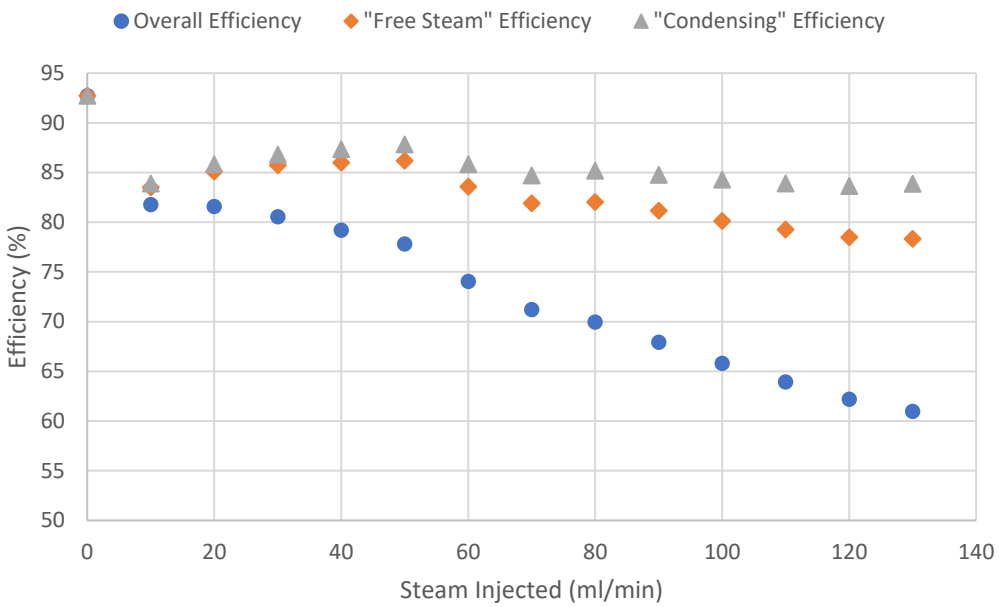

Figure 5-5 - Overall efficiency vs steam injected

Figure 5-5 shows that the overall efficiency decreased 20.8% with steam addition increasing from 10ml/min to 130ml/min. The “Free Steam” efficiency also decreased to a significantly reduced extent, showing that a large proportion of the overall efficiency loss was due to the additional energy required to raise the steam. This means that the latent heat was not being recovered in the boiler, which is to be expected as the boiler is not of the condensing variety.

The “Condensing” efficiency showed that if the heat input to the steam/water was discounted, the resulting efficiency remained fairly constant across the steam injection range, indicating that the majority of the overall efficiency loss was accounted for by the specific and latent heats of the water/steam. A step change in efficiency of over 10% was observed from 0ml/min to 10ml/min, which could not be accounted for with the water vaporisation or specific heat absorption losses. The 0ml/min efficiency of 93% was itself unexpected however, as it was over the boiler’s manufacturer-rated

efficiency of 85.5%. This was later identified to be due to an error introduced by the air and methane volume flow meters, which were subsequently replaced.

In the free steam case, where the energy cost of the latent heat was disregarded, the efficiency showed an increase of 2.7% from 10ml/min to 50ml/min, indicating that the rate of heat transfer to the water increased. As the volume flow of steam was several orders of magnitude less than the volume flow of air, it is unlikely that the increase was due to enhanced turbulence, or a stronger convection coefficient resulting from a velocity increase in the fire tube. It is theorised that this may be due to a condensation/evaporation phenomenon occurring on the fire tube walls. Lienhard IV and Lienhard V (2011) stated that the condensation heat transfer coefficient can be several orders of magnitude higher than the forced air coefficient, therefore in a short timescale the steam in the fire tube could have been condensing on the walls and rapidly re-evaporating. This process would have resulted in a higher overall heat-transfer coefficient and may explain the free steam efficiency increase.

The decrease in efficiency in steam flows of over 50ml/min may have been due to the cooling effect of the steam, as observed by Zou *et al.* (2014), or a disruption of the flame profile, both of which could cause incomplete combustion. This theory is supported by the results presented in Figure 5-6, which show that CO and HC increased with increasing steam injection.

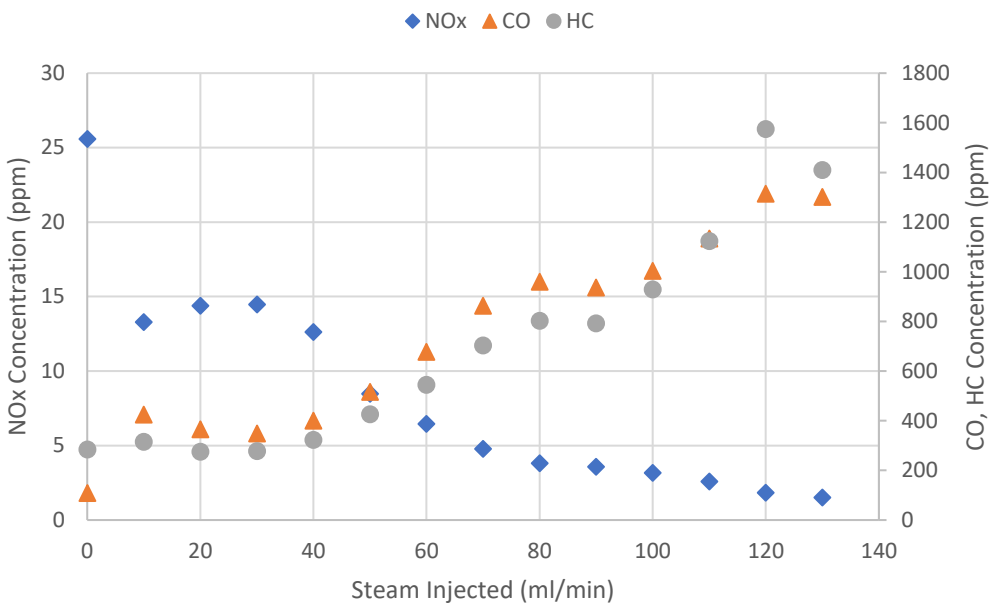

Figure 5-6 - Flue gas concentrations vs steam injected

Figure 5-6 also shows that NO_x decreases with steam injection as predicted, which aligns with observations from Landman, Derksen and Kok (2006) and Zhao *et al.* (2002), despite their studies focusing on gas turbine combustor applications rather than boilers.

There was a step-change in NO_x between 0ml/min and 10ml/min, where it decreased by 12.3ppm, yet there was only an 11.8ppm decrease from 10ml/min to 130ml/min. This could indicate that the 0-10ml/min region was more significant and that the effect of steam injection diminished with increasing flow, as observed by Göke *et al.* (2014). The step-change could however be due to the aforementioned difficulties in controlling the flow of steam, therefore a greater quantity could have been injected than expected. This would also explain the increase in NO_x and decrease in CO between 10ml/min and 30ml/min, which seems anomalous as such an inversion was not observed in any previous studies. To clarify this further experimentation was conducted in Chapter 7 with a focus on the 0-12ml/min range.

The results indicated that retrofitting a burner to accommodate steam injection for NO_x reduction would be viable if the accompanying rise in CO and decrease in efficiency could be addressed. Claeys *et al.* (1993) and Peltier (2006) both reported reductions in CO and NO_x simultaneously, therefore further investigations were conducted in Chapter 7 to identify whether similar results were achievable for the boiler application.

5.2.4. Stability Tests

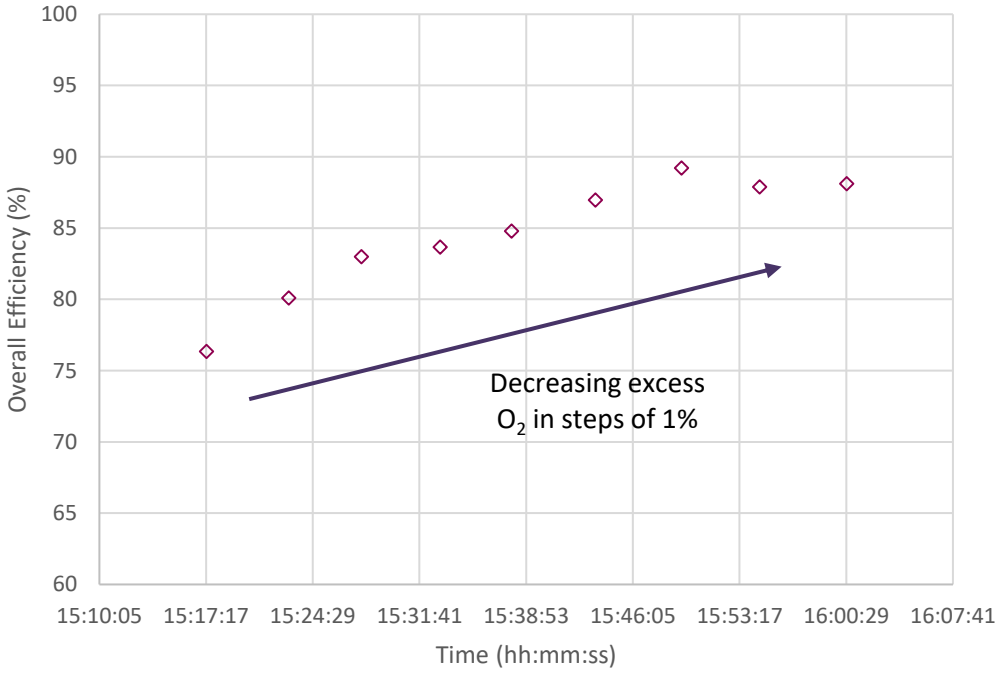

Figure 5-7 – Efficiency vs. Time for 10% to 2% Excess O_2

Figure 5-7 shows that the overall efficiency responds fast enough to allow a 2 minute settling time between tests. It also reveals that efficiency plateaus at low O_2%, showing that there may be a balance between heating less excess air and releasing less heat through incomplete combustion.

Figure 5-8 indicates that the system took 17min 19sec to reach 95% of its stable value. This confirmed that the test rig had a high thermal mass, due to it containing over 30l of water plus the mass of the radiator and boiler.

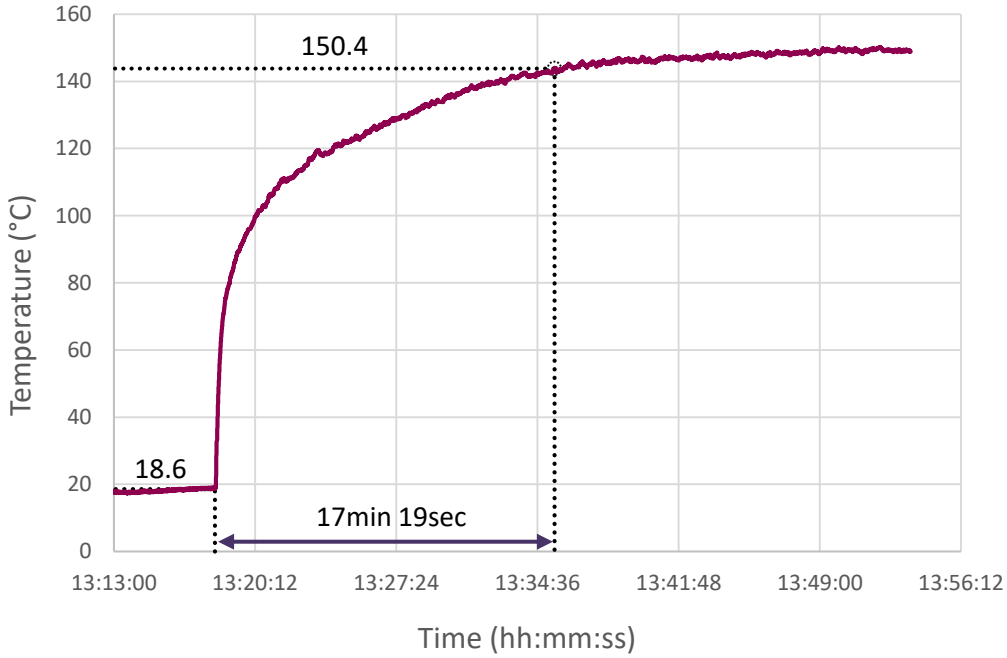

Figure 5-8 – Flue temperature during experimental set-up initialisation

5.2.5. Other Findings

In each of the three investigations there was a significant disparity between repeated experiments at the same conditions. For example, the baseline tests for the water injection experiment featured a standard deviation of 1.56% on an average overall efficiency of 82.0%. The error propagation analysis had identified that significant uncertainty originated from the temperature measurements of the loop water as it entered and exited the boiler. For a representative test, the standard deviation on the temperature rise of the loop water was 1.97°C, while the rise itself was only 6.21°C, which propagated through to a 28.8% relative error in the overall efficiency. The source of the error was found to be the substantial variation in the boiler

water temperature data shown in Figure 5-9. This was caused partially by electromagnetic interference, as the physical location of the thermocouple wires changed the amplitude of the noise.

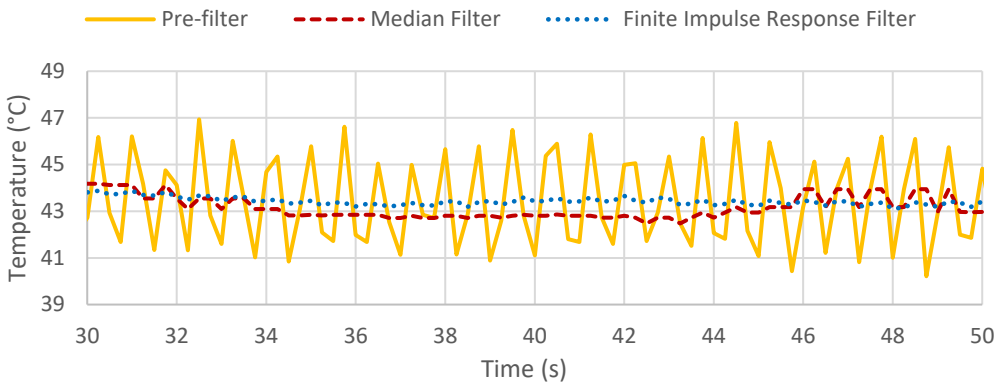

Figure 5-9 - Noise on the boiler water inlet temperature sensor

Even without the noise contribution, the instrument limit of error for the T-type thermocouples was 0.25°C at one standard deviation, which was still significant. To remedy this for the main experiments the T-type thermocouples were replaced with resistance temperature detectors with a 1/10 DIN accuracy, giving an instrument limit of error of 0.04°C at one standard deviation, and all unshielded cable was replaced. Also, a median filter and finite impulse response filter were investigated for noise reduction. Figure 5-9 shows that both filters were effective, though the latter was chosen for subsequent experiments.

Another potential source of error was the positioning of the water volume flow meter for the boiler circuit, which was installed adjacent to a globe valve. This was moved at least 10 pipe diameters away from the valve to limit the effects of flow disruption on the volume measurement. It was also noted that the air flow rate fluctuated somewhat during tests, therefore another air regulator stage was added to spread the pressure drop across two stages, which improved stability.

An equipment limitation was found with the emissions analyser in that it could not be used at flue gas O_2 concentrations of less than 2.0%, as the CO concentration increased to a level that overloaded the analyser sensor. A dilution function was available to extend its CO measurement range, however O_2 measurement was not available while this was active. Additional testing at such high CO concentrations was deemed unnecessary as operating a system in such a fashion has no practical use.

Complications with the HC sensor were also identified. Firstly, it was not designed to be used below 2% O_2, and therefore switched off, however a full power cycle of the analyser was required to reactivate it. Secondly, the measured HC ranged from 300ppm to 1400ppm, however the uncertainty of the sensor was a significant proportion of that at ±400ppm, thus the HC data is of questionable value. Lastly, the HC sensor lifetime was short and the first HC sensor had to be replaced. This was almost prohibitively costly, therefore the decision was made to only activate the sensor if there was specific case worth using it for.

5.3. Conclusions

It was found that reducing the excess oxygen increased the efficiency of the system. CO was lowest between 4% and 7% excess oxygen, and NO reduced with increased oxygen across the range tested.

The experiments confirmed the importance of excess oxygen control in gas-fired boilers, showing that reducing the excess oxygen from 5% to 4% resulted in an efficiency increase of 2.2%. It was also been shown that a burner could be retrofitted with a steam injection system rather than having to incorporate the capability into the original design.

The literature review identified that it was possible to decrease both NO_x and CO simultaneously, however this was not observed during the preliminary tests, possibly due to the identified issues.

5.4. Chapter Summary

This chapter has detailed the results of the preliminary experiments. These involved changing the excess oxygen levels in the flue by varying the intake air, and injecting known amounts if steam and water into the burner. The resulting efficiencies and emissions were measured.

It was found that with 10ml/min to 130ml/min of saturated steam, NOx emissions reduced by up to 88.7%, accompanied by a decrease in overall efficiency of 20.8% and an increase in exhaust CO and HC of 207% and 347% respectively. For water addition rates from 0ml/min to 15ml/min NOx reduced by 30.8%, with a decrease in efficiency of 2.5% and CO increase of 153%.

Due to issues with accurately determining the efficiency the results were inconclusive, however the sources of error were identified and the experimental setup was modified to remove them.

Chapters 6 and 7 expand on the knowledge gained from the preliminary tests and focus on injecting water and steam into the burner, respectively.

6. Water Addition

6.1. Introduction

This chapter focuses on the experimental work involving the addition of water into the primary air of the burner. The literature review found that reductions in the emissions of NO_x and CO could be achieved through the injection of water into the combustion process of a gas turbine. It also discovered that NO_x reduction using steam injection had been demonstrated previously in industrial boilers, however no evidence was found of the use of water injection, or the reduction of CO emissions. Also, no investigations into NO_x reduction on domestic or commercial boilers were identified. There are also no known cases of a boiler burner being retrofitted for water or steam injection.

The chapter details the modifications to the preliminary test rig to enable water injection into the combustion zone, both through the burner directly and separately via the air intake of the burner. It also presents the methodology for the experiments, and an analysis of the results.

Contents

6.2. Methodology

6.2.1. Rig Changes as a Result of Preliminary Testing

The preliminary tests established that there were errors in the data, which were found to be caused by the meters used for the air and fuel volume flows. These were replaced with Bronkhurst thermal mass meters, which were not dependant on pressure, pressure drop, or temperature, thus the errors from the pressure and temperature sensors were negated.

The flow meters were connected digitally using RS232 rather than the previous analogue 4-20mA loop, which eliminated the associated transmission errors. The meters interfaced with the computer directly, allowing data to be captured using a combination of the manufacturer's software, the LabView program, and the Dynamic Data Exchange protocol.

6.2.2. Water Injection System

The original experimental setup described in Chapter 5 was modified to include suitable injection points for the water. There were several injection locations available, including:

1. In the air supply before the burner, which was predicted to be ineffective due to the complex flow path through the burner internals. There was a likelihood of the water depositing inside the burner rather than being entrained in the air and passing through to the flame.
2. In the fuel supply, which was discounted due to safety concerns and reduced access compared with the air supply.

3. Directly into the flame, which would have required modification of the boiler combustion area.
4. In the air supply inside the burner, which provided good access and delivered the water immediately before the swirl diffuser.

Two injection locations were chosen for the experiments. Firstly, into the air supply inside the burner, as it did not require modification of the boiler yet ensured that the water would reach the combustion area, and secondly into the air supply before the burner. Although introducing water before the burner was predicted to be less effective due to the potential for the water to coalesce before it reached the combustion zone, it was the preferred solution as it did not require modification of the burner.

Initial water experiments utilised an injection system that featured a tube that entered the burner via a compression fitting. The tube was effectively open-ended. Water injection rates of up to 100ml/min caused no effect on the flue gas emissions, and further addition extinguished the flame. This was assumed to be due to poor mixing as some effect should have been observed. It was decided to replace the open-ended tube with an atomising nozzle to promote a more homogenous mix of water and air.

Several types of nozzle were available, detailed in Table 6-1.

Table 6-1 – Comparison of injection nozzle types

Nozzle Type	**Advantages**	**Disadvantages**
Solid-cone	High flow rate	Required 4 bar to atomise Coarse atomisation
Hollow-cone	Fine atomization	Required 4 bar to atomise
Pneumatic atomising	Finest atomization Requires little water flow	Required air to atomise, which required metering

The hollow-cone nozzles were selected due to their fine atomisation and ease of use. Although the pneumatic atomising nozzles generated the finest mist, they would have introduced additional air into the system which would have needed to have been measured. This would have required additional pressure and temperature sensors and a flow meter.

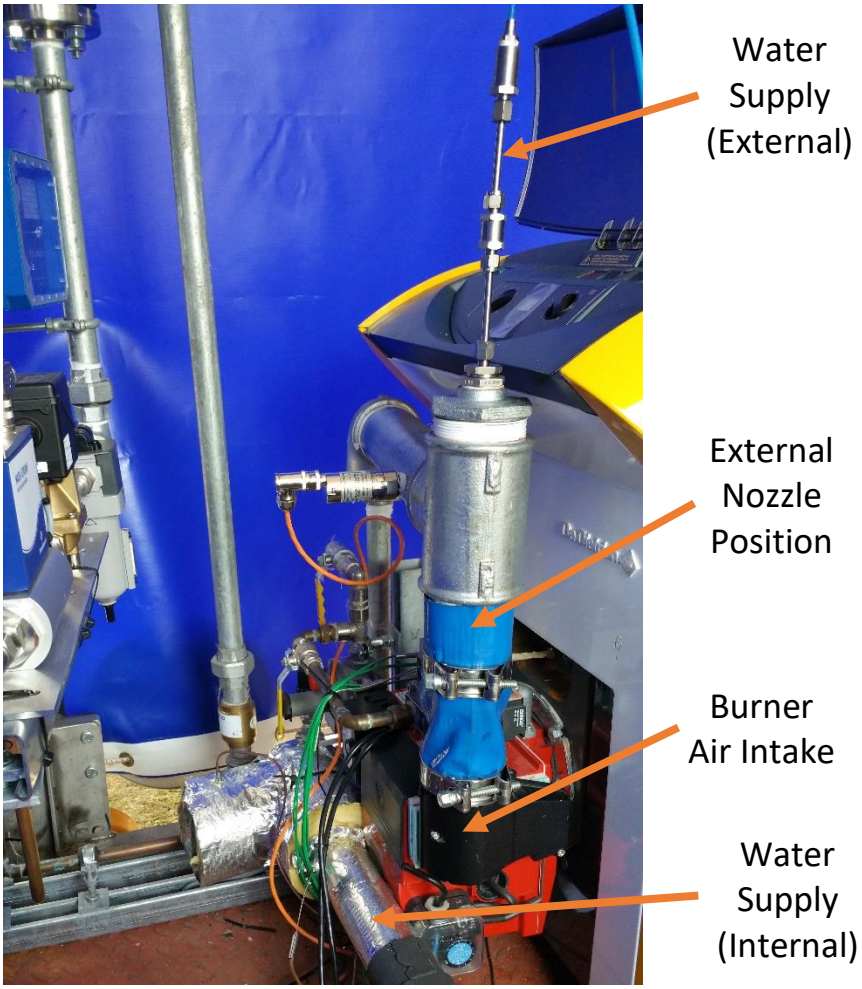

Figure 6-1 – Nozzle location for external injection testing

For the water injection experiments a range of atomising hollow-cone nozzles were acquired which were either mounted inside the burner, before the swirl diffuser, or in the air intake shown by Figure 6-1. Temperature and pressure sensors monitored the condition of the fluid entering the burner, as they influenced the flow rate and dispersion pattern of the nozzles.

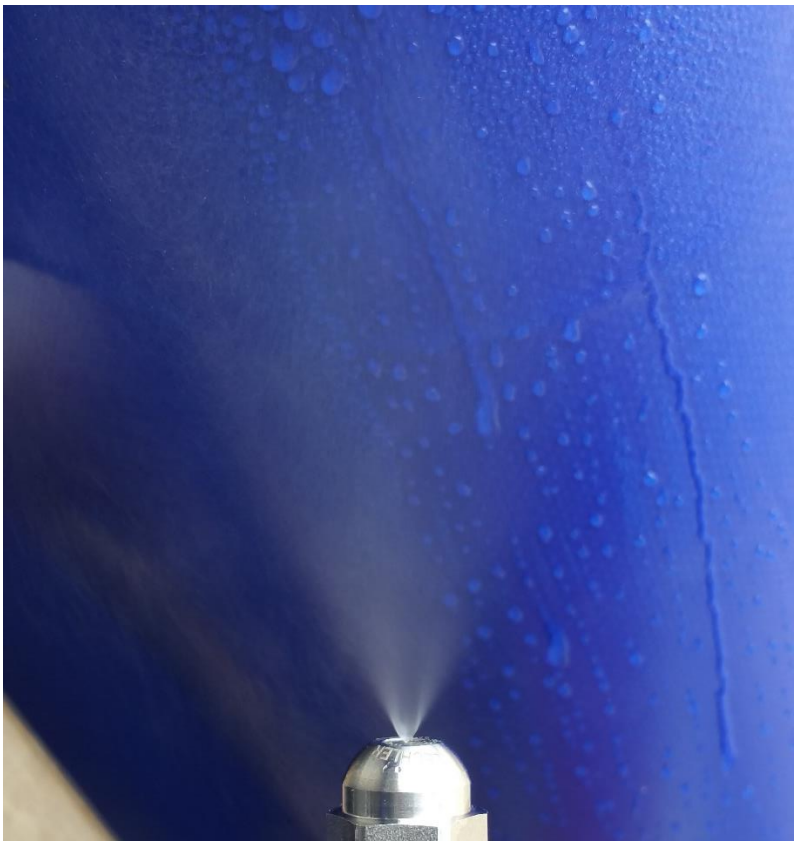

Figure 6-2 – 0.6mm hollow-cone nozzle operating at 12ml/min

6.2.3. Test Procedure

The aims of the experiments were to determine the effect of water addition on the efficiency, CO output, and NO_x emissions of the combustion process. The preliminary experiments showed that these parameters also varied with the level of excess oxygen in the exhaust, therefore it was necessary to conduct a multi-variable investigation. This involved varying the water and the air flowrates individually across a range of cases.

As industrial boilers are generally operated with as little excess oxygen as possible to promote higher efficiencies (Carbon Trust, 2012), it was decided to set a maximum limit of 6% for the experiments. The minimum limit was determined by the amount of CO generated, as the analyser was restricted to 2000ppm. Based on these constraints, air-fuel equivalence ratios were tested ranging from 1.00 to 1.32, in steps of 0.04.

Toqan et al. (1992) suggested that 0.12 kg_{water}/kg_{CH4} was sufficient to cause significant effects on the emissions, which was within the range of the smallest hollow-cone nozzle which had a bore diameter of 0.1mm. This nozzle was tested outside of the burner to assess its atomisation performance at various flow rates. Figure 6-2 shows the droplet distribution at 12ml/min, which was adequately spread. Figure 6-3 shows the distribution at 4ml/min, where the hollow cone was beginning to lose form. It was found that atomisation was lost completely at water flow rates below 4ml/min, and the maximum working pressure of the pump was exceeded above 12ml/min, thus rates of 4ml/min, 8ml/min, and 12ml/min was chosen for the experiments. This was repeated for each λ setpoint.

Four additional nozzles of larger size were tested, however they could not achieve atomisation for the flow rates of interest.

Figure 6-3 – 0.6mm hollow-cone nozzle at 4ml/min

For each combination of water addition rate and λ the volume fraction of CO and NO_x were measured. This was to determine the effects of changing conditions on the flue gas emissions so that the optimal settings could be found. The volume fraction of O_2 was measured to investigate whether it was influenced by steam injection.

No data was collected from the HC sensor as it would not function at excess oxygen levels below 2% volume. The preliminary experiments found that HC followed a comparable trend to CO, therefore the absence of the data was not significant.

The effect of changes in λ and water addition on the flame were also of interest. Direct measurement of the flame would have required a platinum-rhodium thermocouple or similar, as well as a separate data acquisition unit, both of which were prohibitively costly. Instead several type-K thermocouples, capable of measuring up to 1620K, was placed in the fire tube staggered every 100mm from the burner along its axis. Though the sensors were not capable of reading the maximum flame temperature, useful data was gathered from part of the array.

Data was also collected on the flue gas temperature and mass flow rates of reactants. Combined with the species concentrations in the flue this enabled a calculation of the heat rejected through the flue, and in turn the flue-derived efficiency.

Lastly, the ambient temperature was monitored to determine whether environmental changes had an impact on the experiments. For example, a cooler ambient temperature could have resulted in increased heat loss from the boiler to the environment, and would have allowed more heat to be rejected through the radiator.

6.3. Results

6.3.1. Emissions

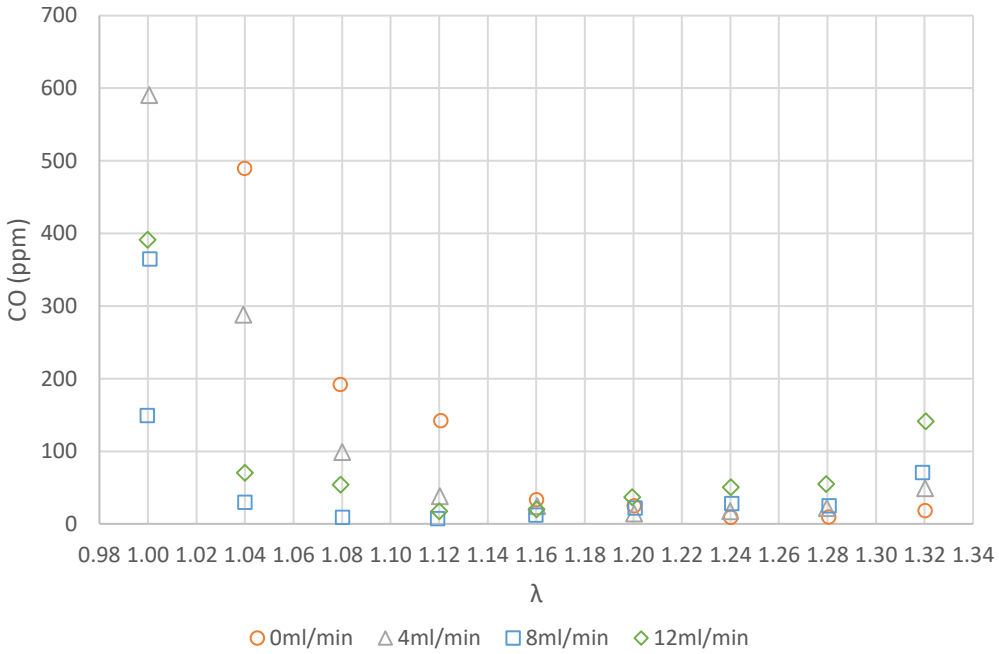

Figure 6-4 - CO vs λ at various water injection rates, internal injection

Figure 6-4 shows that the minimum CO tends to occur at lower λ values for increasing water injection rates; for 0ml/min it is at λ = 1.24, and for 12ml/min it is at λ = 1.12, and it is shown that all the injected cases generate lower maximum CO than the 0ml/min case. For example, at λ = 1.04 the 0ml/min case generated 490ppm CO, which decreased by 93.9% to 30ppm for the 8ml/min case.

Maximum values of CO occur at minimum λ for all water injection rates, and CO increases from its minimum more readily when the λ value is decreased than increased. For example, at 4ml/min, reducing the λ value from 1.20 to 1.08 results in an increase in CO of 607%, whereas increasing to 1.32 increases CO by 250%.

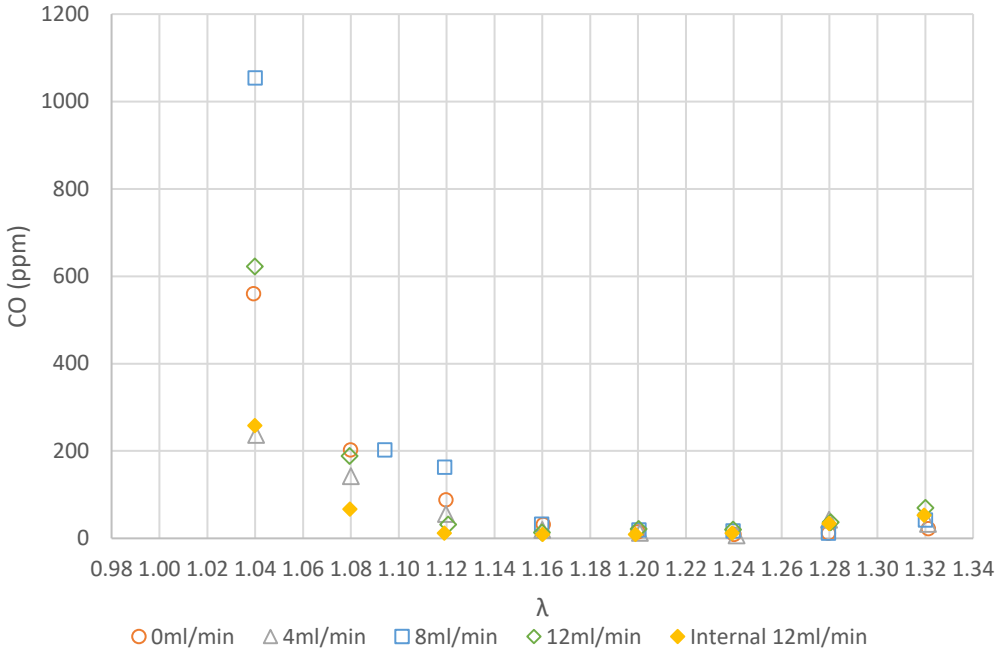

Figure 6-5 - CO vs λ at various water injection rates, external injection

Figure 6-5 shows that injecting water into the air before the burner also affects the CO emissions. As with the internal injection there is a point of minimum CO around the centre of the λ range. This changes for each flow rate, and the CO increases to a greater extent when moving towards stoichiometry. Unlike internal injection, external injection did not reduce emissions in all cases. For example, at λ = 1.04 only the 4ml/min case reduced CO below the 0ml/min case. The 12ml/min external case increased CO by 11%, whereas the corresponding internal case reduced CO by 54%.

The maximum NO_x occurs at the same λ value of 1.08 for injection rates of 0, 4, and 12 ml/min, and at λ = 1.04 for 8ml/min. For the 0ml/min the minimum NO_x was found at the minimum λ value of 1.00, however in the other cases it was found at the maximum λ value of 1.32, though in all cases there are local minima at each end of the experimental λ range. NO_x reduces for all water injection rates, and the 8ml/min case generally appears to be most effective, though it is approximately equal to the 12ml/min cases at

either end of the λ spectrum. The greatest reduction in NO_x can be observed at λ = 1.32, where 4ml/min reduces NO_x by 21.5% from 38.2ppm to 30.0ppm, and the 12ml/min case reduces it by 40.1% to 22.9ppm.

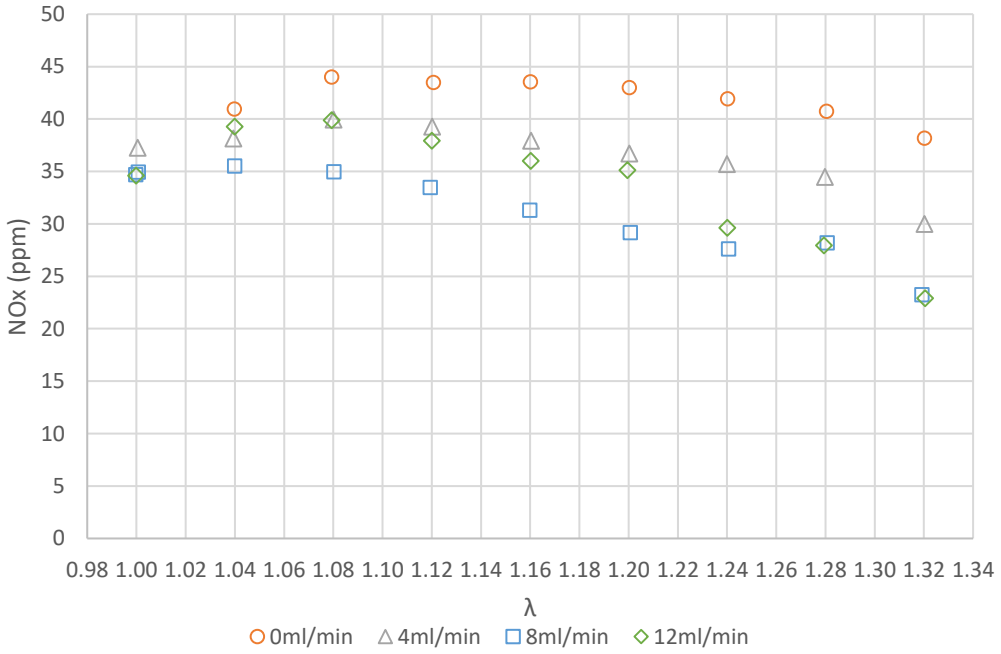

Figure 6-6 - NO_x vs λ at various water injection rates, internal injection

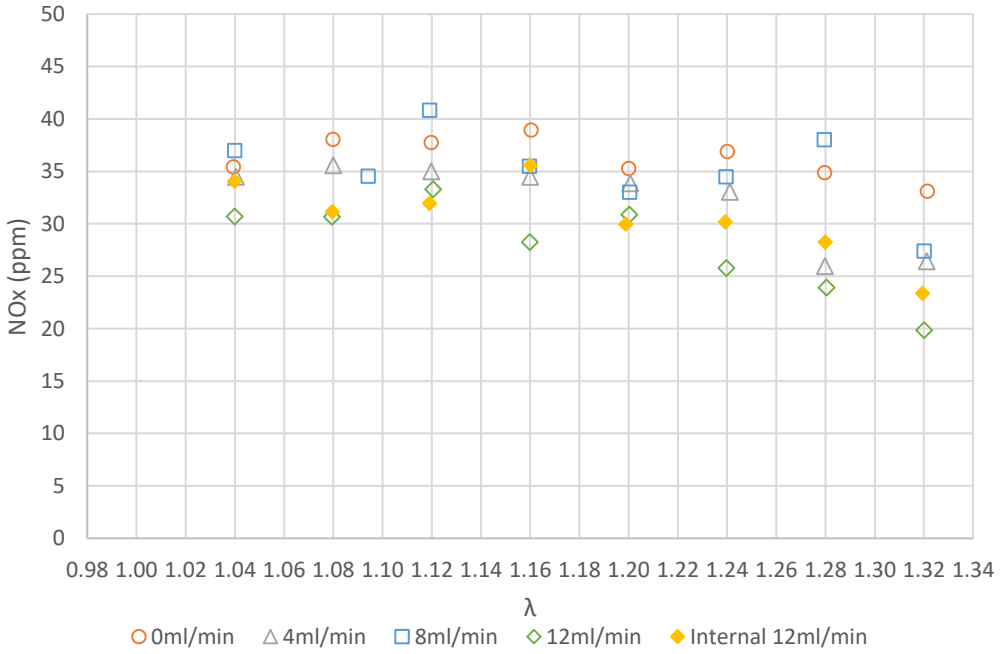

Figure 6-7 - NO_x vs λ at various water injection rates, external injection

Figure 6-7 shows that for all but the 8ml/min case, water injection reduces NO_x for all λ setpoints. At λ = 1.32 NO_x was reduced by up to 40.2% from 33.1ppm to 19.8ppm, and at λ = 1.04 it was reduced by up to 13.2% from 35.4ppm to 30.7ppm. NO_x reduction was generally higher at higher λ values. It is also shown that the 12ml/min external injection case offers better overall performance than the internal case, though individual λ test points vary. The 8ml/min case appears to increase NO_x above the 0ml/min case at 3 λ values.

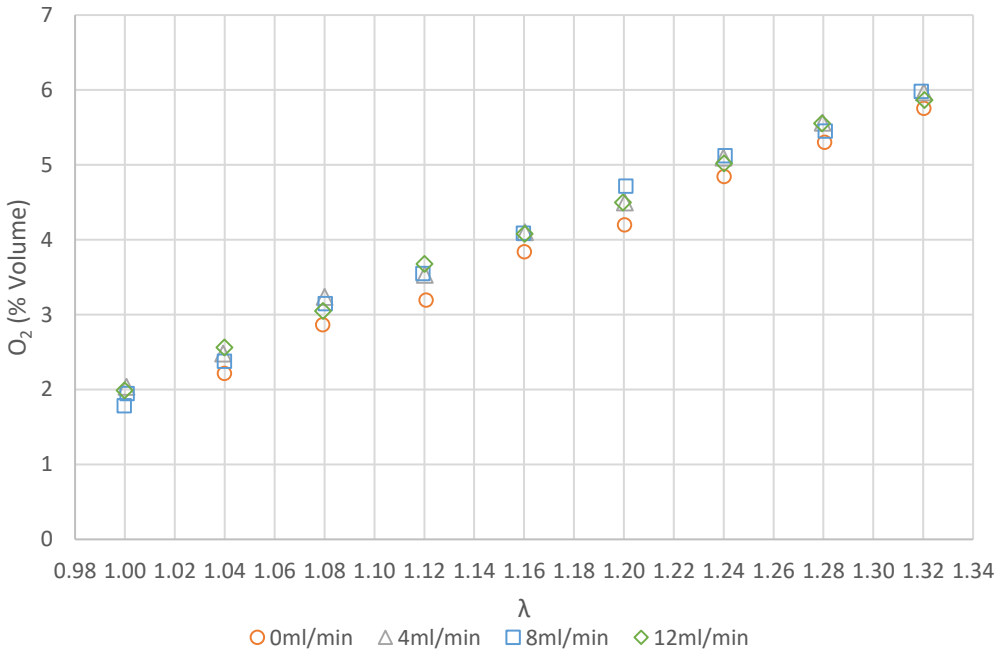

Figure 6-8 – Oxygen vs. λ at various water injection rates, internal injection

Figure 8 shows that O_2 increases with λ. O_2 appears to be constant for a fixed λ value across water injection rates but is lower for the 0ml/min case. For example, at λ = 1.12 the mean O_2 value for the injected cases was 3.6%, while the 0ml/min was 3.2%.

Figure 6-9 indicates that O_2 increased with λ. O_2 generally reduced with increasing water flow rates, up to a maximum reduction of 28% at λ = 1.04 at an injection rate of 12ml/min.

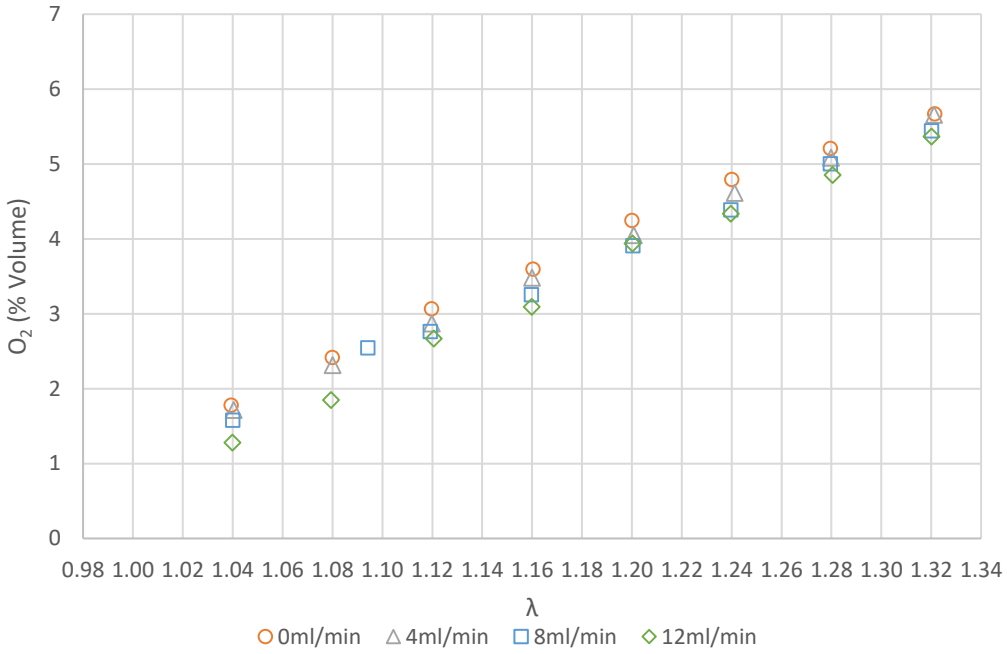

Figure 6-9 - Oxygen vs. λ at various water injection rates, external injection

The fire tube temperatures shown by Figure 6-10 indicates that there is no clear correlation with water injection rate. The maximum average temperature across all four cases is achieved at λ = 1.12. Relative to the 0ml/min case, the 4ml case generally decreased the fire tube temperature, the 8ml/min case was similar, and the 12ml/min case generally increased it.

Figure 6-11 showed similar trends to Figure 6-10, with flame temperatures maximising around λ = 1.12, a general increase with 8ml/min and 12ml/min, and a general decrease with 4ml/min.

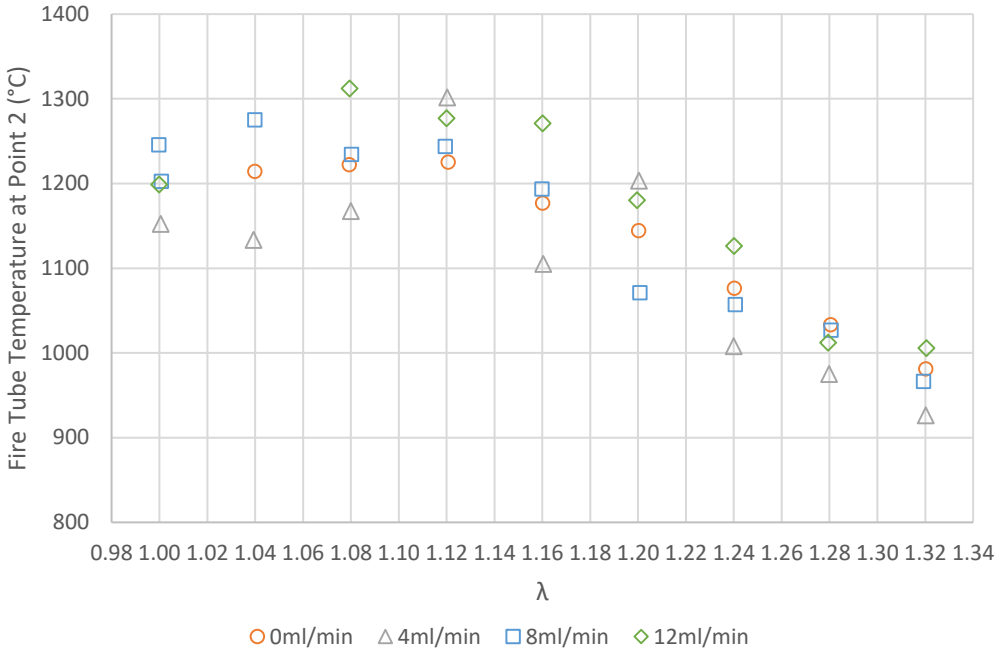

Figure 6-10 - Fire tube temperature vs. λ at various water injection rates, internal injection

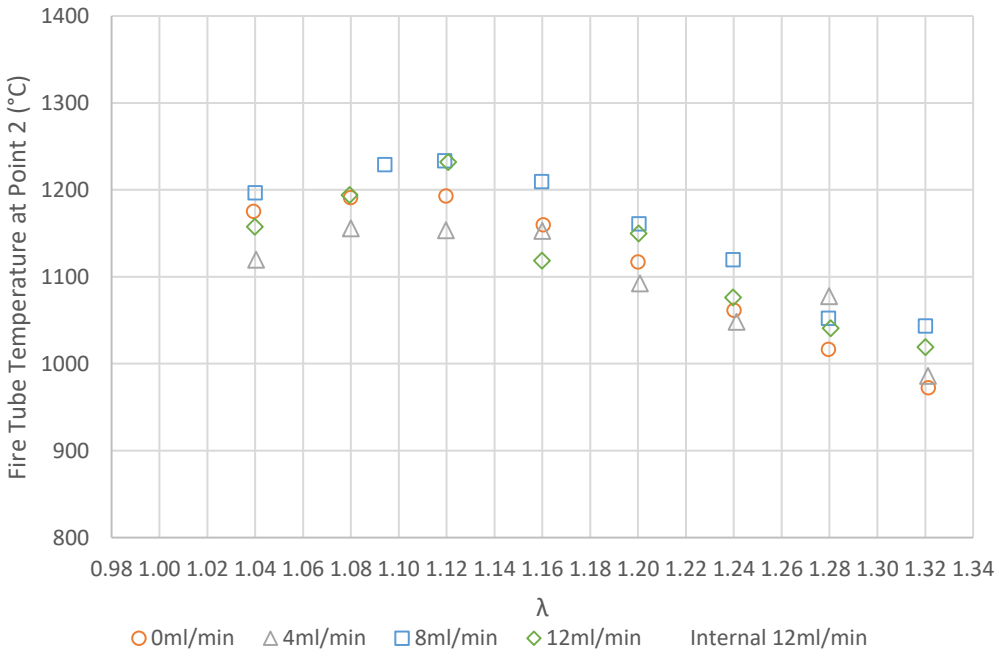

Figure 6-11 - Fire tube temperature vs. λ at various water injection rates, external injection

6.3.2. Efficiency

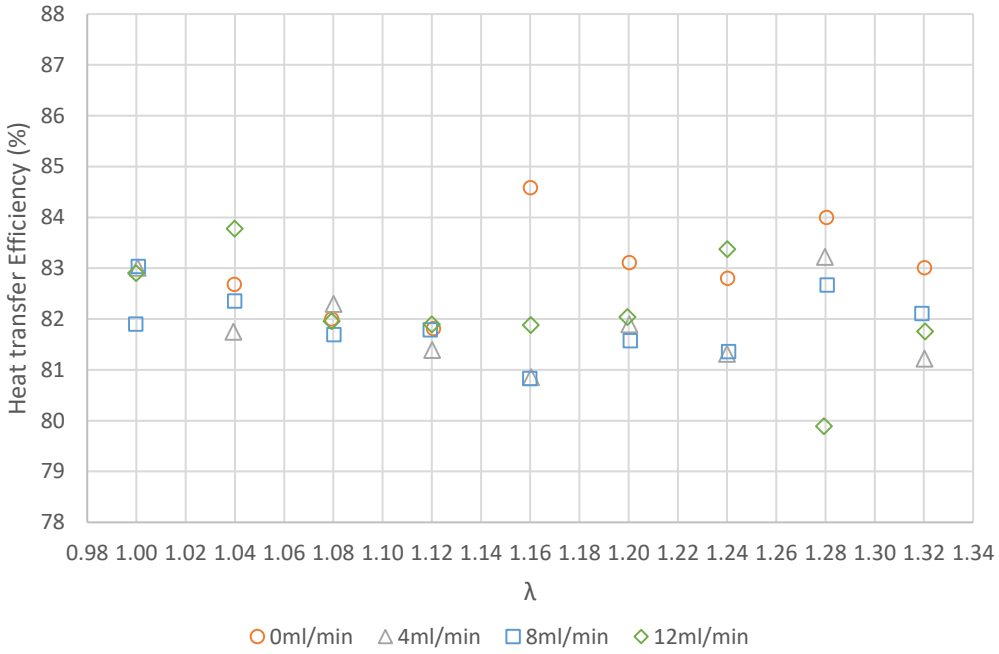

Figure 6-12 - Heat-transfer efficiency vs λ at various water injection rates, internal injection

Figure 6-12 shows that there was no significant correlation between heat transfer efficiency, λ, nor water injection rate.

Figure 6-13 shows that, as with the internally injected cases, there is no distinct correlation between heat transfer efficiency and λ, nor between heat transfer efficiency and rate of water injection.

Both Figure 6-14 and Figure 6-15 show that the flue-derived efficiency decreases approximately linearly with increasing λ. They also show that flue-derived efficiency reduces with increasing water injection rate, again approximately linearly.

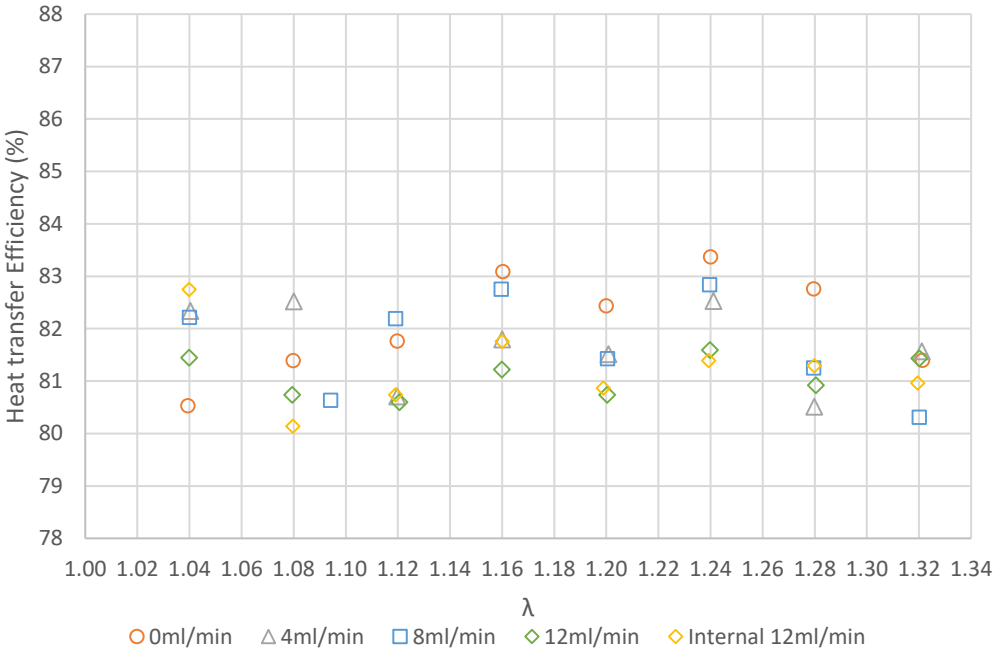

Figure 6-13 - Heat transfer efficiency vs. λ at various water injection rates, external injection

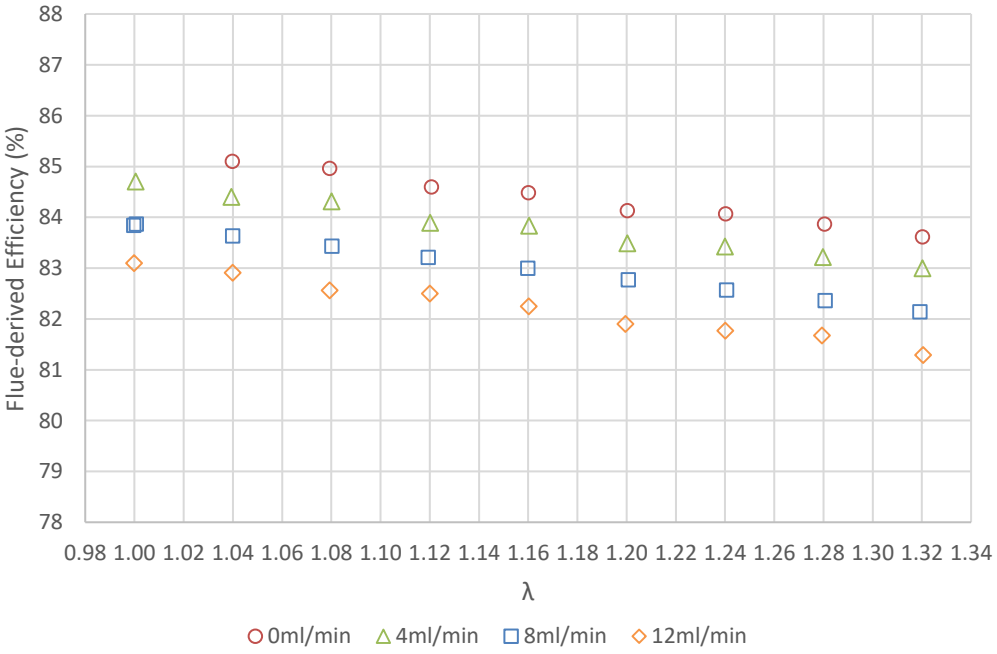

Figure 6-14 - Flue-derived efficiency vs. λ at various water injection rates, internal injection

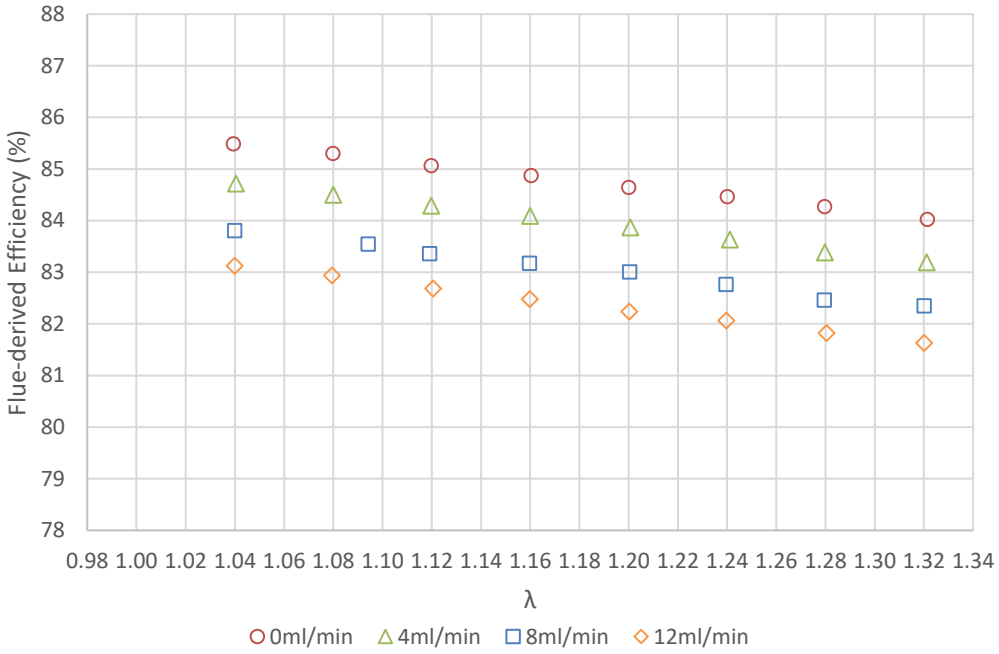

Figure 6-15 - Flue-derived efficiency vs. λ at various water injection rates, external injection

6.3.3. Sensitivity to External Factors

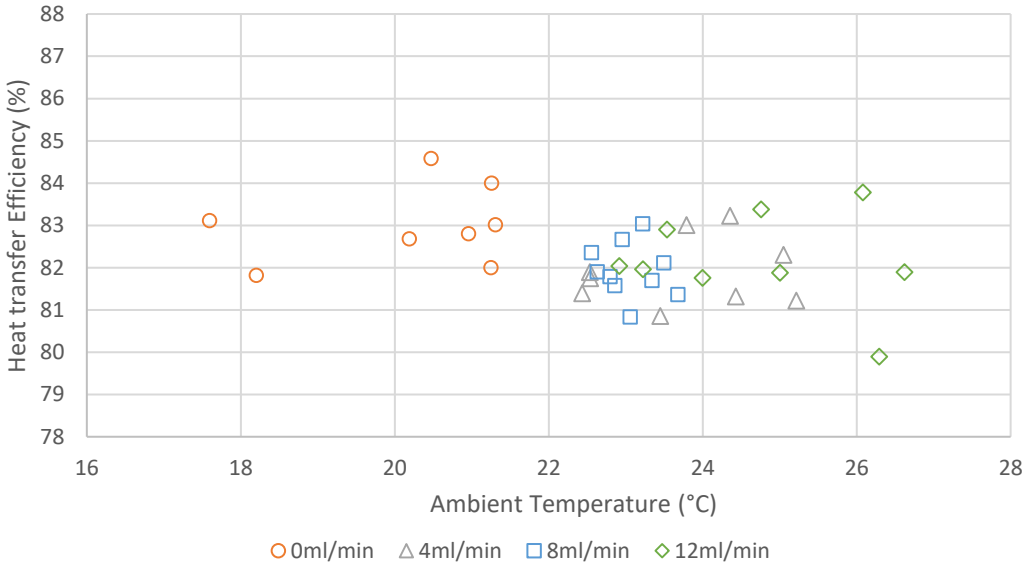

Figure 6-16 - Heat-transfer efficiency vs. ambient temperature at various water injection rates, internal injection

There was no clear correlation between heat-transfer efficiency and the ambient temperature, for either the internal or external cases show in Figure 6-16 and Figure 6-17 respectively. The internal 0ml/min dry case shows approximately 1% higher efficiency than the injected cases.

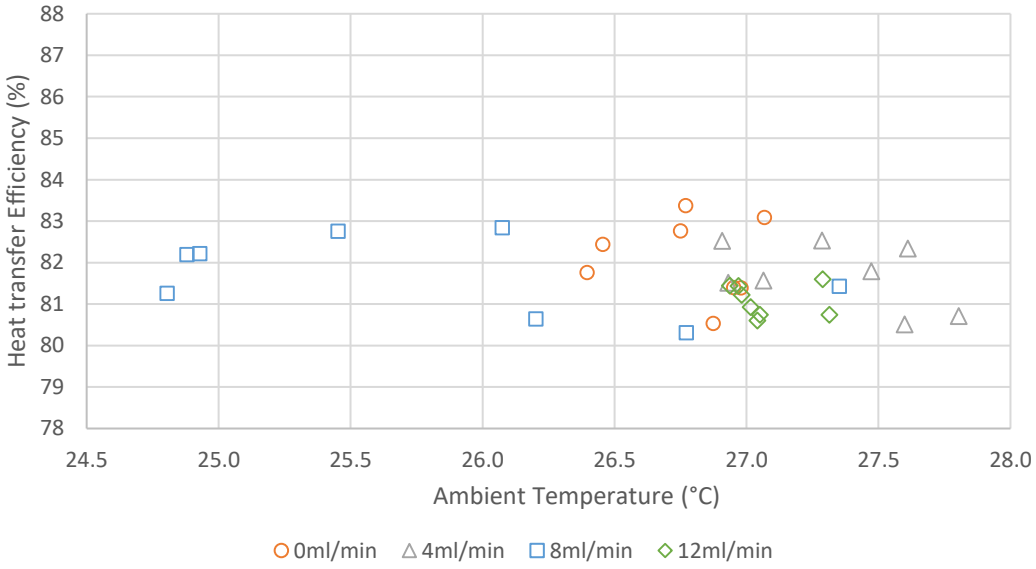

Figure 6-17 - Heat-transfer efficiency vs. ambient temperature at various water injection rates, external injection

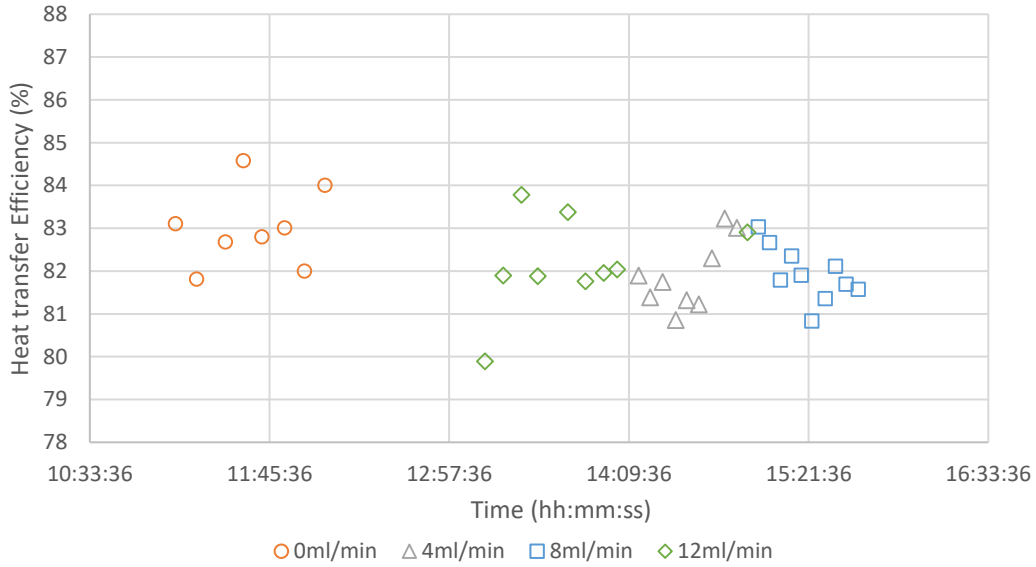

Figure 6-18 - Heat-transfer efficiency vs. time at various water injection rates, internal injection

Figure 6-18 shows that heat-transfer efficiency decreased by approximately 1% between the 0ml/min morning tests and the injected cases in the afternoon. Figure 6-19 shows poor correlation between heat-transfer efficiency and time.

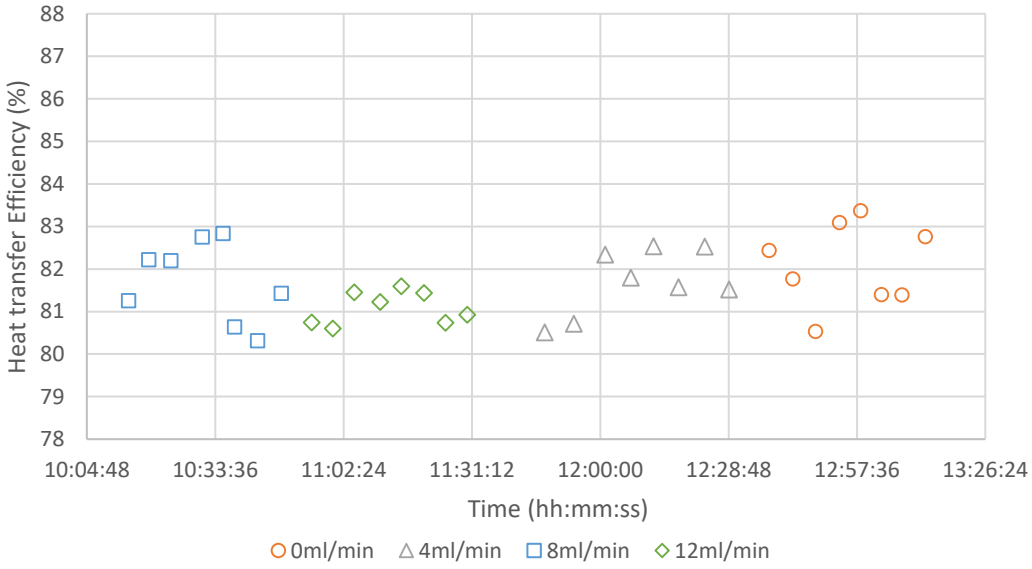

Figure 6-19 - Heat-transfer efficiency vs. time at various water injection rates, external injection

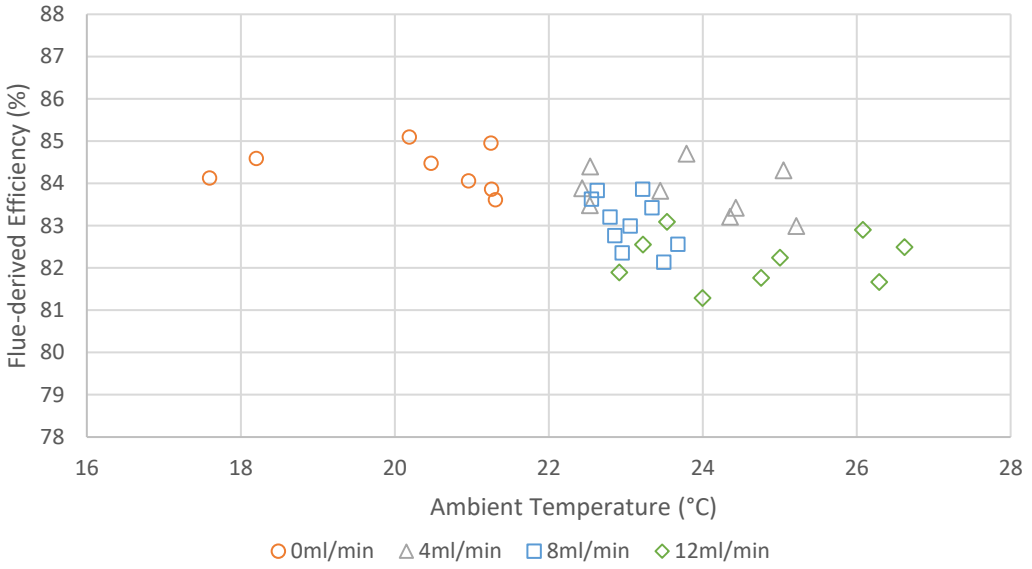

Figure 6-20 - Flue-derived efficiency vs. ambient temperature at various water injection rates, internal injection

Figure 6-20 shows that there is little correlation between flue-derived efficiency and ambient temperature, other than the changes accounted for by the water injection. Figure 6-21 shows no correlation between flue-derived efficiency and ambient temperature.

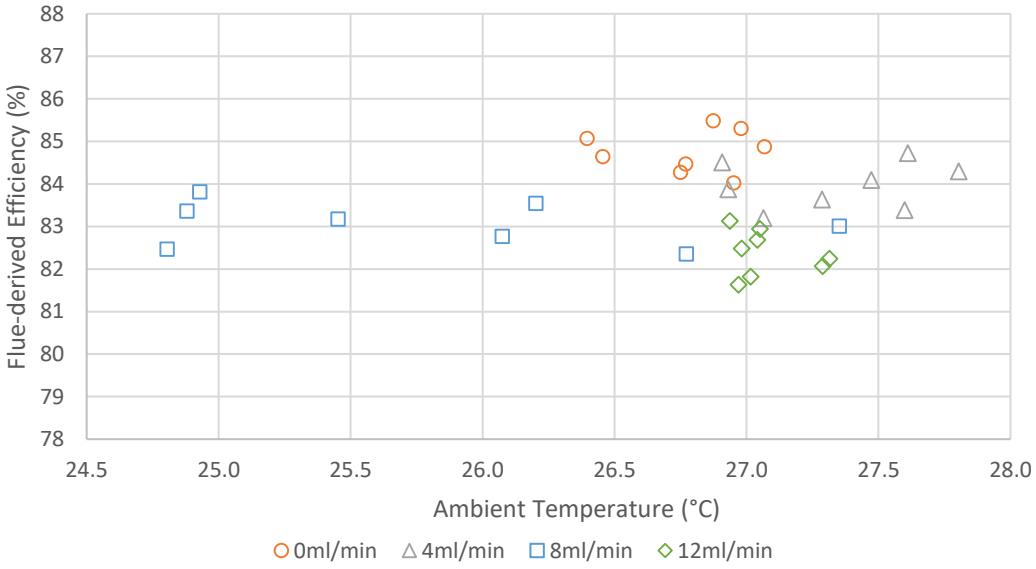

Figure 6-21 - Flue-derived efficiency vs. ambient temperature at various water injection rates, external injection

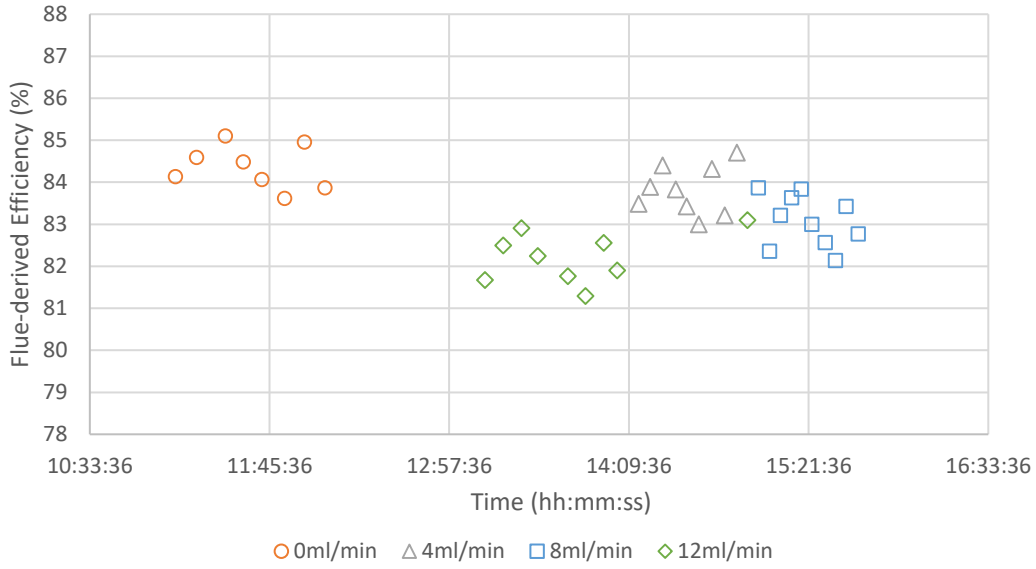

Figure 6-22 - Flue-derived efficiency vs. time at various water injection rates, internal injection

Figure 6-22 shows that there was poor correlation between flue-derived efficiency and time. There is a notable between the 0ml/min and 4ml/min tests, which coincided with a rig shutdown. The results are comparable to Figure 6-23, which was not interrupted by a shutdown, therefore this does not appear to have affected the flue-derived efficiency.

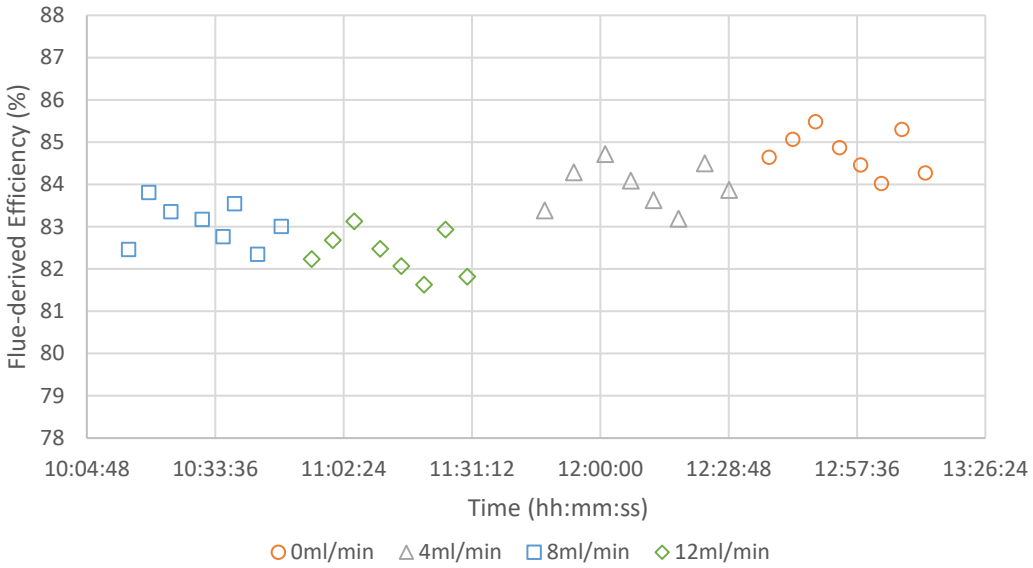

Figure 6-23 - Flue-derived efficiency vs. time at various water injection rates, external injection

6.3.4. Repeatability

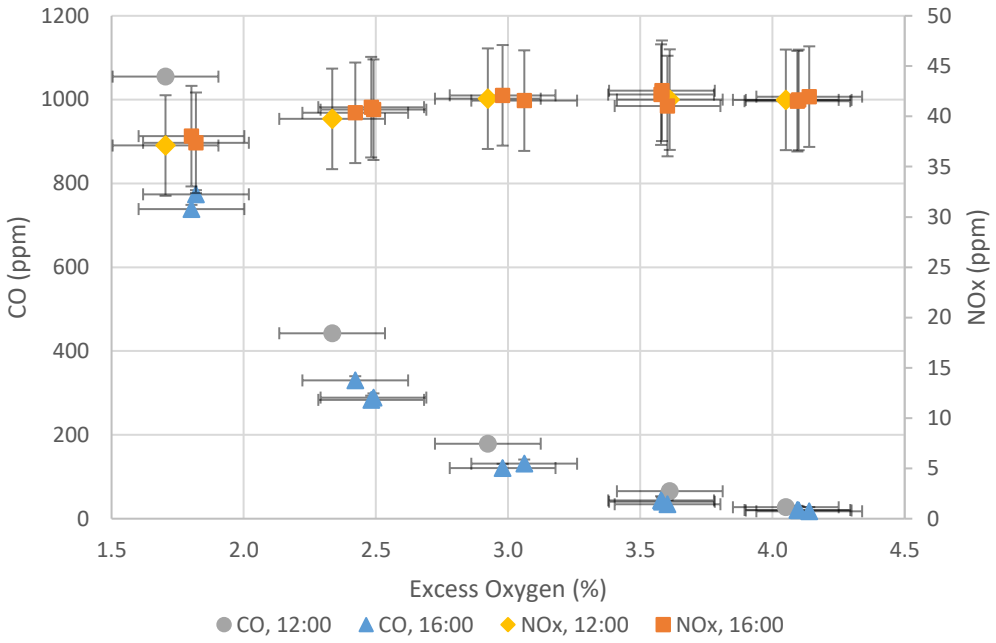

Figure 6-24 – CO and NOx vs. excess oxygen in the flue, no injection, data collected at the beginning and end of a test run, error bars based on sensor measurement uncertainty

Figure 6-24 shows that for both the CO and NO_x, the "dry" reference data collected at the beginning and the end of the experiment clearly correlated within the measurement uncertainty of the sensors. This means that any sensor drift across the duration of the test is within the expected limitations of the measurement equipment.

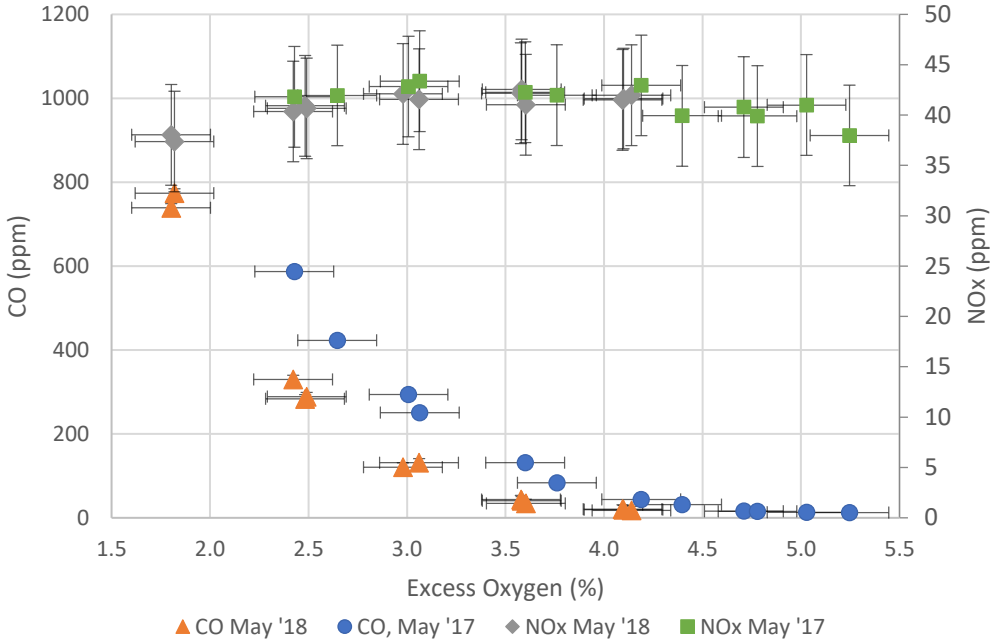

Figure 6-25 – CO and NOx vs. excess oxygen in the flue, no injection, data collected at the end two test runs conducted 1 year apart, error bars based on sensor measurement uncertainty

Figure 6-25 displays poor correlation between two sets of CO data that were collected a year apart, as the deviation between the them is clearly outside of the uncertainty limits. As the analyser was zeroed at the start of each test this is likely due to an actual degradation of the sensor over time, although it was recalibrated each year. Regardless, this highlights the importance of collecting the reference data at the beginning of each test, as Figure 6-24 has shown that the drift was not an issue within a single experiment, therefore relative differences within an experiment are unaffected.

Despite both the CO and NO_x sensors operating on the same principle, the NO_x sensor did not display significant deviation over the year.

6.4. Discussion

6.4.1. Carbon Monoxide

The results show that the reduction in CO emissions is dependent on the injection method, mass flow of water, and λ value. This is evidenced by the reduced effectiveness of the external nozzle compared to the internal nozzle, where the internal experiments resulted in substantial CO reductions in all sub-1.16 λ tests, while there were several cases in the external tests that displayed increased CO emissions.

Increasing CO implies incomplete combustion, as none would exist under stoichiometric combustion, therefore water addition caused incomplete combustion in the cases where CO increased. This could be due to the water causing instabilities in the flame as a result of its evaporation and subsequent expansion. It may also be causing partial quenching of the flame, inhibiting combustion.

It can also be seen that for both the internal and external tests, CO did not consistently decrease with λ. Instead it there were minima around λ 1.20, and CO began to increase for higher λ values. This was also displayed in the preliminary data, which showed an exponential increase with further increases in λ value. It was expected that the CO would decrease at higher λ values due to the increased availability of oxygen, therefore the increased volume flow through the burner must have resulted other effects that decreased the combustion efficiency. For example, the increased axial flow will have affected the flame profile and would also bring the axial velocity closer to the burning velocity, possibly altering the position of the flame or causing lift-off. These effects would result in flame instabilities and reduced combustion efficiency.

For the internal tests the CO minima in the 0ml/min cases also affected whether water addition increased or decreased CO. Below the minima CO tended to decrease with water injection, however it increased with CO above the minima. This inversion may explain why some studies such as De Jager et al. (2007) reported an increase in CO, whilst others such as De Paepe et al. (2016) reported a decrease; they could have been operating on either side of the inversion. It is possible that if any of the studies had expanded their range of λ values they may have also experienced the opposite water/CO effect. This shows that optimisation is required in order to achieve the full emissions reduction potential of water injection.

In the λ range tested for the water injection experiments it is not thought that the CO increase was due to the decrease in flame temperature with increasing air. Other combustions systems, such as in the Göke and Paschereit (2013) study, have been shown to operate at higher λ values with no such issue. As the increase in CO occurs with or without injection, the water appears to amplify the underlying trend rather than being the root cause. Water injection is not thought to cause lift-off as it initially exists in a low-volume liquid state and would therefore not contribute significantly to the volume flow of the reactants entering the combustion zone.

For the internal injection case the 8ml/min case that was most effective rather than the maximum of 12ml/min, and the 4m/min case was most effective for the external injection. This suggests that there is an optimal water flow rate which is dependent upon the injection location.

A decrease in CO with increasing water injection was observed in the mathematical model across all λ values, and it was concluded that this was due to the corresponding reduction in AFT resulting in decreased thermal dissociation of CO_2. The model did not capture the trend inversion in the data, where water injection increased CO towards higher λ values, therefore the experimental trend is likely caused by physical effects rather than chemical effects, which would have been identified by the model. This also explains the discrepancy between the model and the data, as the model did not incorporate fluid dynamics or heat transfer.

The general increase in CO towards stochiometric conditions is well documented in literature (Hanby, 1994).

6.4.2. Oxides of Nitrogen

Both the internal and external injection cases show the potential for reducing NO_x with water injection. It is also clear that the location of the injection nozzle affects the change in emissions, as the internal experiments showed reductions at all injection rates, however the external reductions shows some cases of increase.

As the flow rates of water and the atomisation characteristics of the nozzles where the same in both the internal and external cases, the cause of the variations in NO_x must have been a function of the distance that the nozzles were relative to the flame. In the internal case where the nozzle was directly before the swirl diffuser, the water interacting with the flame would have been fully atomised, increasing its mixing effectiveness and decreasing the time for it to evaporate. In the external case the injected water had to travel a longer path around the various components within the burner, and it is likely that it would have begun to coalesce and attach to the internal surfaces if the burner. This may have resulted in large droplets of water entering the combustion zone and possibly a film of water around the burner shroud, which would have reduced the mixing effectiveness and altered how and where the expanding evaporating water interacted with the flame. This in turn will have influenced NO_x generation.

6.4.3. Efficiency

In both the internal or external injection cases, the efficiency did not correlate with λ value. The lack of significant change in efficiency could be due to competing efficiency increasing and decreasing effects balancing out. It was in the preliminary data that at higher λ values the efficiency decreases, as there was a 30% decrease in efficiency across the range. This was concluded to be a result of thermal dilution, where the increasing flow of air caused an increasing quantity of heat to be lost through the flue. It was also seen in Figure 6-4 and Figure 6-5 that CO increased exponentially towards λ = 1, indicating incomplete combustion and therefore a decrease in combustion efficiency. The relatively constant efficiency in tested range could be due to the expected efficiency gains from decreasing excess air being countered by a decrease in efficiency due to incomplete combustion. Alternatively, the apparently constant efficiency could be due to limitations in the experimental setup, although the preliminary tests showed that the response rate of both the heat-transfer efficiency and emissions were suitable for the testing programme.

The heat-transfer efficiency also appears to be unaffected by the water injection rate as no correlation was exhibited. The injected water must have absorbed heat as it exited the boiler as steam, which would result in a decrease in heat-transfer efficiency if all other factors were constant. Therefore, the additional water in the combustion gases may have improved the heat-transfer between the combustion gases and the working fluid, resulting in a constant heat-transfer efficiency.

The flue-derived efficiency was calculated without consideration of heat transferred to the heated water or lost through insulation. It can be interpreted as the "expected efficiency" that would be achieved if the increased oxidising air and injected water simply absorbed heat from the combustion gases. The discrepancies between the heat-transfer efficiencies and flue-derived efficiencies are likely due to effects not captured by the boiler model. For example, the aforementioned increased humidity of the combustion gases resulting in increased heat transfer, or the cooler combustion gases in the injected cases resulting in reduced insulation losses.

6.4.4. Optimisation

Two of the aims of the research were to reduce CO and NOx emissions from the system. Whilst minimum and maximum values are easily identified, optimising both simultaneously is less straightforward, and depends upon the objective. As the heat-transfer efficiency experienced no measurable change over the range of λ setpoints, it does not factor in to the optimisation.

For both the internal and external nozzle cases, the minimum CO lies between λ values of 1.12 and 1.24, dependant on the water injection rate. For the internal nozzle, the 8ml/min case yielded up to 93.9% CO reductions when $\lambda < 1.12$, whilst none of the injection cases resulted in improvements above 1.24. The internal nozzle tended to result in higher CO reduction than the equivalent external case, for example, at $\lambda = 1.04$, the internal 12ml/min produced 58.6% less CO. Also, for the external cases below λ, both the 8ml/min and 12ml/min cases result in increased CO. It can therefore be deduced that the internal nozzle outperforms the external nozzle with regards to CO reduction. The absolute optimal point for the minimisation of

CO is the internal, 8ml/min, λ = 1.12 case, which resulted in 7ppm CO, a 95% reduction from the 0ml/min case.

For NOx reduction, both the internal and external nozzles cases produced minimum NOx at λ = 1.32, with a maximum between λ = 1.04 and 1.08 for the internal case, and at 1.12 for the external case. For the internal cases, NOx decreased with water injection, with the 8ml/min tests producing the minimum NOx across the λ range. The external nozzle results were less consistent, however the 12ml/min case generally resulted in minimum NOx for most λ setpoints, and achieved the minimum NOx for all the external cases at λ = 1.32. It should also be noted that the external 12ml/min cases tended to reduce NOx beyond the equivalent 12ml/min internal cases. The optimal parameters for NOx reduction would therefore be: external nozzle, 12ml/min water injection rate, λ = 1.32, which resulted in 20ppm NO_x, a 40% improvement over the non-injected case.

The optimal conditions for minimum CO and NOx do not align, indeed the nozzle location, injection rate, and λ setpoint are all different. Optimising for both would therefore cause neither to be optimal. There is also the matter of the optimisation goal, whereas before the minimum was clear, it is not so with two parameters. It could be assumed that both the NOx and CO are equally weighted, and that the overall minimum lies where the sum of both is at a minimum, however there is little justification for such an assumption. In fact, the legislation states limitations only for NO_x, therefore clearly they are not weighted equally.

The research set out to reduce both NO_x and CO, therefore from the perspective of this research increasing one at the detriment of another is not acceptable. It was found that for the internal nozzle, the optimal for both

CO and NO_x resided at λ = 1.16 with 8ml/min injection rate, resulting in reductions of 64% and 28% for CO and NOx, respectively. Similarly, for the external nozzle, the optimal point was at λ = 1.16 but with 12ml/min injection rate, resulting in reductions of 56% and 27% for CO and NO_x, respectively. The overall optimum is therefore the internal nozzle at the aforementioned parameters.

6.4.5. Flame Temperature and Excess Oxygen

Figure 6-8 suggested that internal water addition resulted in increased O_2 in the flue. The reduced NO_x generation will have caused a minor increase in O_2, though that does not account for the 0.4% increase. There was no evidence of the increased O_2 being caused by incomplete combustion, therefore it can only be concluded that the 0ml/min O2 or air mass flow measurements were anomalous. Figure 6-9 displayed a decrease in O_2 when water was added externally. This met expectations as the increased water flow resulted in a higher total volume flow, thus the proportional of O_2 reduced.

It was shown that the maximum flame temperatures at the monitored position were observed around a λ value of 1.12. For λ values above 1.12, the decrease in flame temperature was likely due to the thermal dilution effects of the increasing mass of air. For λ values less than 1.12, the decrease was likely caused by incomplete combustion due to a reducing quantity of available oxygen, resulting in reduced heat release in the combustion chamber. It could also have been related to a change in flame profile with volume flow.

It was also shown that water injection affects the flame temperature, generally decreasing it for the 4ml/min case, and increasing it in the 8ml/min

and 12ml/min. Theoretically the adiabatic flame temperature will decrease with increasing steam injection, however the data represents a point measurement, therefore only the temperature of that specific region of the flame is measured. The increase in flame temperature in the 8ml/min and 12ml/min cases are likely due to the vaporised water changing the flame profile, resulting in a warmer region around the probe, rather than a bulk increase in the flame temperature. Terhaar, Oberleithner and Paschereit (2014) also showed that steam, was shown to affect the flame profile and would therefore coincide with a change of flame temperature at a fixed point. If water affected the flame in a similar fashion, the changes in flame profile could cause incomplete combustion.

6.4.6. Sensitivity to External Effects

The heat-transfer efficiencies for the internal and external experiments appeared to be insensitive to ambient temperature and did not vary significantly with time, with the exception of the internal 0ml/min case, which was 1% higher than the injected cases. This could have been due to heat absorbed by the injected water, or to the cooler ambient temperature.

Figure 6-20 and Figure 6-21 showed that flue-derived efficiency did not vary unexpectedly with temperature. Figure 6-23 appeared to indicate some correlation between flue-derived efficiency and time as there is an increasing trend of approximately 2.39% across the 10:55 to 13:12 time period, however comparisons with Figure 6-15 show that this increase was due to the effect of decreasing steam injection rather than a time related effect. In both Figure 6-22 and Figure 6-23, for each water injection rate in isolation, there is no clear correlation between flue-derived efficiency and time. The observable peaks and troughs corresponded to changing λ

values. This means that the flue-derived efficiency was not influenced by time-based effects.

6.4.7. Limitations of Experimental Approach

The lack of correlation between either water injection or λ and heat-transfer efficiency showed that either their effects were neutralised as discussed, or that the effects could not be measured with the experimental setup. The latter was investigated during the preliminary phase. For example, the boiler water flow rate was adjusted to increase the temperature differential between the inlet and outlet, which minimised the effects of the temperature sensor, however it had negligible effect on the heat-transfer efficiency data. It was also demonstrated that the efficiency responded in a reasonable period at higher λ values, therefore it was concluded that the experimental setup was fit for purpose.

Evaluating the flue-derived efficiency involved calculating the heat lost to the atmosphere via the flue, and therefore indirectly calculated the useful heat transfer to the system. This means that the only difference between the flue-derived efficiency and heat-transfer efficiency should have been due to the heat lost to the environment, however that was not quantified.

The flame temperature was measured at one point, though it would have been preferable to have multiple readings in order to map the flame profile. This was originally intended, however platinum-based thermocouples were not an option, and of the five installed nickel-based thermocouples, only one remained operational during testing due to the excessive temperatures.

6.5. Conclusions

A commercially available burner for a sub-20kW boiler was successfully modified with water injection capabilities. This enabled the demonstration of NO_x and CO reductions across λ values of 1.00 to 1.32, with water injection rates of 4, 8, and 12ml/min.

It was found that CO emissions were dependant on the λ value, water injection rate, and injection location. The overall minimum CO of 7ppm occurred at a λ value of 1.12 with 8ml/min water, injected internally. At λ values less than 1.12 CO increased significantly, reaching 1054ppm in the worst measurable case. At λ values above 1.12 CO reached a peak of 141ppm. For the internal nozzle, at λ values below 1.24, water injection resulted in up to 95% CO reductions, however above 1.24 it caused an increase. With the external nozzle, only the 4ml/min case provided emissions reductions below λ = 1.12.

The minimum NO_x emissions were found at λ = 1.32 for both the internal and external experiments, where an overall minimum of 20ppm was observed for the external nozzle at 12ml/min, a 40% reduction over the non-injected tests. The maximum NO_x generally occurred between λ = 1.08, reaching a peak of 44ppm. For the internal cases increasing water flow rates tended to decrease NO_x, however in the external cases there was less consistency.

The optimal operating conditions for NO_x and CO do not match. However, it was found that using an internal nozzle with a λ setpoint of 1.16 and 8ml/min water resulted in the most favourable overall reductions, yielding simultaneous reductions of 64% and 28% for CO and NO_x, respectively.

The effect of different injection locations on the effectiveness of emissions reduction has been investigated. Generally, for the same nozzle and mass flow rate, injecting water into the air close to the flame yielded superior overall emissions reductions than injecting before the burner, hence the optimum solution utilises internal injection.

The heat-transfer efficiency data did not indicate any significant advantage or disadvantage to injection water, therefore while no efficiency gains were observed, emissions reductions were achieved without sacrificing efficiency.

The influence of injection method on emissions reductions was also explored. An atomising nozzle was required to ensure that the water was entrained by the air, as operating without one flooded the burner.

6.6. Chapter Summary

This chapter has documented the research involving injecting water into the burner of a boiler. This was achieved by modifying the burner to accommodate a hollow cone nozzle, injecting a range of water flow rates at various λ values, and measuring the resultant emissions and efficiency.

It was found that both NO_x and CO emissions could be reduced simultaneously without compromising efficiency. This was dependant on the λ value, the injection method, and the injection location. Generally, injecting the water closer to the flame yielded greater emissions reductions that injecting it before the burner. This was concluded to have been due to the water coalescing during its transit through the burner.

Chapter 7 investigates the addition of steam into the burner.

7. Steam Addition

7.1. Introduction

This chapter details the injection of steam into a natural gas burner. This involved modifying a gas jet-burner to incorporate a steam injection system, and then monitoring the effect of steam injection on the emissions and efficiency of the boiler system.

As shown by the literature review, the reduction of both CO and NO_x using steam injection has been demonstrated in gas turbine applications (Peltier, 2006). The purpose of this research was to determine if the same emissions reductions could be achieved for domestic or commercial boiler applications. NO_x reductions have been observed in industrial boilers, but not for domestic-scale boilers. Additionally, no evidence was found regarding CO reductions in boilers using steam injection, nor for retrofitting a burner for steam injection, therefore research in that area was warranted.

Contents

7.2. Methodology

7.2.1. Modification of Experimental Arrangement

As with the water injection experiments the basic experimental arrangement was modified, in this case for steam injection into the burner.

There were several potential locations at which steam could have been injected, including:

1. Into the air supply before the burner, which would inevitably cause the steam to condense in the ambient temperature air.
2. Into the air supply inside the burner, where the point of injection could be nearer to the combustion zone.
3. Into the fuel supply, which may have caused issues due to the low fuel pressure.
4. Directly into the flame, which would have been an option if the combustion chamber was accessible.

Two injection points were chosen in order to determine the effect of the location on the system. Firstly, into the air supply inside the burner before the diffuser plate, as shown in Figure 7-1. This ensured that the steam only interacted with the burner components that were rated for high temperatures, and that it had minimal residence time in the lower temperature air. The second injection point was into the air before it entered the burner. It was calculated that the steam would not damage the burner due to significantly higher mass of air it was mixing with. Although it was estimated that even superheated steam would condense before it reached the combustion zone, identifying the effect of this on the system was of

interest, as if the results were similar then modification of the burner would not have been necessary.

The position shown in Figure 7-1 was chosen to ensure that the steam did not damage any of the lower temperature components further inside the assembly, yet could still interact with the swirl diffuser.

Figure 7-1 - Burner modification for steam input

For the preliminary steam injection experiments an electric steam generator was used to raise steam fed from the deionised water tank, and the temperature was maintained at 170°C using a temperature controller.

Due to the shortcomings of the electrical steam generator, detailed in Appendix A, an improved steam generation system was designed.

The new steam generator consisted of a brazed plate heat exchanger with high-pressure condensing plant steam on the hot side, and evaporating water on the cold side, as shown in Figure 7-2.

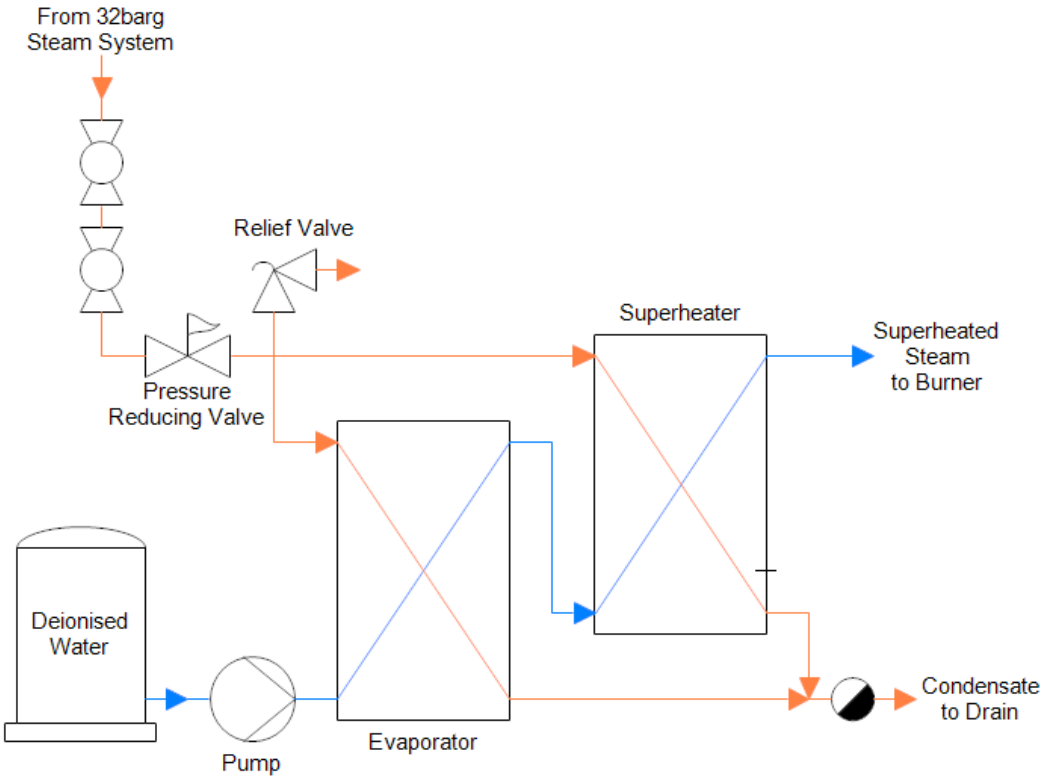

Figure 7-2 - Clean steam generation system

The steam trap was used to ensure that condensate was drained away from the heat exchanger's hot side to promote heat transfer through steam condensation.

The brazed plate heat exchanger was chosen due to its compactness, pressure rating, and large heat transfer area. It was calculated that the steam exiting the cold side of the heat exchanger would be effectively at the

hot side temperature of 184°C. This resulted in steam that was superheated by 84°C at atmospheric pressure. The superheat was important as the steam had to cool to saturation temperature before it began condensing, creating a “buffer” that ensured that only dry steam entered the burner.

During commissioning it was found that the steam inlet temperature was 100°C, indicating that the fluid was at saturation temperature and not superheated. This meant that it also had an unknown vapour fraction, rendering it unsuitable for the experimental work. Achieving superheated steam at the burner required either perfect insulation to eliminate heat loss, or extra heat to counter the loss. Vacuum insulated steam pipe technology existed, however it was still in development and was not designed for such low flows. The saturated steam was therefore routed through the dedicated superheater displayed in Figure 7-2, which resulted in the required superheated steam.

The preliminary experiments also showed that the air flow rate varied despite a fixed valve position, possibly due to other demands on the compressed air system causing pressure fluctuations. To address this an upgraded flow meter was installed, which incorporated a control valve and proportional-integral-derivative controller. By controlling the meter with LabVIEW via RS232, a flow rate could be specified which the flow controller maintained regardless of upstream conditions.

7.2.2. Test Programme

During the preliminary experiments the air flow rate was varied whilst maintaining a constant fuel flow rate, and for each air flow rate set point, varying steam injection rates were tested. It was found that achieving a steady superheated steam temperature could take up to 10min, therefore the approach was changed so that varying air flow rates were examined at constant steam injection flow rates, as this reduced the fuel consumed whilst waiting for equilibrium.

Steam injection rates of 4, 8, and 12ml/min (before vaporisation) were chosen for comparison with the water tests. For each steam flow rate, various air-fuel equivalence ratios were tested, ranging from 1.00 to 1.32.

At the internal injection point tests were initially conducted with the steam outlet show in Figure 7-1. These were then followed by solid-cone nozzle tests at both of the internal and external injection points.

As for the water tests, the volume fraction of CO and NO_x were measured. For the internal jet case HC data was also collected, however a sensor failure prevented data collection for the other cases. The changes in volume fraction of O_2 was also measured.

Flame temperature data was collected at a single point using a type-K thermocouple, to determine its relationship with λ and steam injection rate.

Data was also collected to enable the calculation of heat-transfer and flue-derived efficiencies. Ambient temperature changes were also measured to check for correlation.

7.3. Results

7.3.1. Emissions

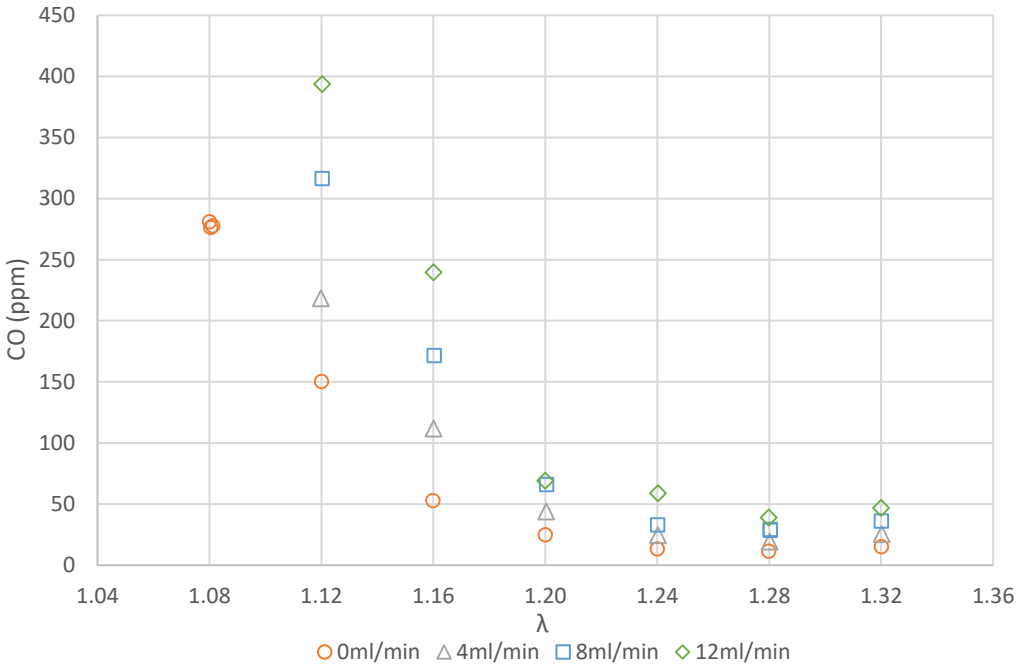

Figure 7-3 – CO vs λ at various steam injection rates (water equivalent), internal steam jet

Figure 7-3 displays the CO volume fraction data for the internal steam jet case. It can be seen that there was a distinct increase in CO with increasing steam flow. At λ = 1.12, 0ml/min steam resulted in 150 ppm CO, increasing to 394ppm at 12ml/min steam, which equated to a 243% increase. This trend remains true across the λ range, with a maximum percentage difference between the 0ml/min and 12ml/min cases of 355% at λ = 1.28.

It can also be seen that there was an exponential increase in CO with decreasing λ in the range of λ = 1.28 to 1.08, and that there was also an increase in CO from λ = 1.28 to 1.32.

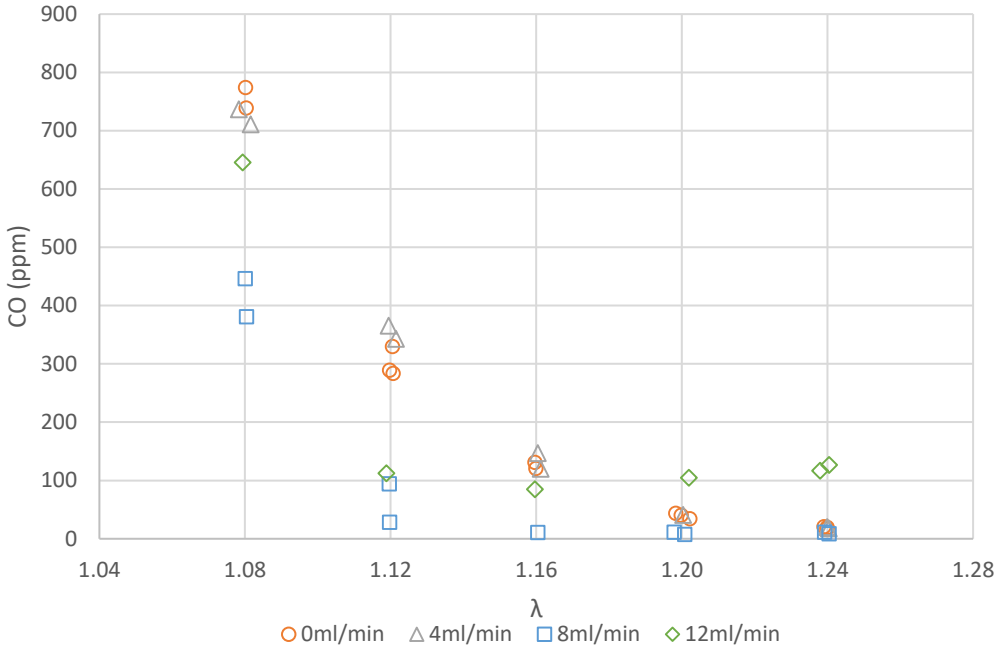

Figure 7-4 – CO vs λ at various steam injection rates (water equivalent), internal steam nozzle

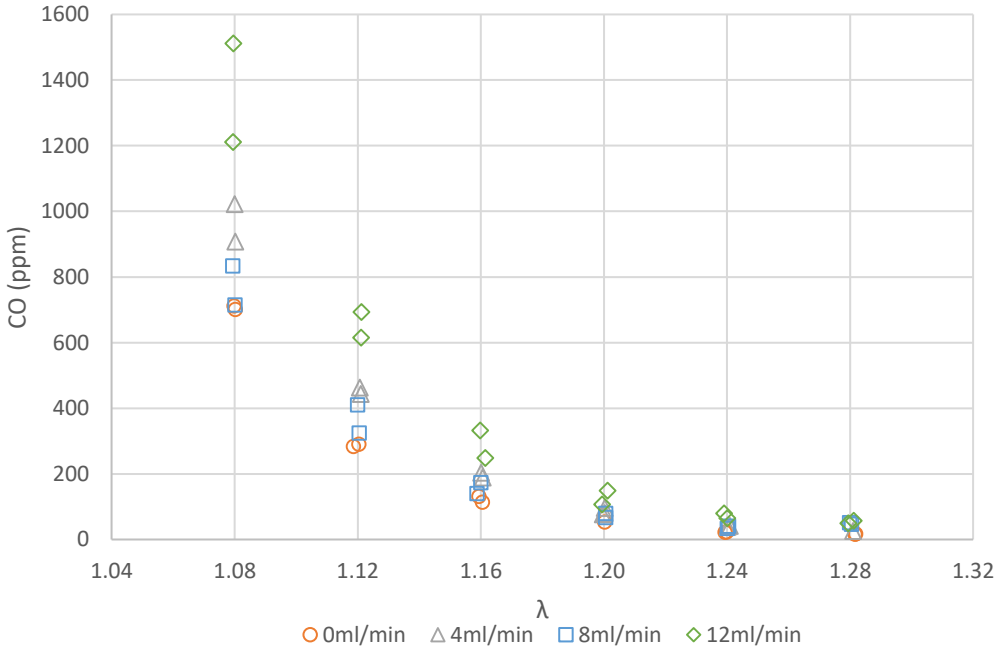

Figure 7-5 – CO vs λ at various steam injection rates (water equivalent), external steam nozzle

Figure 7-4 shows that injecting water through an internal nozzle affected CO emissions in a non-linear fashion. For the 0ml/min, CO increased exponentially from approximately 20ppm at a λ value of 1.24 to 757ppm at 1.08. At 4ml/min there was insignificant change compared to the dry case for any λ value, however at 8ml/min there is a marked reduction. For example, at a λ value of 1.08 there is a 45% reduction in CO from 757ppm to 414ppm. Additionally, for λ values between 1.16 and 1.24, an 8ml/min injection rate maintained CO within a range of 11ppm to 7ppm, whereas the dry case varied between 120ppm and 18ppm. In the 12ml/min CO emissions were reduced approximately 15% to 645ppm at a λ value of 1.08, reached a minimum of 85ppm at 1.16, and then steadily rose to 127ppm at 1.24. At an λ value of approximately 1.17, the 12ml/min steam injection began to increase CO emissions rather than decreasing them, up to approximately 520% at 1.24.

It can be seen in Figure 7-5 that injecting steam into the air through an externally mounted nozzle resulted in increases of CO across all injection cases. For the 12ml/min case, this increase spans from approximately 91% at λ 1.08 to 235% at 1.28. The increase in CO was not proportional to the steam injected. For example, at λ 1.08, 4ml/min resulted in an increase of approximately 35%, while 8ml/min increased CO by approximately 9%. For all cases CO decreased with increasing λ, with the exception of 8ml/min, which showed a 32% increase from λ 1.24 to 1.28.

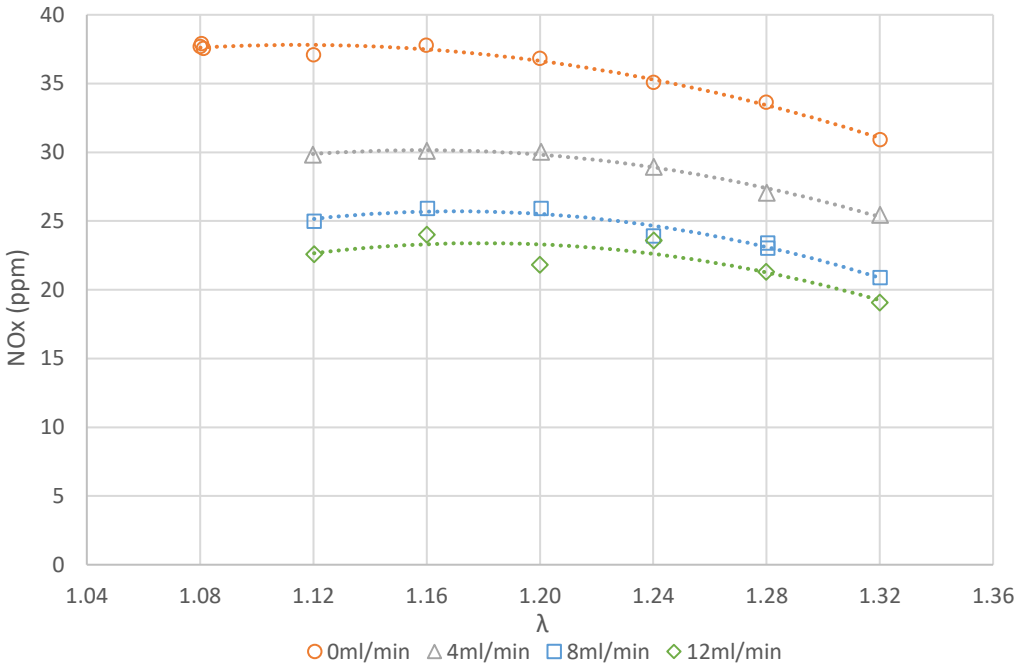

Figure 7-6 - NOx vs λ at various steam injection rates (water equivalent), internal steam jet

For the steam jet case there was a decrease in NO_x with increasing steam flow, shown in Figure 7-6. The NO_x reduction for each additional 4ml/min increment in steam flow rate decreased. NO_x appeared to peak at different λ values for each steam flow rate.

Steam injection through an internal nozzle also resulted in a decrease in NO_x, as shown by Figure 7-7. For the 4ml/min and 8ml/min cases, each 4ml/min reduced NO_x by a mean of 10.5% of the dry case across the 1.08 to 1.24 λ range. The decrease between 8ml/min and 12ml/min was more pronounced, at a mean of 19.3%. The peak NO_x value rested at a λ value of approximately 1.20 for injection rates up to 8ml/min, and moved to 1.16 for 12ml/min.

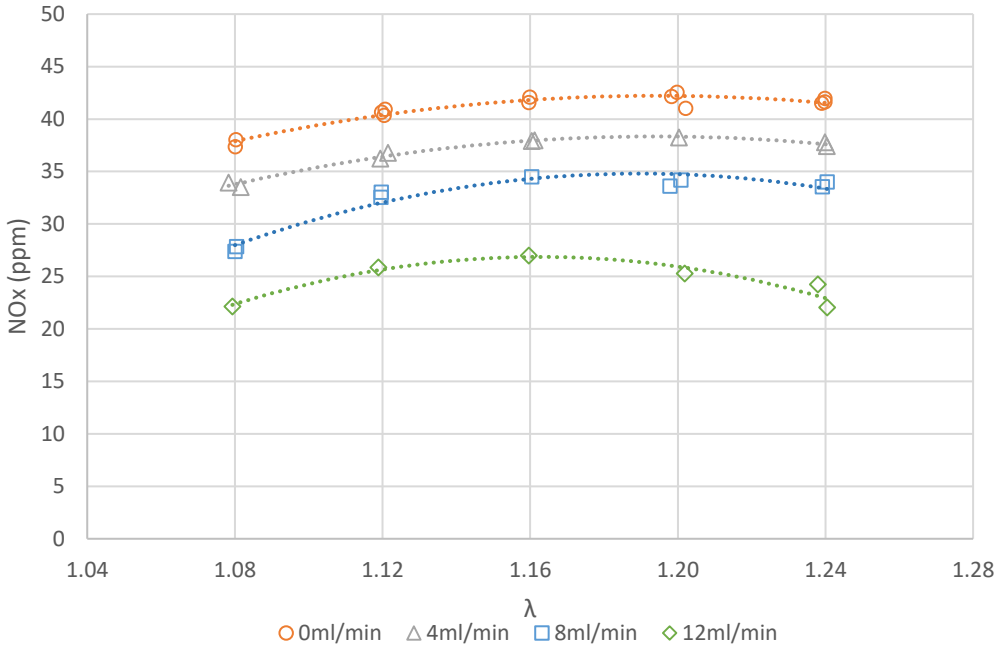

Figure 7-7 – NO_x vs λ at various steam injection rates (water equivalent), internal steam nozzle

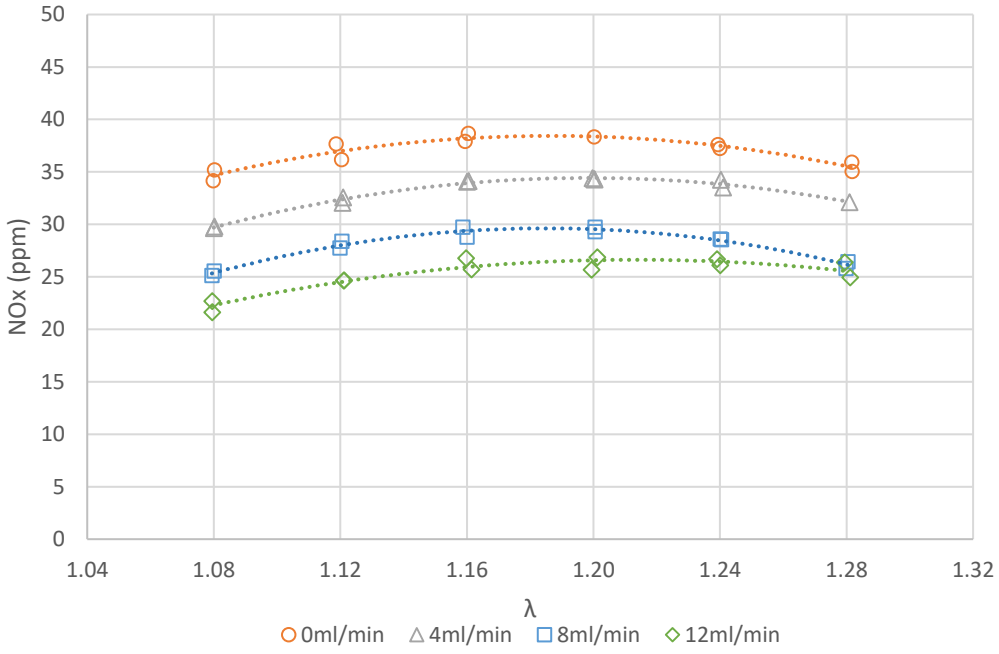

Figure 7-8 – NO_x vs λ at various steam injection rates (water equivalent), external steam nozzle

Figure 7-8 shows that the external steam nozzle case exhibited similar trends to the other cases, as NO_x decreased with steam addition. The 4ml/min, 8ml/min, and 12ml/min cases resulted in mean 10.4%, 24.3%, and 31.3% reductions respectively. The NO_x values peaked around λ 1.20.

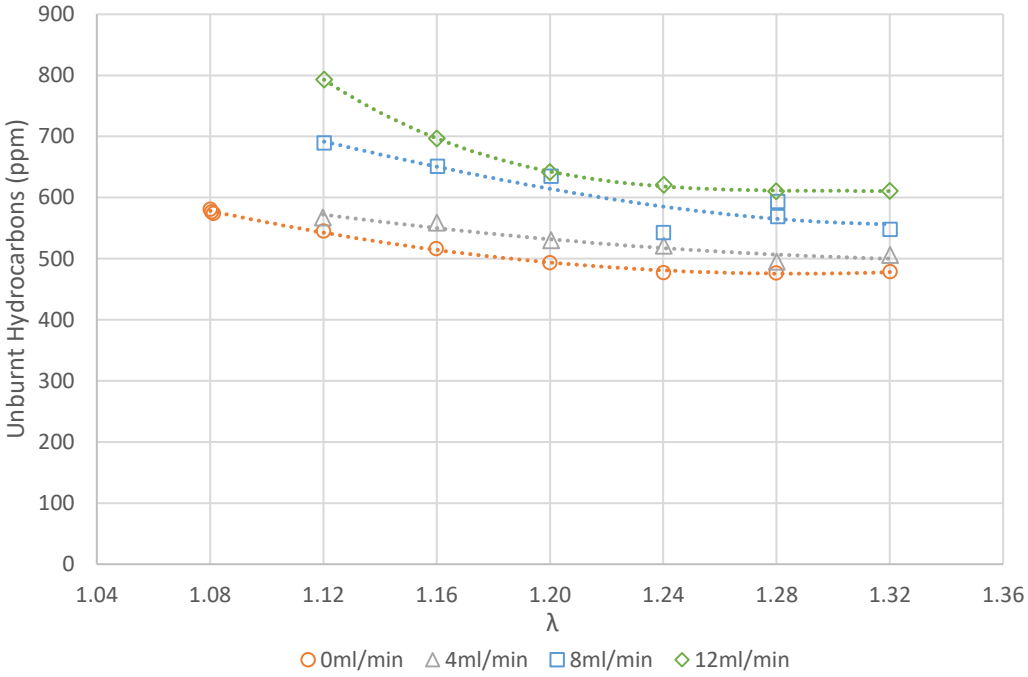

Figure 7-9 – HC vs λ at various steam injection rates (water equivalent), internal steam jet

Figure 7-9 shows that HC increased with increasing steam flow across the range of λ values tested. For example at λ = 1.12, 0ml/min steam results in 545 ppm HC, which increased by 145% to 793 ppm with 12ml/min steam. This indicates that the steam was causing incomplete combustion.

HC tended to decrease with increasing λ regardless of injection rate, which was expected as an increase in oxygen availability resulted in a higher probability of the fuel reacting within the combustion zone.

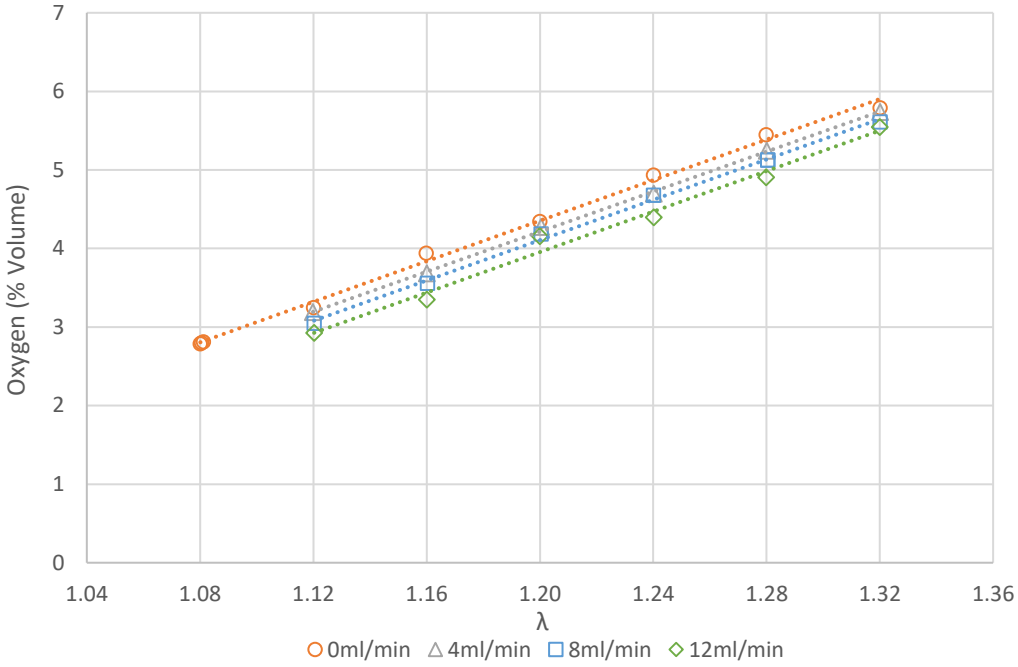

Figure 7-10 – O_2 vs λ at various steam injection rates (water equivalent), internal steam jet

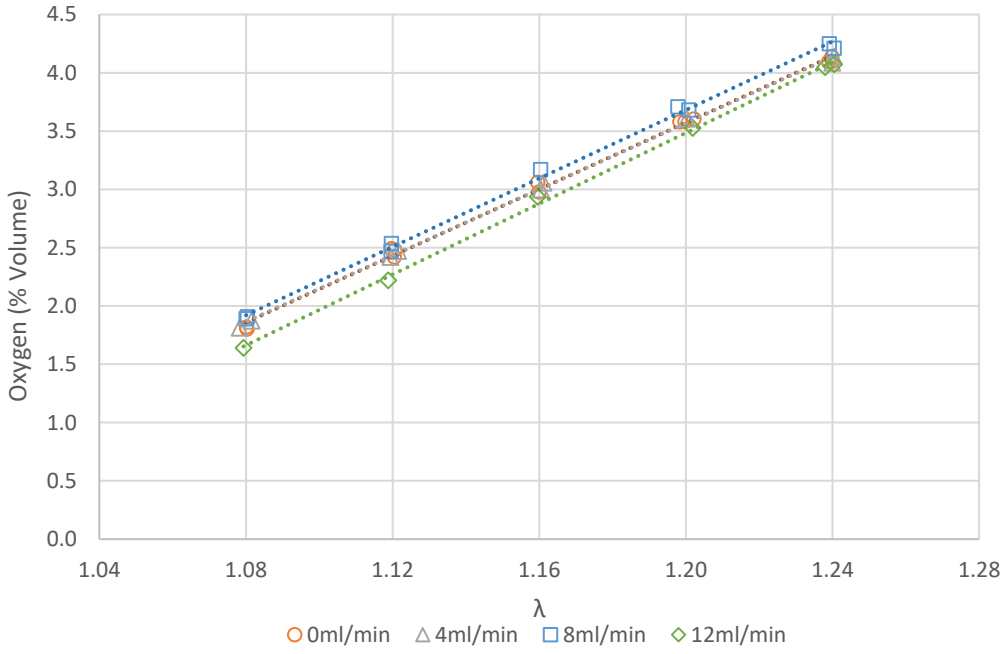

Figure 7-11 – O_2 vs λ at various steam injection rates (water equivalent), internal steam nozzle

Figure 7-10 indicates that the oxygen content in the exhaust decreased approximately linearly with increasing rates of steam injection. It exhibited a mean 8.8% reduction (as a percentage of the dry case O_2) at 12ml/min and increased with increasing λ as expected.

Figure 7-11 shows that O_2 in the flue changes with the various injection rates. As with the CO emissions, the 4ml/min case did not change significantly from the dry case. The 8ml/min case increased O_2 by a mean of 3%, while the 12ml/min case decreased it by a mean of 4%.

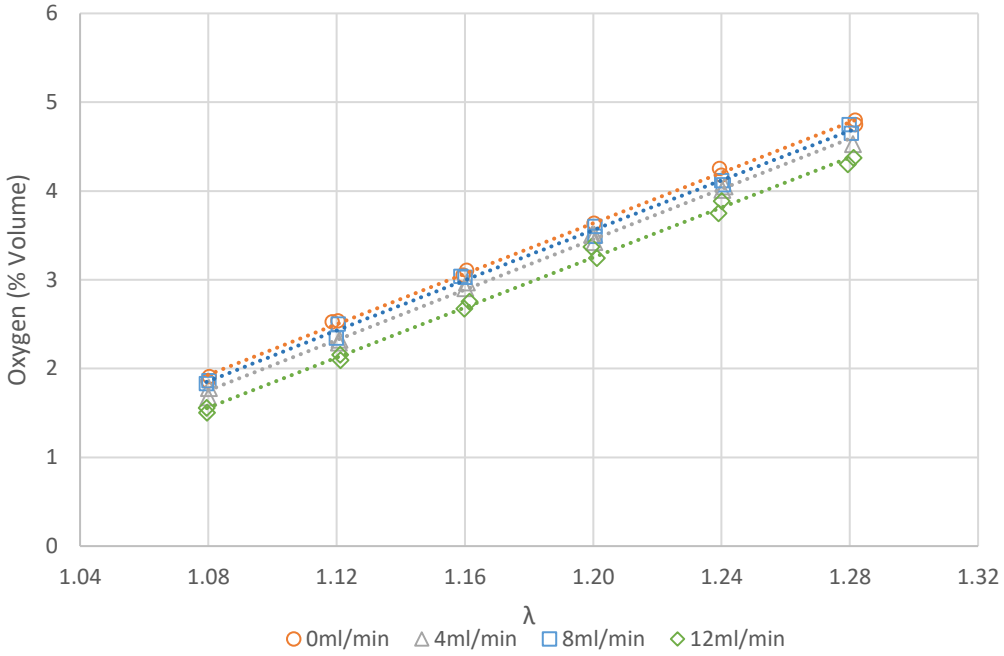

Figure 7-12 – O2 vs λ at various steam injection rates (water equivalent), external steam nozzle

Figure 7-12 again shows a decrease in O_2 with steam injection, though the decrease was not proportional to the injection rate. For the 4ml/min, 8ml/min, and 12ml/min cases the mean O_2 reductions were 8.1%, 2.4%, and 11.4% respectively.

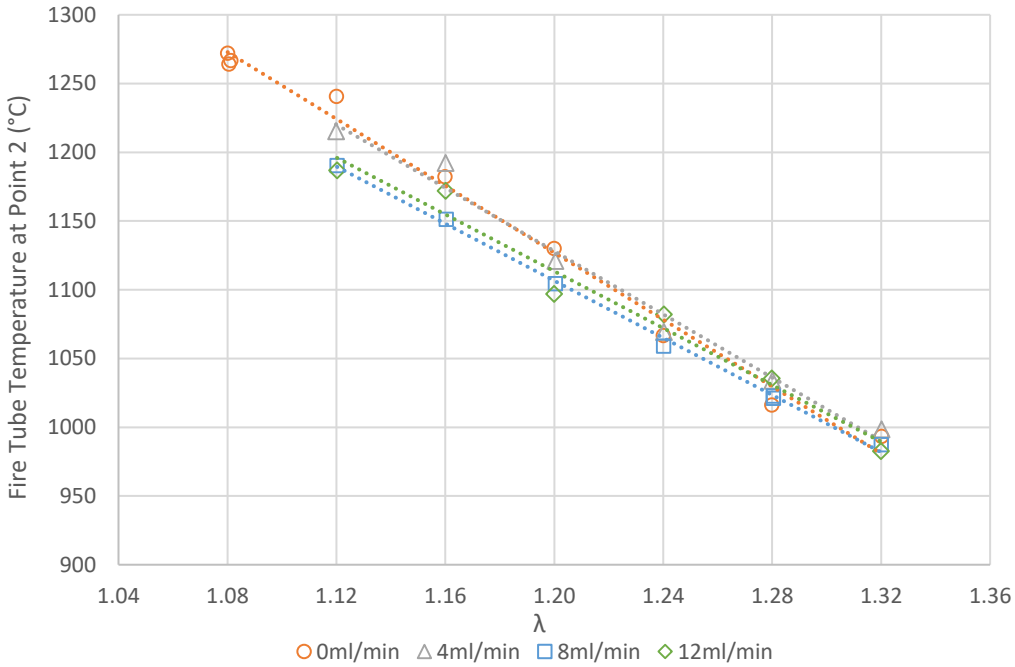

Figure 7-13 – Point 2 flame temperature vs λ at various steam injection rates (water equivalent), internal steam jet

Figure 7-13 shows that there was a distinct linear decrease in the flame temperature at point 2 as the λ value increased for all steam flows tested. In the 0ml/min case, the flame temperature decreased 21.8% from approximately 1270°C at λ = 1.06, to 993°C at λ = 1.32. Figure 7-13 also shows that there was a reduction in flame temperature with steam injection at lower λ values, however the results converge as λ increases.

Figure 7-14 shows that steam injection through the internal nozzle resulted in a reduced flame temperature for the 4ml/min and 12ml/min cases, up to 4% and 21% respectively. The 8ml/min case also reduced flame temperatures in the 1.08 to 1.20 λ range, but resulted in a 2% increase at 1.24. It is also notable that at a λ value of 1.08 there was a progressively increasing temperature reduction with each 4ml/min, and while the other cases followed that pattern up to 1.24, the 8ml/min is distinctly different.

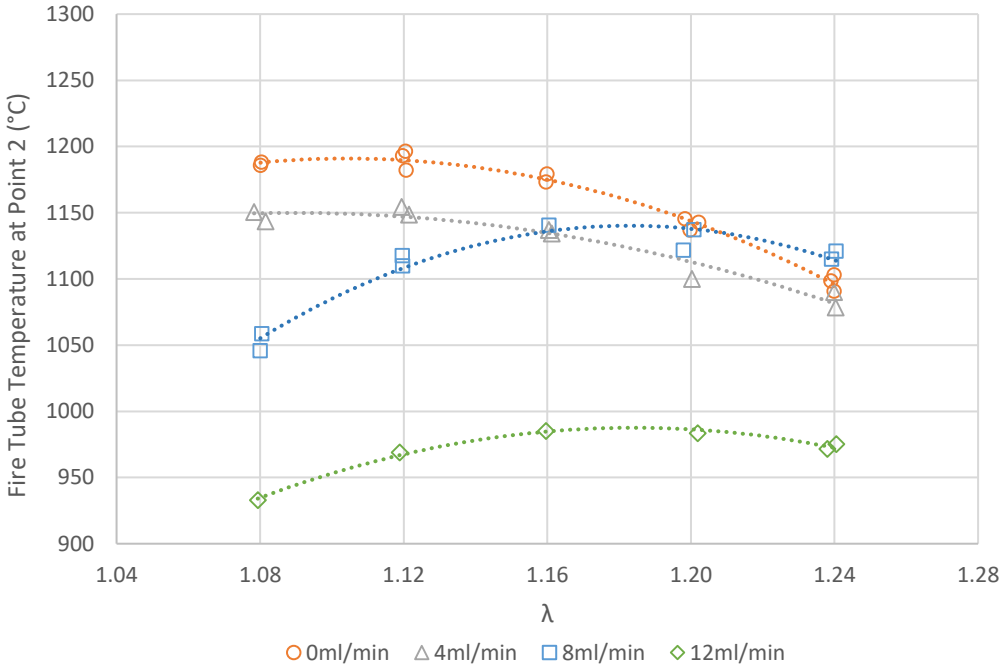

Figure 7-14 – Point 2 flame temperature vs λ at various steam injection rates (water equivalent), internal steam nozzle

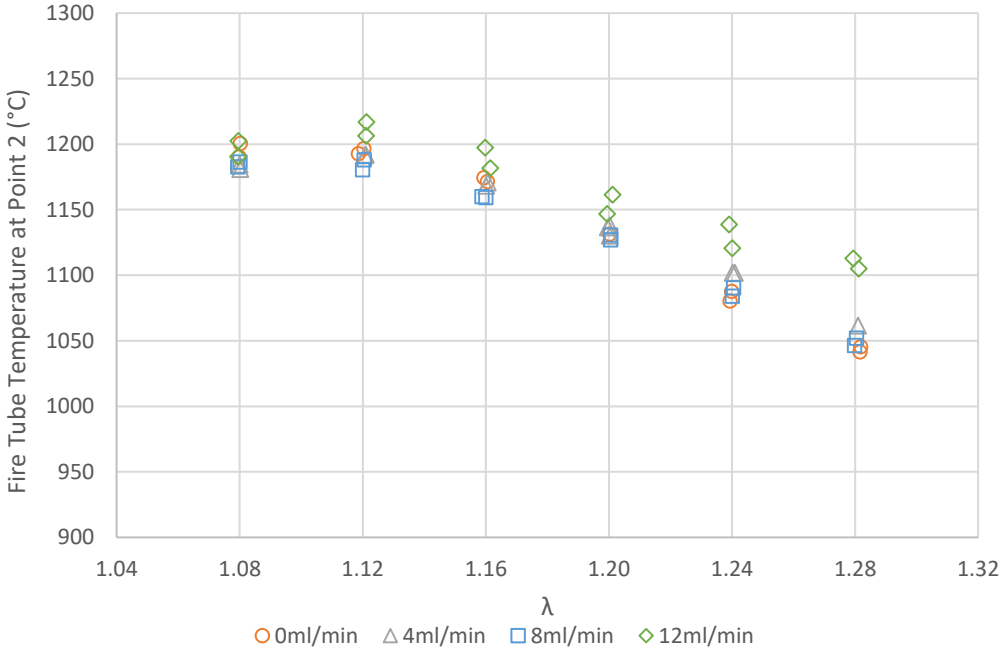

Figure 7-15 – Point 2 flame temperature vs λ at various steam injection rates (water equivalent), external steam nozzle

Each case follows a parabolic trend, with the 0 to 4ml/min cases reaching a maximum between a λ value of 1.08 and 1.12, and the 8 to 12ml/min cases peaking between 1.16 and 1.20.

Figure 7-15 shows that injecting water through an external nozzle increases the point 2 flame temperature by up to 6.3% for the 12ml/min case. For the 4ml/min and 8ml/min cases the flame temperature increased at a λ values less than 1.16 and 1.22 respectively, and increased at higher values. Across all cases there was a general increase in flame temperature between λ 1.08 and 1.12, declining thereafter.

7.3.2. Efficiency

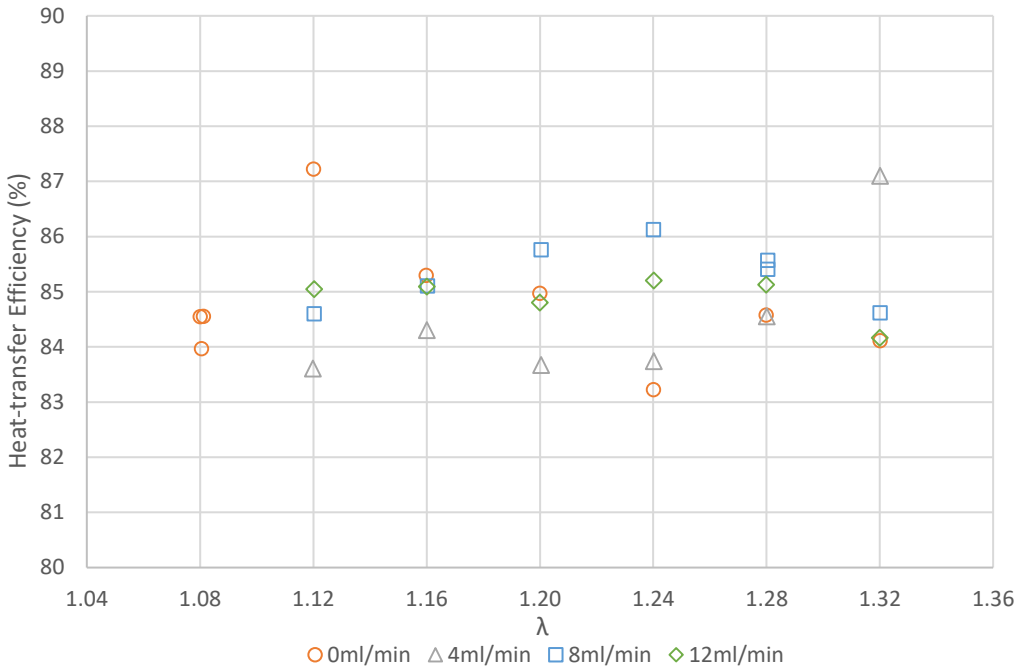

Figure 7-16 – Heat-transfer efficiency vs λ at various steam injection rates (water equivalent), internal steam jet

Figure 7-16 shows that there was poor correlation between λ and heat-transfer efficiency. The 0ml/min case displays a high degree of variability, containing both the maxima and minima of the data sets, and it also shows little discernible trend. In the 4ml/min case the efficiency tends to increase with increasing λ, rising from 80.4% at λ = 1.20 to 83.7% at 1.32%. The 8ml/min case shows another different trend, increasing from 81.3% to a peak of 82.8% at λ = 1.24, before decreasing back to 81.3% at λ = 1.32. Finally, the 12ml/min case remains within 81.5% to 81.8% other than for λ = 1.32, where it falls to 80.9%.

There was no correlation between steam injection and heat-transfer efficiency. Each of the cases exhibited individual, overlapping trends. The internal steam nozzle experiment resulted in similar trends to the steam jet as shown by Figure 7-17. None of the four cases show a definitive trend, and all lie within a 2% efficiency band.

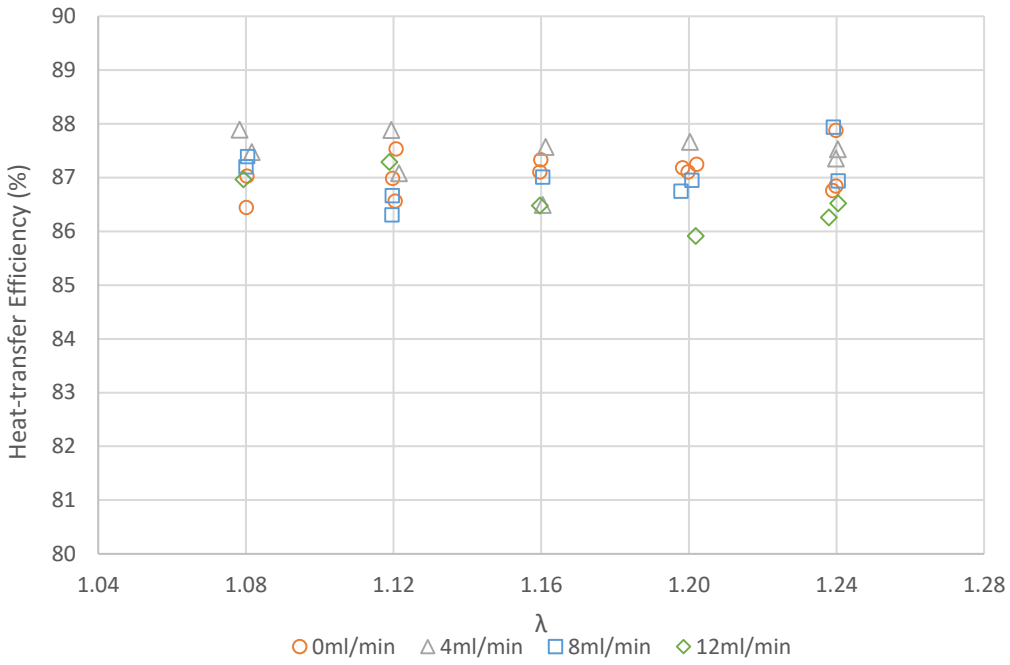

Figure 7-17 – Heat-transfer efficiency vs λ at various steam injection rates (water equivalent), internal steam nozzle

As with the steam jet and internal nozzle experiments, the external nozzle heat-transfer efficiency shows an insensitivity to the steam injection rate. This is shown by Figure 7-18 where all the results are scattered within a 3% range.

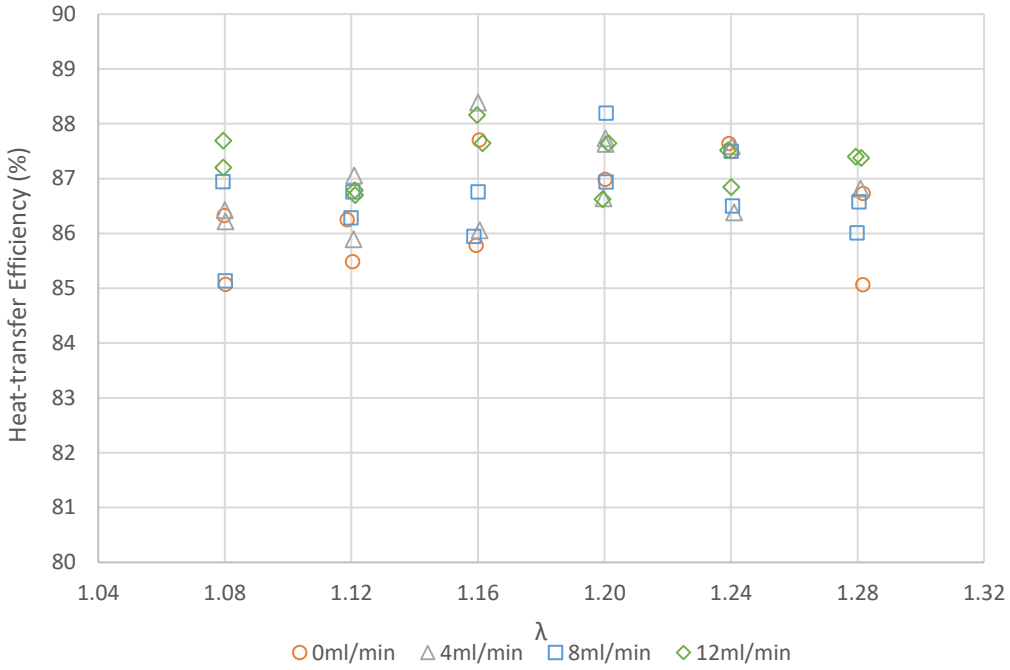

Figure 7-18 – Heat-transfer efficiency vs λ at various steam injection rates (water equivalent), external steam nozzle

Figure 7-19 shows clear correlation between λ, steam injection, and flue-derived efficiency. The flue-derived efficiency decreases linearly with increasing λ, an effect which is consistent regardless of steam injection rate and equates to a 0.55% decrease for each 0.1 increase in λ. There is approximately a 0.2% efficiency loss when the steam injection rate is increased from 0ml/min to 12ml/min. Figure 7-20 shows similar trends for the internal steam nozzle experiment, where efficiency decreases by approximately 0.45% for each 0.1 increase in λ. There was a 0.09% efficiency loss from the 0ml/min to the 12ml/min case, however the 4ml/min resulted in a 0.03% increase.

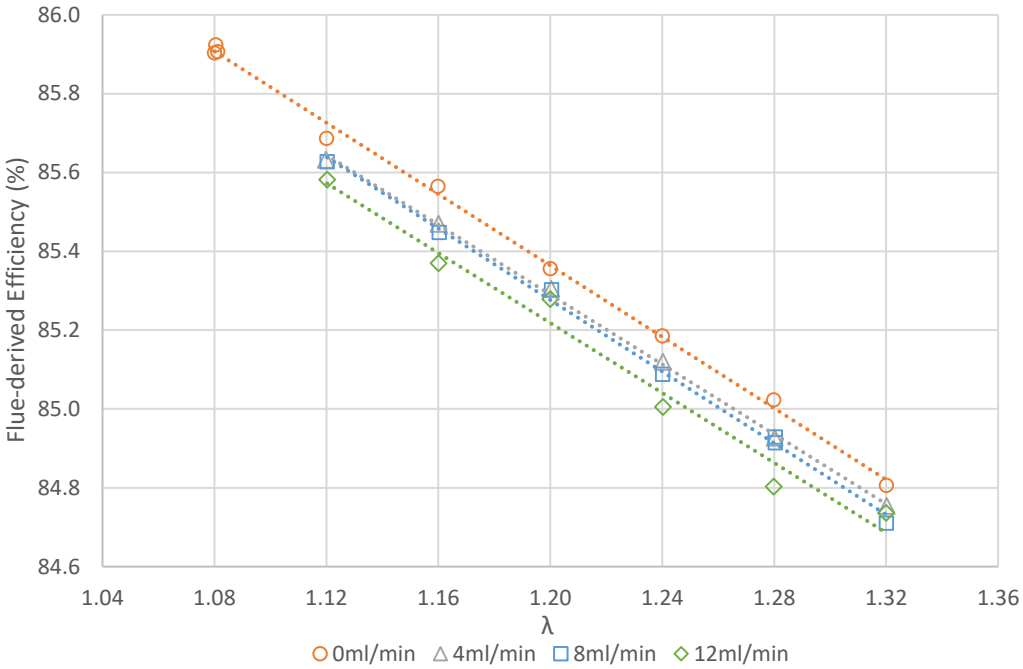

Figure 7-19 – Flue-derived Efficiency vs λ at various steam injection rates (water equivalent), internal steam jet

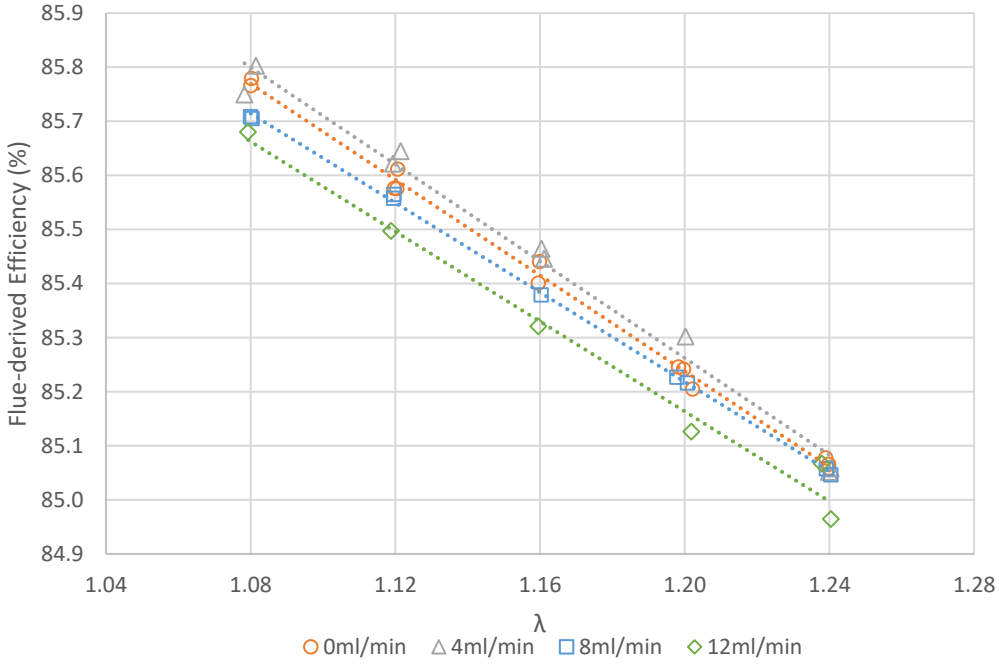

Figure 7-20 – Flue-derived Efficiency vs λ at various steam injection rates (water equivalent), internal steam nozzle

For the external nozzle case Figure 7-21 displays a 0.53% decrease for each 0.1 increase in λ regardless of steam injection rate. Steam addition resulted in 0.12%, 0.11%, and 0.27% decreases in flue-derived efficiency for the 4ml/min, 8ml/min, and 12ml/min cases respectively.

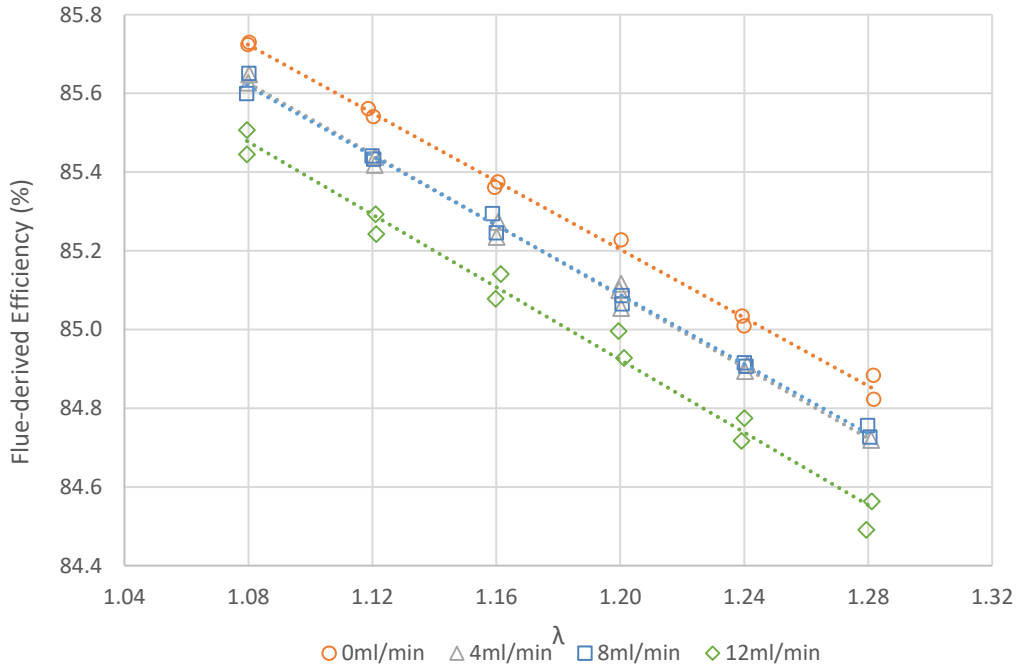

Figure 7-21 – Flue-derived Efficiency vs λ at various steam injection rates (water equivalent), external steam nozzle

7.3.3. Sensitivity to External Factors

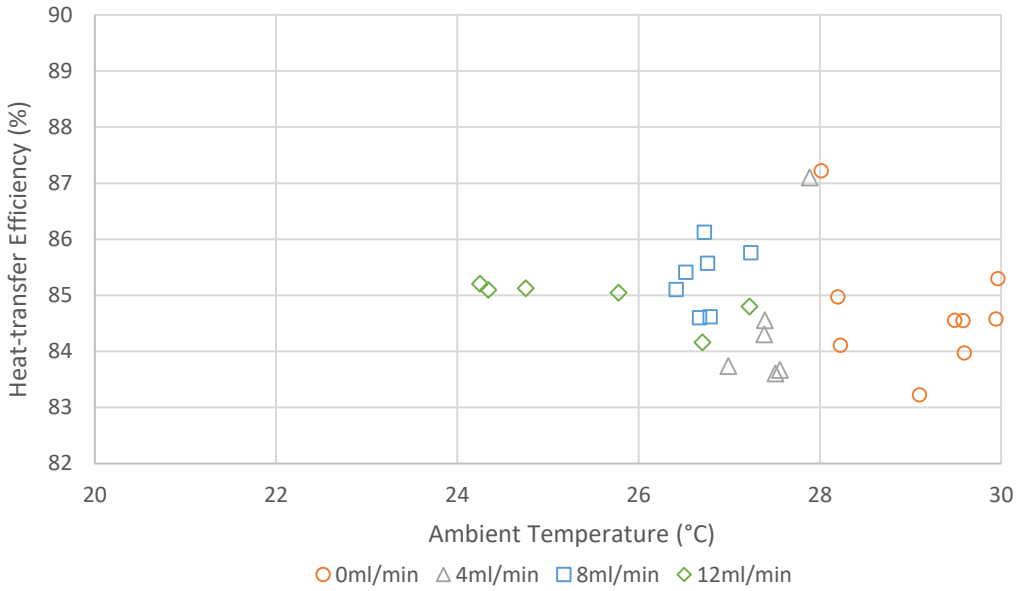

Figure 7-22 – Heat-transfer efficiency vs. ambient temperature at various steam injection rates (water equivalent), internal steam jet

Figure 7-22 shows that the ambient temperature ranged from 24.3°C to 30.0°C over the course of the experiment. Comparing Figure 7-22 with Figure 7-25 shows that the temperature rise corresponded approximately to the time of the test. Despite the increase in ambient temperature, it did not correlate with the heat-transfer efficiency for any steam flow rate. This shows that the experimental results in the range tested were insensitive to the 5.7°C variability in ambient temperature. Despite the 12ml/min case having the greatest temperature range of 3.0°C, it had minimal efficiency deviation. This shows that ambient temperature fluctuations were not the cause of the variability in the 0ml/min case.

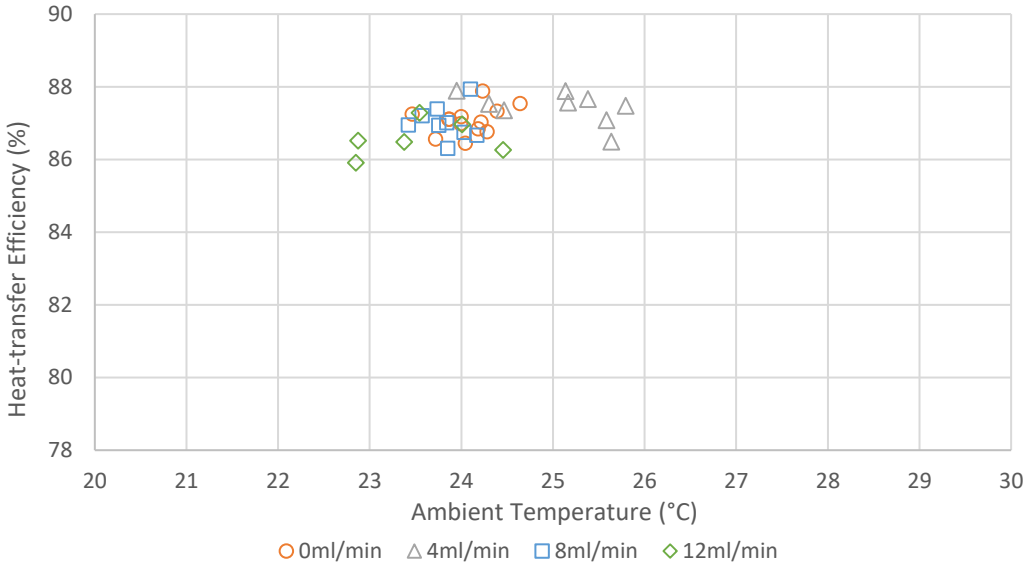

Figure 7-23 – Heat-transfer efficiency vs. ambient temperature at various steam injection rates (water equivalent), internal steam nozzle

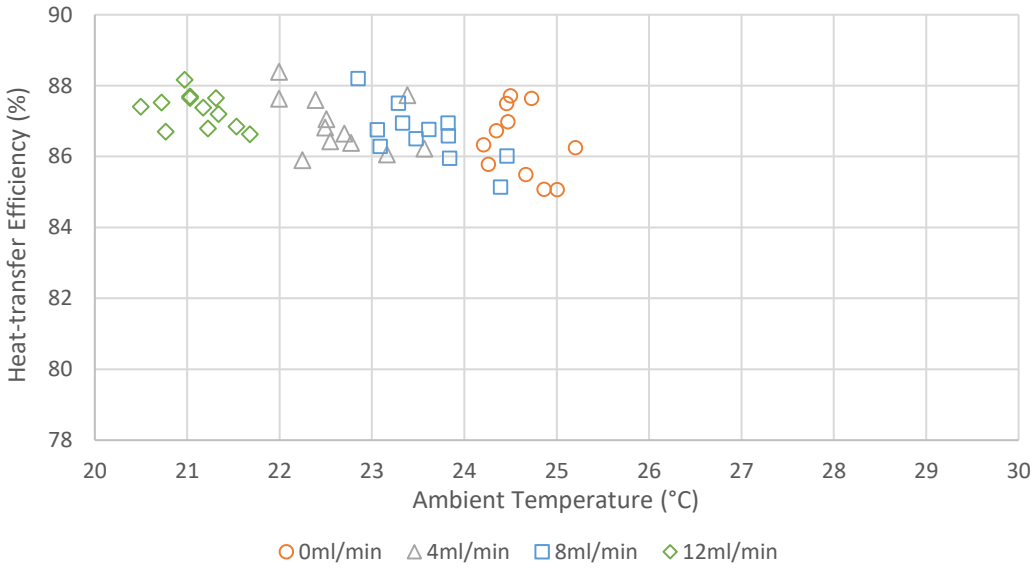

Figure 7-24 – Heat-transfer efficiency vs. ambient temperature at various steam injection rates (water equivalent), external steam nozzle

Figure 7-23 again shows no significant correlation between the 2.0% range of heat-transfer efficiencies and the 3.0°C ambient temperature variation for the internal nozzle experiment. The external nozzle results displayed in Figure 7-24 show an approximate 1.5% decrease in heat-transfer efficiency as the temperature increases from 20.5°C to 25.2°C, indicating that the experiment may have been influenced by the ambient temperature.

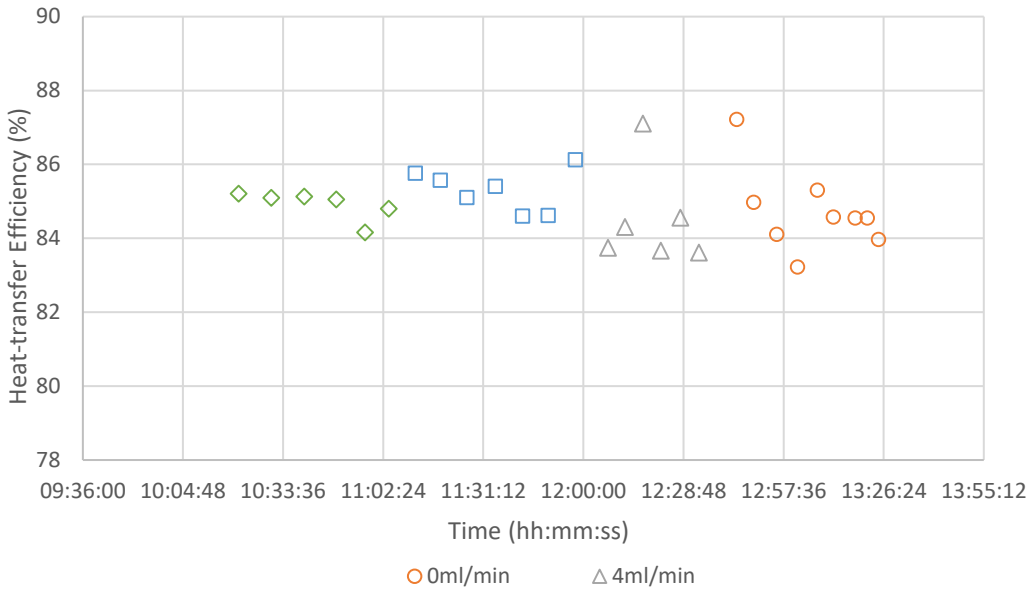

Figure 7-25 – Heat-transfer efficiency vs time at various steam injection rates (water equivalent), internal steam jet

Figure 7-25 and Figure 7-26 show no correlation between heat-transfer efficiency and time, therefore the internal results were time-independent and not subject to errors caused by effects such as equipment warm-up. The external experiment in Figure 7-27 features a decrease in heat-transfer efficiency with time, which corresponds with the increase in ambient temperature in Figure 7-24.

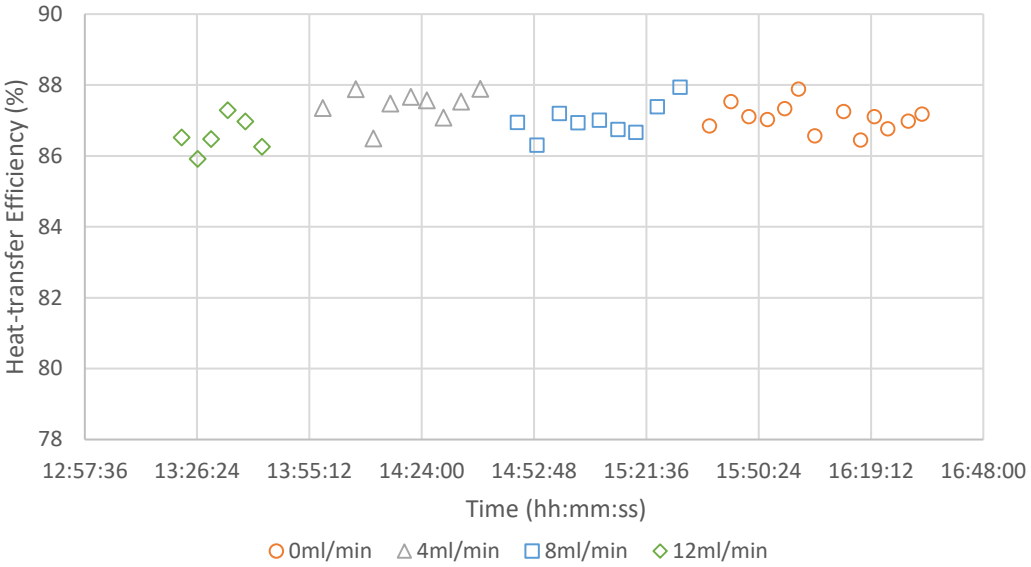

Figure 7-26 – Heat-transfer efficiency vs time at various steam injection rates (water equivalent), internal steam nozzle

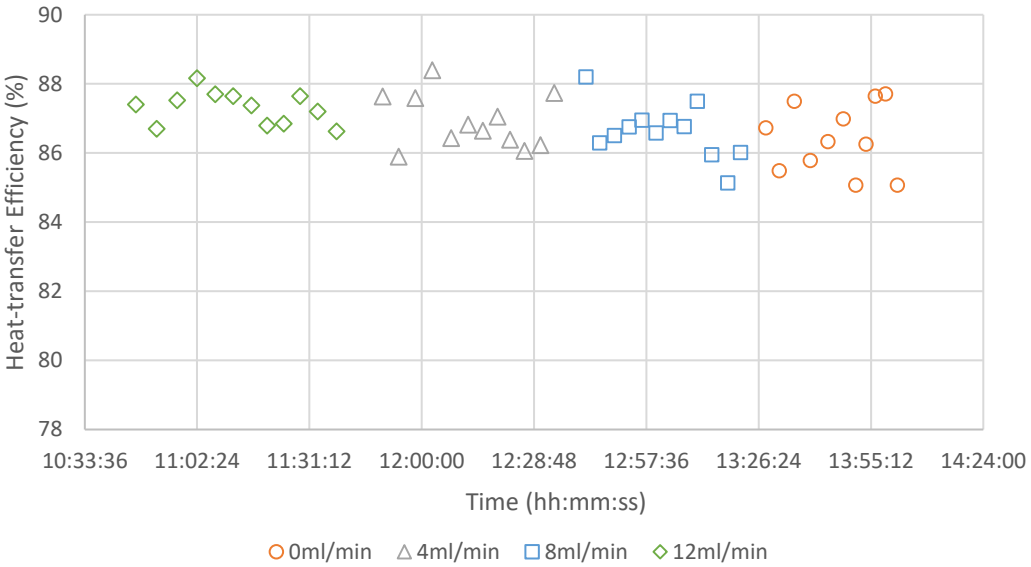

Figure 7-27 – Heat-transfer efficiency vs time at various steam injection rates (water equivalent), external steam nozzle

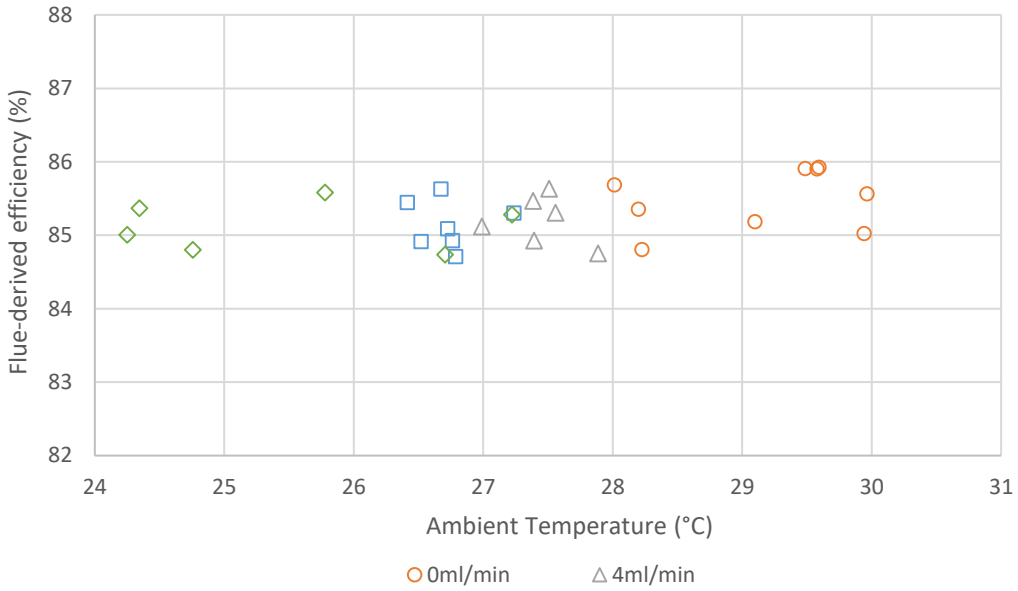

Figure 7-28 – Flue-derived efficiency vs ambient temperature at various steam injection rates (water equivalent), internal steam jet

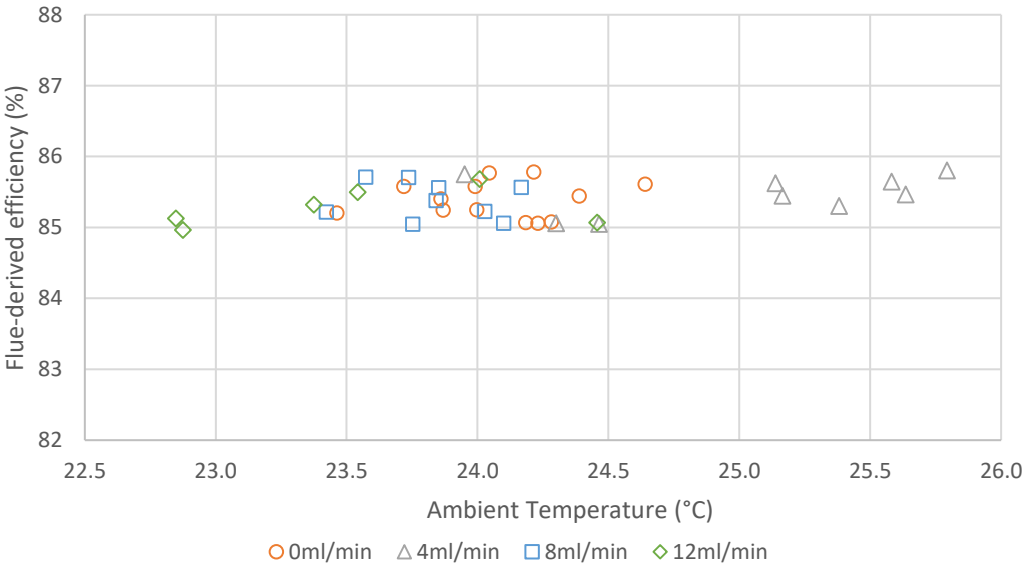

Figure 7-29 – Flue-derived efficiency vs ambient temperature at various steam injection rates (water equivalent), internal steam nozzle

As with the heat-transfer efficiencies, Figure 7-28 and Figure 7-29 show that there was no correlation between the flue-derived efficiency and ambient temperature for the internal case, therefore those experiments were not sensitive to ambient temperature. Figure 7-30 shows a minor 0.35% increase in flue-derived efficiency from 20.5°C to 25.2°C for the external case, which is the opposite of the decreasing trend for its heat-transfer efficiency.

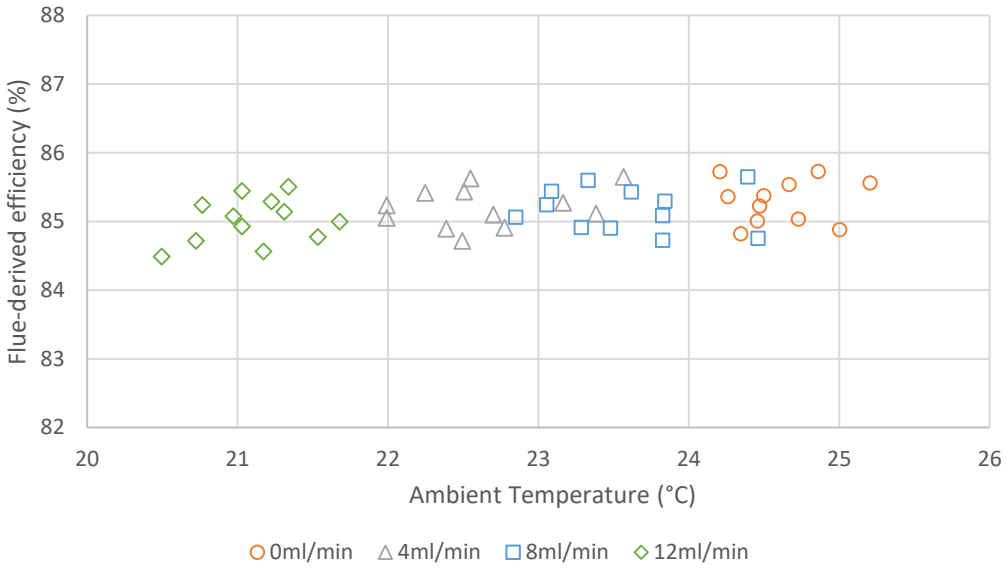

Figure 7-30 – Flue-derived efficiency vs ambient temperature at various steam injection rates (water equivalent), external steam nozzle

Figure 7-31 and Figure 7-32 demonstrate that there was no correlation between flue-derived efficiency and time, as with the heat transfer and ambient temperature studies. Figure 7-33 shows the same minor increase in efficiency as Figure 7-30, due to the ambient temperature correlating with time.

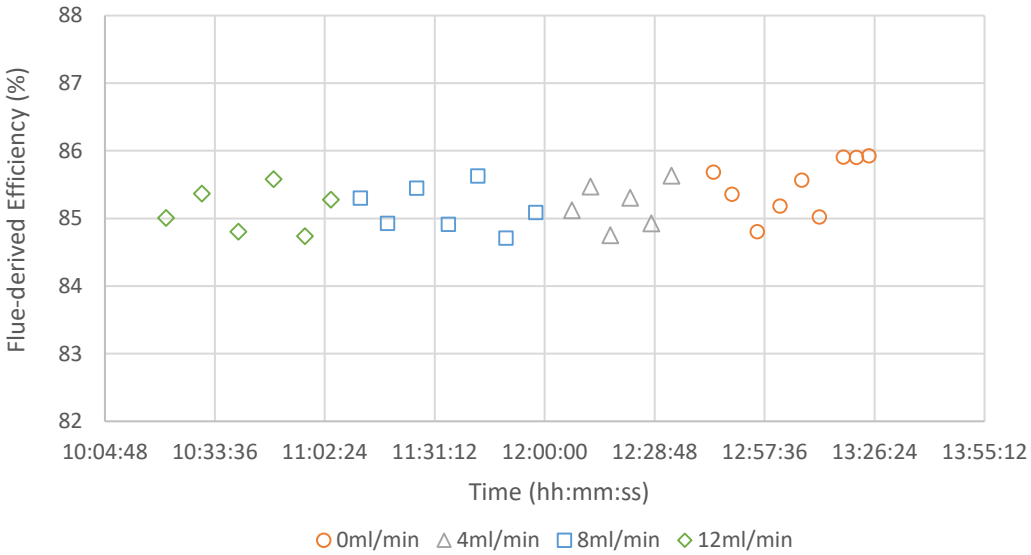

Figure 7-31 – Flue-derived efficiency vs time at various steam injection rates (water equivalent), internal steam jet

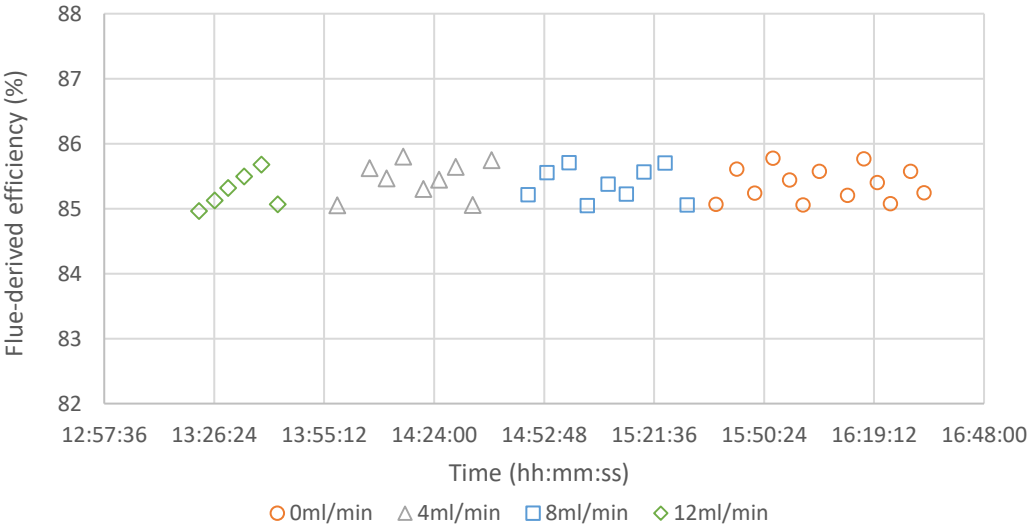

Figure 7-32 – Flue-derived efficiency vs time at various steam injection rates (water equivalent), internal steam nozzle

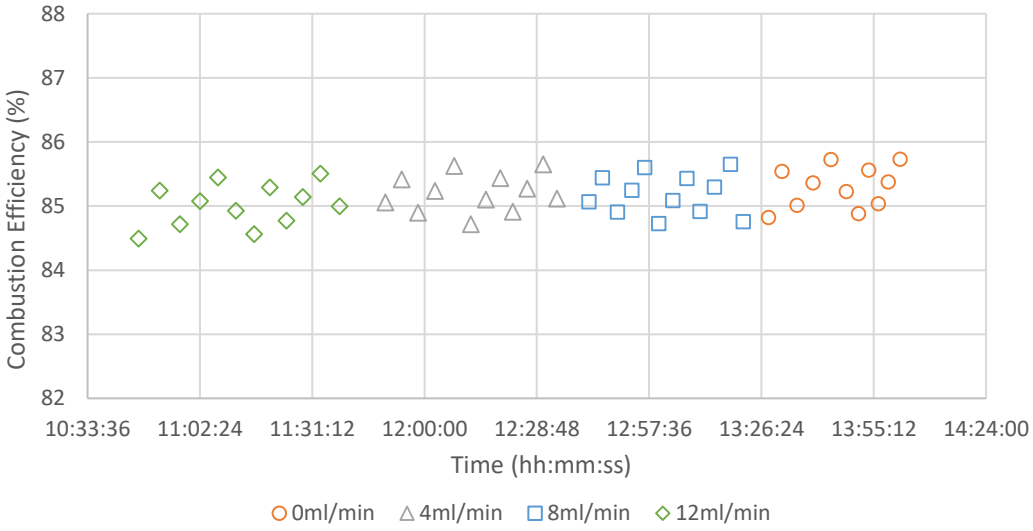

Figure 7-33 – Flue-derived efficiency vs time at various steam injection rates (water equivalent), external steam nozzle

7.4. Discussion

7.4.1. Carbon Monoxide

The increases in CO and HC for the steam jet and external nozzle experiments align with the investigation by De Jager, Kok and Skevis (2007), however investigations by Peltier (2006) and Claeys *et al.* (1993) demonstrated the CO reduction trends observed in the internal steam nozzle case. As the sole difference between the steam jet and internal nozzle tests was the injection method, it can be concluded that the method of steam addition affects the CO emissions of the system. Similarly, the location of the nozzle also affects CO emissions, as the same nozzle was used for both the internal and external cases. The variation is likely due to alterations in the effectiveness of the steam/fuel/air mixing within the combustion process, and the physical effect of the steam addition on the flame stability.

The three aforementioned studies focused on gas turbines, and three different injection experiments were conducted for the current research. The differing CO trends in the studies could therefore be explained by the differing trends from the injection experiments; it is possible that any one of the studies could have produced the opposite effect if the injection method or location had been altered.

The CO results also highlighted the need for optimisation of λ and injection rate, as the minimum CO values occurred at different λ values depending on the injection rate. This was first observed in the preliminary tests, where there was a non-linear response for CO emissions with increasing O_2.

The injection rate appears to modify both where the minima occur and their magnitudes, and the effect of injection rate is not always linear. For example, in the internal nozzle case the 8ml/min rate reduced emissions beyond that of all other cases, and although the 12ml/min offered reductions at λ 1.16 and below, it caused increased emissions above. Göke *et al.* (2014) proposed that excessive cooling of a flame can cause local quenching. It is also widely known that high temperatures and low oxygen availability can cause CO_2 dissociation and incomplete combustion respectively, which result in an increase in CO. It can be concluded that the optimum point for minimum CO rests between the two extremes, which was observed by the non-linear changes in CO with λ or injection rate, hence the need to optimise both.

In the chemical equilibrium study CO decreased with increasing steam injection and λ, however the experimental work only agreed for certain cases. This shows that that a more sophisticated model would be required to accurately calculate the combustion products, such as a computational fluid dynamics approach that included the influence of the burner and nozzle geometries on the mixing and steam dispersion processes.

7.4.2. Oxides of Nitrogen

The results showed clear trends of NO_x decreasing with increasing steam injection rate across all the experiments. This means that in the ranges tested there appears to be no optimum rate of injection, simply that more steam results in lower NO_x. The internal jet case showed diminishing returns however, therefore it is possible that at higher injection rates the beneficial effects would cease and emissions would increase. As the flame is premixed and thermal-NO_x dominated, further reductions in flame temperature due to increasing steam flow are predicted to result in decreasing emissions up till flame failure.

The reductions observed in the experiments were also demonstrated by various previous studies such as the gas turbine application presented by Landman, Derksen and Kok (2006) and the burner application investigated by Toqan *et al.* (1992). This validates both the experimental setup and the NO_x results.

The experiments also demonstrate that a commercially available burner can be modified to provide NO_x control, meaning that existing burners could be retrofitted rather than demanding replacement with new burner designs. This could enable boiler owners to achieve reduced NOx emissions at a lower cost than purchasing a new system.

7.4.3. Efficiency

Each of the three sets of results showed heat-transfer efficiencies that remained within a 3.9% range, and in no set did the efficiency correlate with λ value or steam injection rate. The theoretical modelling indicated that there should have been a decrease in efficiency with increasing λ due to increased thermal dilution, and a similar trend with steam injection rate for the same reason. The loss of efficiency through heat absorbed by the steam may have been negated as its temperature was approximately equal to the exhaust temperature, which would explain the insensitivity to steam flow rate. The effect of the increase in excess air was expected to have resulted in a measurable change in heat-transfer efficiency, however.

The preliminary experiments detailed in Chapter 2 showed clear negative correlation between O_2 value and heat-transfer efficiency over a range of O_2 values from 6% to 16%. It was seen that the change in efficiency at λ values less than 6% was more difficult to distinguish, which coincides with the range of the steam injection experiment. It is possible that although the model suggested an increase in efficiency with reducing excess air, those increases were counteracted by a reduction in efficiency due to incomplete combustion, as indicated by the rise in CO and HC towards stoichiometric conditions. This would explain the insensitivity to λ. The residual variance in the efficiency is reflective of the uncertainty of the measuring equipment.

Contrary to the heat-transfer efficiency, the flue-derived efficiency clearly showed a decreasing trend with increasing steam injection rate across each of the three experiments, which aligned with the predictions of the thermal model. The steam jet experiment also aligned with the model, however the nozzle cases featured some discrepancies. For the internal nozzle the 4ml/min case increased efficiency, which was possibly due to the reduced CO resulting in more complete combustion, or the humidification of the combustion gases resulting in improved heat transfer within the boiler and therefore lower flue gas temperatures. The losses in efficiency with additional steam could be due to thermal dilution overcoming these gains.

In the external case there was no change in flue-derived efficiency between the 4ml/min and 8ml/min cases, even though the emissions data did see a change. This means that the change in steam flow rate was having a measurable effect on the combustion process, which eliminates the possibility of the steam simply not reaching the combustion zone, therefore it can be concluded that for the external case there was a non-linear response to increasing steam flow rate, resulting in the lack of change between the 4ml/min and 8ml/min cases. This is further evidenced by the observation that the efficiencies at each of the λ values are consistently aligned, therefore it was a repeatable response rather than an outlier in the data.

7.4.4. Flame Temperature and Excess Oxygen

With some exceptions each of the three experiments exhibited reducing point 2 flame temperature with increasing λ, which aligned with the model, however the relationship with steam injection was more varied. In some cases steam increased the flame temperature, rather than decreasing it as in the model. This could mean that for those conditions there was a bulk increase in flame temperature, which would require additional heat release in the combustion process. Although Larionov, Mitrofanov and Iovleva, (2014) observed such effects for an inefficiently burning diffusion flame, there was no heat release potential in the premixed flame in this study, where combustion is almost complete. It is therefore more likely that the bulk flame temperature was reducing, and that the temperature at measurement point 2 increased due to the steam altering the flame profile such that a hotter region of the flame was being measured.

The steam jet and external steam nozzle experiments show a lower change in temperature with steam injection than the internal nozzle, which indicates that the internal nozzle causes more a disturbance to the flame profile. The internal nozzle experiment also featured reductions in CO whereas the other trials resulted in increased CO. It is therefore argued that the alteration of the flame profile caused by the flow from the internal nozzle resulted in the reduced CO, and that the CO emissions are dependent on the method and location of the steam injection.

7.4.5. Optimisation

As discussed in Chapter 6, the aims of the research were to reduce both CO and NO_x emissions, meaning that reductions in in one parameter that caused an increase in another did not satisfy these aims. As the CO increases for all the internal steam jet and external nozzle cases, they are eliminated from this comparison. As in the water injection study, the λ value and injection rate have an indistinguishable effect on the heat-transfer efficiency, therefore only reductions in NO_x and CO are considered.

For CO there was clear optimum injection rate as the 8ml/min case produced the minimum CO across all λ setpoints. The minimum 8ml/min, and therefore the overall minimum, occurred at λ = 1.2, with an average of 9ppm at a 77% reduction compared to the non-injected case.

The 12ml/min case resulted in the lowest NO_x across the tested range, featuring an overall minimum at λ = 1.08. Here, NO_x emissions were 41% below the 0ml/min case at 22.1ppm. Although the 12ml/min case resulted in the lowest NO_x, it also increased CO at λ > ~1.18.

With the goal of reducing both CO and NO_x simultaneously, the optimal setpoint for 12ml/min was λ = 1.16, yielding CO and NO_x emissions of 85ppm and 27ppm, 71% and 36% below the 0ml/min cases. The optimal for 8ml/min was λ = 1.16, yielding CO and NO_x emissions of 11ppm and 35ppm, 96% and 18% below the 0ml/min cases. Although the overall improvement for both the optimal 12ml/min and 8ml/min solutions was similar, the 8ml/min case offers an 87% CO improvement over the 12ml/min case, whereas the 12ml/min case only improves NO_x by 22%, therefore the overall optimal is considered to be the 8ml/min at the stated parameters.

7.4.6. Sensitivity to External Effects

For the internal case heat-transfer efficiency was generally stable over time and despite increases ambient temperature, though the external case showed a decline. It is possible that the increased ambient temperature resulted in reduced heat rejection from the radiator, which would have increased the inlet temperature of the water, however the internal experiments also displayed similar changes in ambient temperature with no loss of efficiency. As the mean decline in efficiency across all cases was less than the range of any single case, it is not considered significant.

The flue-derived efficiency showed an insensitivity to temperature and remained stable over time.

7.4.7. Limitations of Experimental Approach

The steam addition experiments shared similar limitations to the water injection experiments described in Chapter 6.

An additional factor in the steam experiments was the vapour fraction of steam entering the combustion zone. Though extensive modifications were made to the experimental setup to ensure superheated steam entered the injection point, it could not be guaranteed that the steam was free from liquid at the point of entering the combustion zone.

7.5. Conclusions

The experimental work has shown that a commercially available burner can be modified to enable steam to be injected into its combustion process. Both the location and the method of injection were examined.

For other combustion systems described in the literature, it was found that steam addition generally resulted in the reduction of NO_x. The NO_x trends aligned with the current experimental work which showed reductions across all cases. A minimum of 22.1ppm was achieved during the internal nozzle experiments, with a λ value of 1.08 and 12ml/min steam injection, equivalent to a 41% reduction over the 0ml/min case.

The effect of steam injection on CO emissions was dependant on both the location and method of injection. For the internal nozzle case CO reductions were achieved. The optimal conditions were found to be at 8ml/min with λ = 1.2, where 9ppm CO was reached, amounting to a 77% reduction over the 0ml/min test. However, in the same location without a nozzle, and for the same nozzle injecting outside the burner, CO increased with steam injection, by up to 355% over the base case.

The optimum conditions for reducing both CO and NO_x were 8ml/min steam injected internally through a nozzle at λ = 1.16. This resulted in NO_x and CO emissions of 35ppm and 11ppm respectively, equivalent to reductions of 18% and 96% over the corresponding 0ml/min case.

The heat-transfer efficiency data remained within a 3.9% range across all tests, and did not correlate with either λ or steam injection rate. This indicates that the process was not adversely affected by steam injection, therefore the emissions reductions were achieved with no loss in efficiency.

The research has found that for the internal nozzle case, it was possible to achieve both reduced CO and NO_x simultaneously, with no significant effect on efficiency. Therefore, steam injection is a viable method of reducing emissions in sub-20kW boiler systems.

7.6. Chapter Summary

This chapter has detailed the investigation into injecting superheated steam into the burner of the boiler. A review of relevant literature found that for the majority of combustion systems, steam addition resulted in a reduction of NO_x, though its effect on CO varied across studies. The theoretical analysis indicated that both NO_x and CO reduced under ideal conditions.

A commercially available burner was modified to enable steam to be injected into the primary air, approximately 100mm before the swirl diffuser. A range of steam flow rates were investigated at various air-fuel equivalence ratios.

It was found that for all cases examined, NO_x reduced with increasing steam addition. The reduction was attributed to reduced flame temperatures. The effect of steam on CO emissions was found to vary with injection method and location, with reductions only found in the internal nozzle case.

It was concluded that steam injection could provide an overall benefit for a sub-20kW boiler if the nozzle design and location are optimal.

Chapter 8 will conclude the thesis, and Chapter 9 will suggest routes for further investigation.

8. Conclusions

8.1. Research Goals

The purpose of this research was to improve the environmental sustainability of improve the environmental sustainability of natural gas fuelled steam boilers. This was primarily due to increasing international concern for the natural environment, resulting in legislation that restricts emissions and encourages fuel economy.

The research therefore has the following aims:

1. A reduction of NO_x emissions
2. The reduction of CO emissions
3. An improvement in heat-transfer efficiency, and thus a reduction in fuel consumption

A literature review was conducted to identify techniques that could achieve these objectives. It was found that injecting steam or water into the combustion process of a gas turbine could reduce NO_x and CO emissions to 2ppm or less (Peltier, 2006), whilst simultaneously improving efficiency. It was hypothesised that similar techniques could be applied to gas fuelled steam boilers, and mathematical modelling of the air/methane/steam indicated that the approach had merit, thus it was chosen as the focus of the research.

8.2. Experimentation

Due to practicalities it was not possible to conduct the research on a full-scale industrial steam boiler, therefore a ~20kW scale commercial water "boiler" was used in situ.

The experimental setup featured the boiler at its core, with a burner attached to its front. The burner took methane, air, and steam/water as its inputs. The mass flow, temperatures, and pressure of each of these were instrumented so that the energy input to the system could be derived. The flow rate and temperature of the heated water were also monitored, allowing the useful heat transferred to be calculated. This water was passed through a fan-cooled radiator which simulated a heat demand.

Emissions of NO_x and CO, excess oxygen, and temperature of the outlet combustion gases were measured using a flue gas analyser.

8.3. Water Addition

Water injection rates of 4, 8, and 12ml/min were investigated across λ values of 1.00 to 1.32. The water was injected through a hollow-cone nozzle at two locations, before the burner air intake and inside the burner before the swirl diffuser. The enabled the determination of the effect of injection rate, air/fuel ratio, and injection location on CO and NO_x emissions, as well as heat-transfer efficiency.

The results indicated that CO emissions were dependant on all three of these parameters. It was found that for both the internal and external cases a minimum CO was found between λ = 1.12 and 1.24, depending on water injection rate. At λ = 1.04, CO reached a maximum of 1054ppm, and at λ = 1.32, 141ppm was observed. A minimum CO of 7ppm occurred at a λ value of 1.12 with 8ml/min water, injected internally.

The minimum NO_x emissions were found at λ = 1.32 for both the internal and external experiments, where an overall minimum of 20ppm was observed for the external nozzle at 12ml/min, equal to a 40% reduction over the non-injected tests. The maximum NO_x was observed between λ = 1.08, reaching a peak of 44ppm. In the internal cases increasing water flow rates tended to decrease NO_x, however in the external cases there was less consistency.

The optimal operating conditions for simultaneous NO_x and CO reduction were found at using an internal nozzle at a λ setpoint of 1.16 with 8ml/min water. This yielded reductions of 64% and 28% for CO and NO_x, respectively.

Generally, for the same nozzle and mass flow rate, injecting water into the air close to the flame yielded improved emissions reductions than injecting before the burner.

The heat-transfer efficiency data did not indicate any significant advantage or disadvantage to injection water, therefore although no efficiency gains were observed, this does mean that the aforementioned emissions reductions were achieved without sacrificing efficiency.

The water addition experiments have shown that the first two objectives of the research were achieved: the reduction of CO and NO_x emissions. The third objective, improving efficiency, was not, however as the emissions reductions did not cause a loss in efficiency, there an overall benefit has been demonstrated.

8.4. Steam Addition

The steam addition experiments involved injecting superheated steam into the combustion air at the same locations as the water injection: into the air before the burner intake, and inside the burner before the swirl diffuser. Two different methods of injecting the steam were tested, firstly through a simple orifice, resulting in a steam jet, and secondly through a solid-cone nozzle. The steam jet experiments were only conducted internally.

The results indicated that NO_x reduction increased for increasing steam injection rate, for both the two internal cases and the external case. A minimum of 22.1ppm was achieved during the internal nozzle experiments, with a λ value of 1.08 and 12ml/min steam injection, equivalent to a 41% reduction over the 0ml/min case. This aligned with trends observed in the literature.

The effect on CO emissions varied depending on the location and the use of the nozzle. Only the internal nozzle cases resulted in CO reductions. A minimum of 9ppm was achieved at 8ml/min injection rate with $\lambda = 1.2$, equivalent to a 77% reduction from the non-injected test. For the internal steam jet and external nozzle CO increased with steam injection, by up to 355% over the base case.

The optimal conditions for reducing both CO and NO_x were 8ml/min steam injected internally through a nozzle at $\lambda = 1.16$. This resulted in NO_x and CO emissions of 35ppm and 11ppm respectively, equivalent to reductions of 18% and 96% over the corresponding non-injected case.

The heat-transfer efficiency data remained within a 3.9% range across all tests, and did not correlate with either λ or steam injection rate. This indicated that the process was not adversely affected by steam injection, therefore the emissions reductions were achieved with no perceivable loss in efficiency.

As with the water injection experiments, the CO and NO_x reduction research objectives have been met, using the internal steam nozzle. Again, these were obtained with a measurable loss in efficiency, resulting in an overall improvement versus operating the system without injection.

8.5. Other Findings

The configuration of the injection system was shown to be critical to its performance. Different injection methods, locations, and fluid states resulted in varying emissions for the same mass flow, highlighting the influence of the injection system design on the emission reduction potential. The importance of a full geometric computational model was made apparent, as the dimensionless chemical kinetic model used in the research did not capture the effect of the injection system or burner designs.

From the reviewed literature steam appeared to be the preferred injection fluid, rather than liquid water. However, this research has shown that liquid water, when appropriately atomised, achieved comparable emissions reductions to steam. The use of water simplifies and reduces the cost of the injection system as a steam generator is not required, liquids require smaller pipework due to decreased volume flow, and energy does not have to be expended to raise the steam.

8.6. Contributions to Knowledge

1. Emissions reductions on a 20kW scale system

   This research is the first known instance of the application of water injection for the reduction of CO and NO_x in a ~20kW scale commercial system. Emissions reductions of up 64% CO and 28% NO_x were achieved with no apparent effect on heat-transfer efficiency.

   This has proven that it is technically viable to introduce the environmental benefits of water injection to commercial/domestic-scale boilers. This means that technology currently only featured on industrial megawatt-scale systems could be used in the domestic or commercial market, creating a new opportunity that would improve environmental sustainability, reduce fuel costs for end-users, and lead to new sales.

Additionally, many applications of steam injection highlighted in the literature review featured water/air ratios of over 30%, whereas the current research achieved up to 77% CO reductions and 41% NOx reductions with ratios of ~2.5%. This shows that smaller injection systems could still yield significant emissions savings in those applications and could be less costly to implement.

Though the research was focused on a 20kW-scale system, the principle of operation for steam boilers is similar, and the research output will result in the development of a product for an industrial system.

2. Retrofitting a commercially available burner for NO_x/CO reduction

This research is the first known study of a retrofitted commercially available burner for water or steam injection. Prior research has featured the design of burners for water injection, however in this research a standard burner was modified to incorporate the same functionality.

It was shown that a modification of the burner enclosure in an optimal location enabled emissions savings to be achieved. This means that burners that were not originally designed for water injection could be retrofitted with the technology, potentially reducing implementation costs and making the technology accessible by a wider market.

3. Reducing emissions to access lower fuel-air equivalence ratios, thus improving efficiency

   This research has led to a patent submission for a multi-variable optimisation system that reduces NO_x, CO, and SO_x emissions, in addition to improving potential efficiency.

   This is achieved by controlling the air/fuel and water/fuel ratios, which enables operating the burner under richer conditions than would normally be accessible. Typically, emissions increase as excess air is reduced, however operating closer to stoichiometric offers efficiency improvements. By harnessing the emissions reducing potential of water injection, the system can operate close to stoichiometric whilst maintaining an acceptable emissions output.

4. Identification of the importance of injection location to the performance of water injection systems for boilers

   The research investigated the effect of water injection point and the use of atomising nozzles on the CO and NO_x emissions from the system. The locations included inside the burner before the swirl diffuser, and into the air supply before the burner air intake. Experiments were conducted both with and without nozzles, and on steam and water, at each location.

   It was identified that the injection point and the nozzle type used for the water injection was critical to the resultant emissions of the boiler system, as injecting internally and with the use of a nozzle offered clear improvements. This had not previously been investigated for this application.

8.7. Closing Statement

In conclusion, the research has met its first and second objectives of reducing CO and NO_x emissions, achieving simultaneous reductions of up to 64% and 28%, respectively. These reductions were obtained without compromising the third objective of improving efficiency, however no measurable efficiency gains were yielded either.

Chapter 9 explores routes for further research and commercialisation.

9. Further Work

9.1. Introduction

This chapter highlights potential routes for investigation and commercialisation based on the outputs of the current research, including both industrial applications and further research opportunities.

Contents

9.2. Limitations of Current Research

The research concluded that there was no measurable correlation between water/steam injection rate or λ value and heat-transfer efficiency, for λ values of 1.04 to 1.32. This contradicted the theoretical analysis which suggested that water/steam addition should have caused an increase in efficiency. Reasons for this were hypothesised, such as the thermal dilution effects being countered by more complete combustion, however they were not possible to prove with the current experimental arrangement. This was due to the boiler/burner system being optically inaccessible; it was essentially a “black box” with air/fuel/water entering and flue gas exiting. This meant it was impossible to precisely determine how the various parameters were affecting the combustion process.

Lab-based experiments have been conducted which have optically-accessible flame arrangements, as demonstrated by Ge, Zang and Guo (2009), however the literature review found that the design of the system was critical to its performance, therefore recreating a similar arrangement would likely yield different results. Instead, it is proposed that either the current system is modified to incorporate an optical window, or that the existing burner is installed into an optically accessible boiler with similar configuration.

An optically-accessible system, with the appropriate seeding and measurement equipment, would enable the flame profile, burning velocity, flame speed, and chemical processes to be measured. The experiments could then be repeated and the effect of the water/steam on the combustion process would be measurable. For example, the use of OH chemiluminescence would provide data on the increase of OH radicals due to water injection, or particle image velocimetry could provide information as to how the internal steam jet case caused a disruption to the flame.

Lastly, more data on the temperature distribution in the combustion chamber and through the boiler could provide useful information on how the heat-transfer between the combustions gases and the boiler water is affected by the various parameters.

9.3. Further Research

9.3.1. System Design

There are various extensions to the research which could also be investigated, such as the design of the injection system. For the water addition experiments a hollow-cone nozzle was used for atomisation, however different types of nozzle, such as solid-cone or air-atomising could be used, which may produce different results. Further investigation into the locations of the injection points could also be conducted. For example, the water could be added to the fuel rather than the air, or directly into the flame rather than before the swirl diffuser.

The effect of the burner design could also be explored. The burner in the current research is a premixed, single stage type, however counter-flow burners or multi-staged burners could also be tested. Each manufacturer's designs will vary, which may or may not affect the effectiveness of the injection system. For example, it was found that under certain conditions increasing λ resulted in an increase in CO, however it is known that other combustion systems can operate at higher lambda values without increases in CO (Arsenie *et al.*, 2015). It was concluded that this was due to the increased volume flow causing instabilities, therefore modifying the burner to accommodate the increased volume flow could have resulted in reduced CO. Modifications could also involve altering the slot angle or slot width of the swirl diffuser, changing the position of the diffuser, or increasing the proportion of secondary air entering the combustion zone.

9.3.2. Fuel

It was assumed that natural gas had similar combustion characteristics to methane, hence the use of methane in the research, however this could be experimentally verified. It would also be useful to examine the emission-reducing effects of water injection on biogas or synthetic gas to determine whether emissions reductions could be achieved.

A liquid fuelled boiler could also be investigated, as Larionov *et al.* (2016) have shown that steam addition can enhance oil flames in a laboratory setting. There is an opportunity to test whether the benefits of that research and the current research yield improvements on an industrial scale oil-fired burner system, which could lead to a significant expansion of the market opportunity. Similarly, applying the water injection techniques to a coal or biomass application could lead to further opportunities, as there is even greater potential for emissions reductions due to the presence of other contaminants in coal, such as sulphur (Hanby, 1994).

9.3.3. Air

Further research could also involve preheating the air before the water injection stage, which would enable it to attain a higher absolute humidity. This could be part of an investigation into the difference in water injection effectiveness between water droplets entrained in the air and water vapour in the air. Similarly, in applications where the air is pre-heated and combustion temperatures are higher, water injection could reduce the formation of temperature-dependant species such as NO_x by reducing the peak flame temperature (Arsenie *et al.*, 2015).

9.3.4. Water

Preheating of the injection water could also be researched. This would reduce the overall cooling capacity of the water, however it would also reduce the heat required to raise it to the saturation point. An effect of this would be to reduce the time taken until vaporisation within the combustion process, which would physically change where vaporisation occurred in the flame, potentially altering its properties.

In the current research either steam or water was used in the injection process, however the effect of a liquid-vapour mixture could be investigated. A two-phase mixture may offer another option for controlling the cooling and expansion effects, other than adjusting the temperature, pressure, or mass flow rates of the injection fluid. By adjusting the vapour fraction, the level of liquid expansion in the combustion could be controlled, which would offer further optimisation potential.

9.3.5. Other

Other routes for investigation could include combining currently known efficiency increasing technologies with this research. For example, economisers can be used to recover energy from exhaust gases, and injecting water or steam into the combustion process would alter the mass flow through the flue, potentially leading to a change in heat transfer within the economiser. Condensing boiler applications could also be investigated for water injection, due to their ability to recovery the enthalpy of evaporation from the injection water, improving efficiency. This would also lead to the possibility of recycling the condensate for use in the injection process, which would reduce water usage and recover its sensible heat, although the acidic condensate would need to be neutralised or its corrosive effects mitigated.

The effect of water injection in systems with flue gas recirculation could be investigated. As the flame temperature would be lower due to the extra inert gases the benefits of water injection would need to be determined. It is possible that the positive chemical effects would still justify an injection system, however over-cooling of the combustion process could be detrimental.

It was shown in Chapters 6 and 7 that the dimensionless theoretical study only partially reflected the experimental data, due to it not encompassing the effect of burner design, injection location, or flame profile. Further work could therefore include a full CFD analysis of the system, with emphasis on the interaction on fluids injected into the burner by different means, such as through a nozzle or entrained in the air. The model could then be validated against the data from the current research, and used to predict the performance of other systems.

9.4. Industrial Applications

One of the planned extensions to the research is to scale-up the injection technology to measure its effectiveness on an industrial steam boiler. The research water boiler system generated 20kW of thermal power, whereas a representative industrial system could output over 500kW and would generate steam. The difference between heating water and raising steam is that for a water heater, the heat transfer mechanism on the water side is mainly convective, though for a steam boiler it is a mixture of convection and evaporation, which may affect the chemical kinetics in the fire tubes.

Figure 9-1 features an instrumentation diagram of a possible system setup. It would take the form of water injection into the air before the burner to avoid burner modification. Most of the components would simply need to be scaled up, such as the flowmeter and pump, with no change required for the analyser or pressure and temperature sensors.

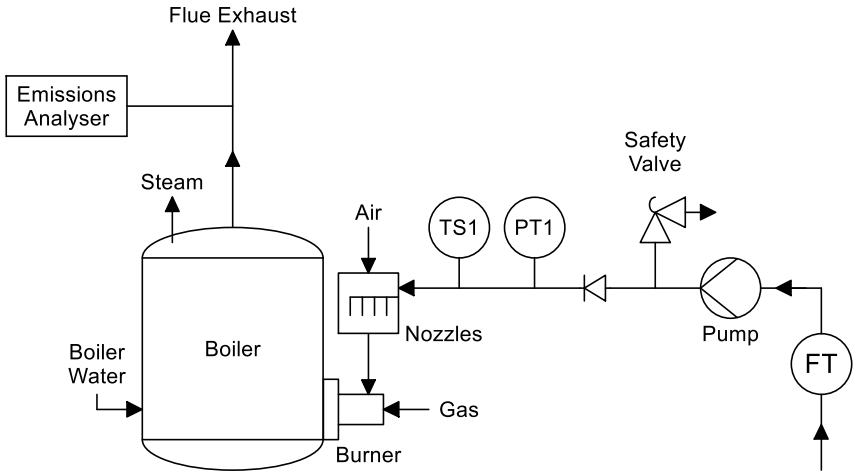

Figure 9-1 – System diagram of a full-scale system

A new multi-variable control system will be designed for the full-scale system which will replace the manual control of the injection fluid and air. Figure 9-2 shows a representative visualisation of the process. On the y-axis is the “Water Addition (%)”. This represents the amount of water relative to either the fuel or air. On the x-axis is the air-fuel equivalence ratio (λ). The contours represent bands of efficiency. The red dotted line represents the emissions boundary.

The plot shows that emissions increase towards λ = 1 and that the emissions boundary prevents operating at maximum efficiency. The boundary is shown to subside when water is added, enabling higher efficiencies to be achieved. It also shows a decrease in efficiency with water injection, though it is less than the efficiency gained by moving the emissions boundary.

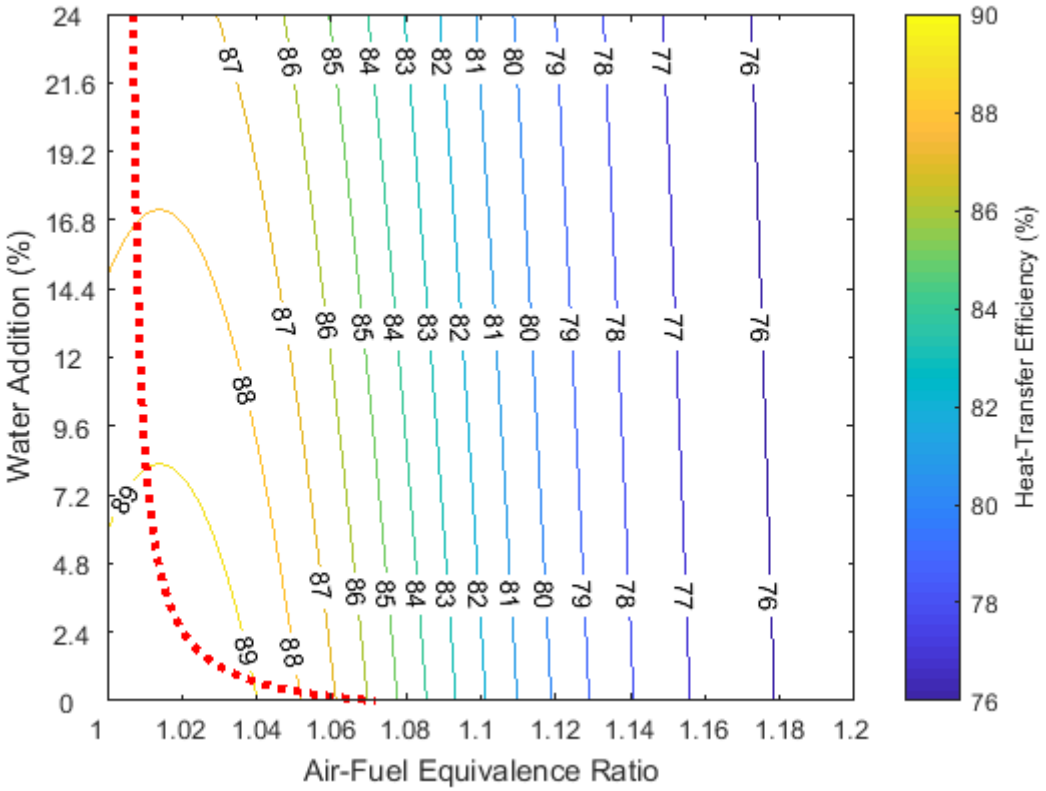

Figure 9-2 – Visualisation of multi-variable optimisation

The multi-variable control system coupled with the theoretical model could also form the basis of a wider boilerhouse energy monitoring system. Energy flows in to and out of the system would be calculated from flow rates, temperatures, and pressures fed into the model, which could then reveal such things as thermal wastage or potential for energy recovery. This information could then be used to optimise the whole boilerhouse rather than just only the heat transfer efficiency, or to determine whether upgrades such as economisers would provide advantages.

The benefit of scaling up the technology would be the commercial and environmental opportunity. It is estimated that there are approximately 3700 boilers in the UK, with emissions that could be reduced using the current research. Similarly, the research could be scaled down to suit residential boilers, which could lead to the exploitation of a market comprising some 25 million fuel-burning households in the UK alone (Department of Energy & Climate Change, 2013). The technology also has the potential to be applied at a power station scale.

9.5. Chapter Summary

This chapter has suggested future extensions to the research and explained why they would be worthy of investigation. These included research into different fuels, the design of the burner, and the type of nozzles used in the injection system. It also described a larger scale system that is being designed based on the results of the research, along with its corresponding control system.

This is the closing chapter, and thus concludes the record of the research.

References

Acampora, L. and Marra, F. S. (2015) 'Numerical strategies for the bifurcation analysis of perfectly stirred reactors with detailed combustion mechanisms', *Computers and Chemical Engineering*. Elsevier Ltd, 82, pp. 273–282. doi: 10.1016/j.compchemeng.2015.07.008.

Altafini, C. R., Wander, P. R. and Barreto, R. M. (2003) 'Prediction of the working parameters of a wood waste gasifier through an equilibrium model', *Energy Conversion and Management*, 44(17), pp. 2763–2777. doi: 10.1016/S0196-8904(03)00025-6.

Arsenie, P. *et al.* (2015) 'Technologies for the Reduction of Nitrogen Oxides Emissions', *TransNav, the International Journal on Marine Navigation and Safety of Sea Transportation*, 9(2), pp. 251–256. doi: 10.12716/1001.09.02.13.

Asgari, O., Hannani, S. K. and Ebrahimi, R. (2012) 'Improvement and experimental validation of a multi-zone model for combustion and NO emissions in CNG fueled spark ignition engine', *Journal of Mechanical Science and Technology*. Heidelberg, 26(4), pp. 1205–1212. doi: 10.1007/s12206-012-0229-6.

Assad, M. S., Penyazkov, O. G. and Skoblya, S. G. (2011) 'Calculation of the equilibrium composition of multicomponent thermodynamic systems by the method of entropy maximization', *Journal of Engineering Physics and Thermophysics*, 84(1), pp. 13–22. doi: 10.1007/s10891-011-0451-6.

Barba, D. *et al.* (2011) 'The Gibbs Free Energy Gradient Method for RDF gasification modelling', *Fuel*, 90(4), pp. 1402–1407. doi: 10.1016/j.fuel.2010.12.022.

van Baten, J. and Szczepanski, R. (2011) 'A thermodynamic equilibrium reactor model as a CAPE-OPEN unit operation', *Computers and Chemical Engineering*. Elsevier Ltd, 35(7), pp. 1251–1256. doi: 10.1016/j.compchemeng.2010.07.016.

Baukal, C. E. *et al.* (2007) 'Controlling emissions during cold furnace startup', *Chemical Engineering Progress*, 103(2), pp. 42–46.

BEIS (2018) 'Energy Consumption in the UK (ECUK) 2018', *Energy Consumption in the UK*, (July), pp. 1–39. doi: 10.1073/pnas.1423686112.

BOC (2015) 'SAFETY DATA SHEET Methane, compressed', p. 14. Available at: https://www.boconline.co.uk/en/images/tg_8321_methane_tcm410-61346.pdf.

Borman, G. L. and Ragland, K. W. (1998) *Combustion Engineering*. McGraw-Hill.

Carbon Trust (2012) *How to implement oxygen trim control*. Available at: https://www.carbontrust.com/media/147167/j8054_ctl147_how_to_implement_oxygen_trim_control_aw.pdf.

Cengel, Y. A. and Boles, M. A. (2015) *An Engineering Approach*. Eighth in. Edited by M. A. Boles. doi: 10.1017/CBO9781107415324.004.

Cheikhravat, H. *et al.* (2015) 'Effects of water sprays on flame propagation in hydrogen/air/steam mixtures', *Proceedings of the Combustion Institute*. The Combustion Institute, 35(3), pp. 2715–2722. doi: 10.1016/j.proci.2014.05.102.

Claeys, J. P. *et al.* (1993) 'Combustion system performance and field test results of the MS7001F gas turbine', *Journal of Engineering for Gas Turbines and Power*, 115(3), p. 537.

Cong, L. and Dagaut, P. (2009) 'Experimental and detailed modeling study of the effect of water vapor on the kinetics of combustion of hydrogen and natural gas, impact on NOx', *Energy and Fuels*. Edited by P. Dagaut, 23(2), pp. 725–734. doi: 10.1021/ef800832q.

Conte, G., Scaradozzi, D. and Cesaretti, M. (2006) 'Combustion control in domestic boilers'.

Department for Business Energy & Industrial Strategy (2018) *ANNUAL STATEMENT OF EMISSIONS*.

Department of Energy & Climate Change (2013) *United Kingdom housing energy fact file*. doi: URN: 12D/354.

Deydier, A. *et al.* (2011) 'Equilibrium model for a travelling bed gasifier', *Biomass and Bioenergy*. Elsevier Ltd, 35(1), pp. 133–145. doi: 10.1016/j.biombioe.2010.08.022.

Faungnawakij, K., Viriya-Empikul, N. and Tanthapanichakoon, W. (2011) 'Evaluation of the thermodynamic equilibrium of the autothermal reforming of dimethyl ether', *International Journal of Hydrogen Energy*, 36(10), pp. 5865–5874. doi: 10.1016/j.ijhydene.2011.02.027.

Freitas, A. C. D. and Guirardello, R. (2012) 'Oxidative reforming of methane for hydrogen and synthesis gas production: Thermodynamic equilibrium analysis', *Journal of Natural Gas Chemistry*, 21(5), pp. 571–580. doi: 10.1016/S1003-9953(11)60406-4.

Freitas, A. C. D. and Guirardello, R. (2014) 'Comparison of several glycerol reforming methods for hydrogen and syngas production using Gibbs energy minimization', *International Journal of Hydrogen Energy*. Elsevier Ltd, 39(31), pp. 17969–17984. doi: 10.1016/j.ijhydene.2014.03.130.

Ge, B., Zang, S.-S. S. and Guo, P. Q. (2009) 'Experimental study on turbulent structure of humid air flame in a bluff-body burner', *Journal of Thermal Science*. Heidelberg, 18(2), pp. 185–192. doi: 10.1007/s11630-009-0185-3.

Glassman, I., Yetter, R. A. and Glumac, N. G. (2014) *Combustion: Fifth Edition*, *Combustion: Fifth Edition*.

Göke, S. *et al.* (2013) 'Influence of steam dilution on the combustion of natural gas and hydrogen in premixed and rich-quench-lean combustors', *Fuel Processing Technology*. Elsevier B.V., 107(x), pp. 14–22. doi: 10.1016/j.fuproc.2012.06.019.

Göke, S. *et al.* (2014) 'Influence of Pressure and Steam Dilution on NOx and CO Emissions in a Premixed Natural Gas Flame', *Journal of Engineering for Gas Turbines and Power*. Edited by S. Goke. American Society of Mechanical Engineers, 136(9), p. 091508. doi: 10.1115/1.4026942.

Göke, S. and Paschereit, C. O. (2013) 'Influence of Steam Dilution on Nitrogen Oxide Formation in Premixed Methane/Hydrogen Flames', *Journal of Propulsion and Power*. Edited by S. Goke. American Institute of Aeronautics and Astronautics, 29(1), pp. 249–260. doi: 10.2514/1.B34577.

Goodwin, D. G. *et al.* (2018) 'Cantera: An Object-oriented Software Toolkit for Chemical Kinetics, Thermodynamics, and Transport Processes'. doi: 10.5281/zenodo.1174508.

Government Digital Service (2018) *Environmental taxes, reliefs and schemes for businesses*. Available at: https://www.gov.uk/green-taxes-and-reliefs/climate-change-levy (Accessed: 11 September 2018).

Gunawardena, D. A. and Fernando, S. D. (2014) 'a Thermodynamic Equilibrium Analysis of Glucose Conversion To Hydrocarbons', *Chemical Engineering Communications*. Taylor & Francis Group, 201(8), pp. 1115–1124. doi: 10.1080/00986445.2013.803078.

Hanby, V. I. (Victor I. (1994) *Combustion and pollution control in heating systems*. Springer-Verlag. doi: 10.1007/978-1-4471-2071-1.

Hosseini, M., Dincer, I. and Rosen, M. A. (2012) 'Steam and air fed biomass gasification: Comparisons based on energy and exergy', *International Journal of Hydrogen Energy*, 37(21), pp. 16446–16452. doi: 10.1016/j.ijhydene.2012.02.115.

IPCC (2014) ‘Summary for Policymakers’, *Climate Change 2014: Mitigation of Climate Change. Contribution of Working Group III to the Fifth Assessment Report of the Intergovernmental Panel on Climate Change*, pp. 1–33.

De Jager, B., Kok, J. B. W. and Skevis, G. (2007) ‘The effects of water addition on pollutant formation from LPP gas turbine combustors’, *Proceedings of the Combustion Institute*, 31 II(2), pp. 3123–3130. doi: 10.1016/j.proci.2006.07.147.

Jarungthammachote, S. and Dutta, A. (2007) ‘Thermodynamic equilibrium model and second law analysis of a downdraft waste gasifier’, *Energy*, 32(9), pp. 1660–1669. doi: 10.1016/j.energy.2007.01.010.

Jarungthammachote, S. and Dutta, A. (2008) ‘Equilibrium modeling of gasification: Gibbs free energy minimization approach and its application to spouted bed and spout-fluid bed gasifiers’, *Energy Conversion and Management*, 49(6), pp. 1345–1356. doi: 10.1016/j.enconman.2008.01.006.

Jones, W. P. and Rigopoulos, S. (2005) ‘Rate-controlled constrained equilibrium: Formulation and application to nonpremixed laminar flames’, *Combustion and Flame*, 142(3), pp. 223–234. doi: 10.1016/j.combustflame.2005.03.008.

Katoh, A. *et al.* (2006) ‘Visualization of Steam Addition Effect on OH Distribution in a Flame by Isotope Shift/Planar Laser-Induced Fluorescence (IS/PLIF) Spectroscopy’, *Journal of Engineering for Gas Turbines and Power*, 128(1), p. 8. doi: 10.1115/1.2056528.

Kayadelen, H. K. (2017) ‘Effect of natural gas components on its flame temperature, equilibrium combustion products and thermodynamic properties’, *Journal of Natural Gas Science and Engineering*. Elsevier B.V, 45, pp. 456–473. doi: 10.1016/j.jngse.2017.05.023.

Kayadelen, H. K. and Ust, Y. (2013) ‘Prediction of equilibrium products and thermodynamic properties in H 2O injected combustion for CαH βOγNδ type fuels’, *Fuel*. Elsevier Ltd, 113(x), pp. 389–401. doi: 10.1016/j.fuel.2013.05.095.

Kobayashi, H. *et al.* (2009) ‘Dilution effects of superheated water vapor on turbulent premixed flames at high pressure and high temperature’, *Proceedings of the Combustion Institute*. The Combustion Institute, 32 II(2), pp. 2607–2614. doi: 10.1016/j.proci.2008.05.078.

Kuo, K. K. (2005) *Principles of combustion*, *Combustion and Flame*.

Kuprianov, V. I. (2005) 'Applications of a cost-based method of excess air optimization for the improvement of thermal efficiency and environmental performance of steam boilers', *Renewable and Sustainable Energy Reviews*, 9(5), pp. 474–498. doi: 10.1016/j.rser.2004.05.006.

Landman, M. J., Derksen, M. A. F. and Kok, J. B. W. (2006) 'Effect of combustion air dilution by water vapor or nitrogen on NOxemission in a premixed turbulent natural gas flame: An experimental study', *Combustion Science and Technology*. Taylor & Francis Group, 178(4), pp. 623–634. doi: 10.1080/00102200500241214.

Langer, R. *et al.* (2018) 'A Comparison of Numerical Frameworks for Modelling Homogenous Reactors and Laminar Flames', *Joint Meeting of the German and Italian Sections of the Combustion Institute*. Available at: http://www.combustion-institute.it/proceedings/XXXXI-ASICI/papers/41proci2018.VI9.pdf.

Larionov, V. M. *et al.* (2016) 'Mechanism of influence water vapor on combustion characteristics of propane-air mixture', *Journal of Physics: Conference Series*. IOP Publishing, 669(1), p. 012041. doi: 10.1088/1742-6596/669/1/012041.

Larionov, V. M., Mitrofanov, G. A. and Iovleva, O. V. (2014) 'Effect of supplementation of water vapor to the environmental characteristics of the combustion of propane-air mixture', *Journal of Physics: Conference Series*, 567(1), p. 12028. doi: 10.1088/1742-6596/567/1/012028.

Lemmon, E. W. *et al.* (2018) 'NIST Standard Reference Database 23: Reference Fluid Thermodynamic and Transport Properties-REFPROP, Version 10.0, National Institute of Standards and Technology'. doi: https://dx.doi.org/10.18434/T4JS3C.

Leonard, G. and Stegmaier, J. (1994) 'Development of an Aeroderivative Gas Turbine Dry Low Emissions Combustion System', *Journal of Engineering for Gas Turbines and Power*, 116(3), p. 542. doi: 10.1115/1.2906853.

Li, M. *et al.* (2017) 'Influence of the Steam Addition on Premixed Methane Air Combustion at Atmospheric Pressure', *Energies*. Multidisciplinary Digital Publishing Institute, 10(7), p. 1070. doi: 10.3390/en10071070.

Li, X. *et al.* (2001) 'Equilibrium modeling of gasification: A free energy minimization approach and its application to a circulating fluidized bed coal gasifier', *Fuel*, 80(2), pp. 195–207. doi: 10.1016/S0016-2361(00)00074-0.

Lienhard IV, J. H. and Lienhard V, J. H. (2011) *A Heat Transfer Textbook: Fourth Edition*. 4th edn. Dover Publications.

Liu, D. D. S. and MacFarlane, R. (1983) 'Laminar burning velocities of hydrogen-air and hydrogen-airsteam flames', *Combustion and Flame*, 49(1–3), pp. 59–71. doi: 10.1016/0010-2180(83)90151-7.

Livingston, R. A. (2016) 'Acid rain attack on outdoor sculpture in perspective', *Atmospheric Environment*. Elsevier Ltd, 146, pp. 332–345. doi: 10.1016/j.atmosenv.2016.08.029.

Mathioudakis, K. (2002) 'Evaluation of steam and water injection effects on gas turbine operation using explicit analytical relations', *Proceedings of the Institution of Mechanical Engineers, Part A: Journal of Power and Energy*, 216(6), pp. 419–432. doi: 10.1243/095765002761034195.

Mayur, M. *et al.* (2019) 'Modeling and simulation of the thermodynamics of lithium-ion battery intercalation materials in an open-source software', *Electrochimica Acta*. Elsevier Ltd, p. 134797. doi: 10.1016/j.electacta.2019.134797.

McBride, B. J., Gordon, S. and Reno, M. A. (1993) *Coefficients for calculating thermodynamic and transport properties of individual species*, *Unknown*. Available at: http://adsabs.harvard.edu/abs/1993cctt.rept.....M.

National Grid (2018) 'Future Energy Scenarios in five minutes', (July). Available at: http://fes.nationalgrid.com/fes-document/.

Pabian, S. E. *et al.* (2012) 'Effects of liming on forage availability and nutrient content in a forest impacted by acid rain', *PLoS ONE*, 7(6). doi: 10.1371/journal.pone.0039755.

De Paepe, W. *et al.* (2016) 'Experimental Investigation of the Effect of Steam Dilution on the Combustion of Methane for Humidified Micro Gas Turbine Applications', *Combustion Science and Technology*. Taylor & Francis, 188(8), pp. 1199–1219. doi: 10.1080/00102202.2016.1174116.

Pang, M. *et al.* (2017) 'Trade-off between carbon reduction benefits and ecological costs of biomass-based power plants with carbon capture and storage (CCS) in China', *Journal of Cleaner Production*. Elsevier Ltd, 144, pp. 279–286. doi: 10.1016/j.jclepro.2017.01.034.

Park, J. *et al.* (2004) 'Numerical study on steam-added mild combustion', *International Journal of Energy Research*. Chichester, UK, 28(13), pp. 1197–1212. doi: 10.1002/er.1027.

Peltier, R. V. (2006) 'Cheng Cycle flirts with 2 ppm NOx- and CO', *Power*. Edited by R. Peltier, 150(4), pp. 5–8.

Ptasinski, K. J., Prins, M. J. and Pierik, A. (2007) 'Exergetic evaluation of biomass gasification', *Energy*, 32(4), pp. 568–574. doi: 10.1016/j.energy.2006.06.024.

Randall, C. and Beaumont, J. (2011) *Housing*.

Rashidi, M. (1997) 'Calculation of equilibrium composition in combustion products', *Chemical Engineering and Technology*, 20(8), pp. 571–575. doi: 10.1002/ceat.270200809.

Roy, P., Schlader, A. F. and Odgers, J. (1974) 'Premixed Combustion in a Baffle Combustor and the Effect of Steam Injection', *Journal of Engineering for Power*, 96(4), p. 387. doi: 10.1115/1.3445862.

Sathiah, P. and Roelofs, F. (2014) 'Numerical modeling of sodium fire - Part I: Spray combustion', *Nuclear Engineering and Design*, 278, pp. 723–738. doi: 10.1016/j.nucengdes.2013.11.081.

Shabbar, S. and Janajreh, I. (2013) 'Thermodynamic equilibrium analysis of coal gasification using Gibbs energy minimization method', *Energy Conversion and Management*, 65, pp. 755–763. doi: 10.1016/j.enconman.2012.02.032.

Singh, D. *et al.* (2012) 'An experimental and kinetic study of syngas/air combustion at elevated temperatures and the effect of water addition', *Fuel*, 94, pp. 448–456. doi: 10.1016/j.fuel.2011.11.058.

Skevis, G. *et al.* (2004) 'Numerical investigation of methane combustion under mixed air-steam turbine conditions - FLAMESEEK', *Applied Thermal Engineering*, 24(11–12), pp. 1607–1618. doi: 10.1016/j.applthermaleng.2003.10.027.

Smith, G. P. *et al.* (2000) 'GRI-Mech 3.0', *http://www.me.berkeley.edu/gri_mech/*. doi: 10.1016/j.jinf.2014.08.011.

Smith, W. R. and Missen, Ronald William (1982) *Chemical reaction equilibrium analysis: theory and algorithms*. Edited by Ronald W Missen. New York ; Chichester: Wiley. Available at: https://books.google.co.il/books/about/Chemical_reaction_equilibrium_analysis.html?id=YzdRAAAAMAAJ&pgis=1.

Sohn, C. H. *et al.* (1999) 'A burning velocity correlation for premixed hydrogen/air/steam flames', *KSME International Journal*. Seoul, 13(3), pp. 294–303. doi: 10.1007/BF02970488.

De Souza, T. L. *et al.* (2014) 'Thermodynamic analysis of autothermal reforming of methane via entropy maximization: Hydrogen production', *International Journal of Hydrogen Energy*, 39(16), pp. 8257–8270. doi: 10.1016/j.ijhydene.2014.03.078.

Sreejith, C. C., Arun, P. and Muraleedharan, C. (2013) 'Thermochemical Analysis of Biomass Gasification by Gibbs Free Energy Minimization Model—Part: I (Optimization of Pressure and Temperature)', *International Journal of Green Energy*. Taylor & Francis Group, 10(3), pp. 231–256. doi: 10.1080/15435075.2011.653846.

Sun, S. *et al.* (2016) 'Experimental and theoretical studies of laminar flame speed of CO/H2in O2/H2O atmosphere', *International Journal of Hydrogen Energy*. Pergamon, 41(4), pp. 3272–3283. doi: 10.1016/j.ijhydene.2015.11.120.

Terhaar, S., Oberleithner, K. and Paschereit, C. O. (2014) 'Impact of steam-dilution on the flame shape and coherent structures in swirl-stabilized combustors', *Combustion Science and Technology*. Taylor & Francis, 186(7), pp. 889–911. doi: 10.1080/00102202.2014.890597.

Testo Ltd. (2019) *Testo 350 Manual*. Available at: https://www.testo350.com/downloads/350/literature-manuals/ (Accessed: 20 August 2019).

Toqan, M. A. *et al.* (1992) 'Low NOx emission from radially stratified natural gas-air turbulent diffusion flames', *Symposium (International) on Combustion*, 24(1), pp. 1391–1397. doi: 10.1016/S0082-0784(06)80162-1.

Touchton, G. L. (1984) 'An Experimentally Verified NOx Prediction Algorithm Incorporating the Effects of Steam Injection', *Journal of Engineering for Gas Turbines and Power*. American Society of Mechanical Engineers, 106(4), p. 833. doi: 10.1115/1.3239647.

Vaezi, M. *et al.* (2011) 'Gasification of heavy fuel oils: A thermochemical equilibrium approach', *Fuel*, 90(2), pp. 878–885. doi: 10.1016/j.fuel.2010.10.011.

Washington State University (2003) *Boiler Combustion Monitoring and Oxygen Trim Systems*.

World Energy Council (2017) 'World Energy Trilemma Index | 2017 MONITORING THE SUSTAINABILITY OF NATIONAL ENERGY SYSTEMS', p. 145. Available at: https://www.worldenergy.org/wp-content/uploads/2017/11/Energy-Trilemma-Index-2017-Report.pdf.

Xiao, R. and Song, Q. (2011) 'Characterization and kinetics of reduction of CaSO4 with carbon monoxide for chemical-looping combustion', *Combustion and Flame*, 158(12), pp. 2524–2539. doi: 10.1016/j.combustflame.2011.05.011.

Xin, G., Shusheng, Z. and Bing, G. (2007) 'Characteristic modes and flow structure of non-premixed flame in humid-air combustion', *Korean Journal of Chemical Engineering*. New York, 24(2), pp. 354–360. doi: 10.1007/s11814-007-5046-8.

Xiong, J., Zhao, H. and Zheng, C. (2011) 'Exergy analysis of a 600 MWe oxy-combustion pulverized-coal- fired power plant', *Energy and Fuels*, 25(8), pp. 3854–3864. doi: 10.1021/ef200702k.

Zainal, Z. A. *et al.* (2001) 'Prediction of performance of a downdraft gasifier using equilibrium modeling for different biomass materials', *Energy Conversion and Management*, 42(12), pp. 1499–1515. doi: 10.1016/S0196-8904(00)00078-9.

Zhao, D. *et al.* (2002) 'Behavior and effect on NOx formation of OH radical in methane-air diffusion flame with steam addition', *Combustion and Flame*, 130(4), pp. 352–360. doi: 10.1016/S0010-2180(02)00385-1.

Zou, C. *et al.* (2014) 'The chemical mechanism of steam's effect on the temperature in methane oxy-steam combustion', *International Journal of Heat and Mass Transfer*. Elsevier Ltd, 75, pp. 12–18. doi: 10.1016/j.ijheatmasstransfer.2014.03.051.

Appendix A – Steam Generator Limitations

The initial steam addition experiments did not progress as planned due to issues involving the electric steam generator. Firstly, the generator that arrived was not a superheater as was specified. That meant that the vapour fraction of the steam could not be determined. In an attempt to overcome the issue, 6bar of back-pressure was exerted on the steam generator using a precision valve, which when expanded to atmospheric pressure, was calculated to result in steam that was superheated by 43.2°C. This did not occur, with steam temperatures of around 100°C detected downstream of the steam generator. Calculating the water content required to absorb the 43.2°C of superheat revealed that the steam being generated was carrying at least 5% liquid.

Secondly, the steam generator was over-sized for the lower flow rates. The manufacturer gave assurances that the generator could cover the entire range of flows, however it repeatedly overheated the fluid. By changing the proportional, integral, and derivative control settings some progress was made towards achieving stability but it was insufficient. The controller was changed to a model with more precise control over the electrical element relays, and one of the 3 heating elements was disabled, but this resulted in only minor improvements. The generator had too much thermal mass and over-sized heating elements.

Thirdly, the steam generator appeared to operate by maintaining a level of liquid within itself. This would not have been a problem if the level was maintained, so that the incoming mass flow of water matched the outgoing mass of steam, however more steam was being generated than was

replaced. This resulted in the level falling until the generator “ran dry” and overheated. Also, this made it impossible to accurately determine how much steam was being generated at any particular time. As the capacity of the generator was approximately 2 litres and took around 90 minutes to empty, the draining of the water would have caused an additional 22ml/min of steam to be generated, which in the worst case would have resulted in an error of over 100%.

Without a reliable measurement of the vapour fraction and mass flow of steam it was decided to stop the experiments until the issues could be resolved. The improvements involved the removal of the electric steam generator and the installation of a steam/water evaporating heat exchanger, where fixed pressure steam was used on the hot side to evaporate the water fed to the burner. This prevented overheating as the injection water/steam could only be heated to the steam side temperature. It also provided a stable temperature with relatively little complexity, as the hot side was fixed at saturation temperature for whichever pressure was set.

Due to space limitations, the new heat exchanger was positioned outside of the test rig, and despite the relatively short 2m length of pipework to the burner, it was calculated that the steam would have begun condensing before reaching the injection point. To overcome the heat loss a trace-heating system was implemented. It was calculated that the heat loss from the injection line would be 240W in the worst case, and so a 500W heater rope was sourced, which provided extra capacity for inaccuracies in the calculations and increased superheating. The heating element was bound to the pipework near to the burner.

Unfortunately, the trace heating system also faced control problems, where temperatures would rapidly oscillate between 100°C to 200°C, likely due to evaporation and condensation causing sudden changes in volume flow. The decision was then made to completely redesign the steam injection system and relocate the experimental setup to minimise the distance between the steam generator and burner. This resulted in the system displayed in Figure 7-2.